

Fermi–Dirac machines as quantizations of neurons

Alexander He,¹ Nana Liu,^{2,3,4,5} and Mark M. Wilde⁶

¹*Department of Physics, Cornell University, Ithaca, New York 14850, USA*

²*Institute of Natural Sciences, Shanghai Jiao Tong University, Shanghai 200240, China*

³*School of Mathematical Sciences, Shanghai Jiao Tong University, Shanghai 200240, China*

⁴*Ministry of Education Key Laboratory in Scientific and Engineering Computing, Shanghai Jiao Tong University, Shanghai 200240, China*

⁵*Global College, Shanghai Jiao Tong University, Shanghai 200240, China*

⁶*School of Electrical and Computer Engineering, Cornell University, Ithaca, New York 14850, USA*

Fermi–Dirac machines have been proposed recently as an approach to solving semidefinite optimization problems on quantum computers. Here, we reinterpret them as canonical quantizations of classical neurons. By viewing a classical neuron as an activation function applied to a parameterized classical Hamiltonian, we quantize this model by replacing classical variables with operators whose eigenvalues encode their possible values. This follows the standard approach to canonical quantization in quantum mechanics. Crucially, when the Hamiltonian consists of commuting operators, our construction reduces exactly to a classical neuron. More generally, our approach yields an activation observable, defined as an activation function applied to a parameterized quantum Hamiltonian. The output of this quantized neuron is a random variable with expectation value equal to that of the activation observable with respect to an input state. We develop efficient hybrid quantum–classical algorithms for evaluating outputs and gradients of our quantized neurons, enabling evaluation and training. These algorithms rely on basic primitives that include random sampling, Hamiltonian simulation, and the Hadamard test. We also quantize a whole host of other activation functions, including the smooth rectified linear unit (ReLU), sigmoid linear unit, Gaussian-smoothed ReLU, and Gaussian error linear unit (GeLU), which are known to be useful for deep learning applications. Numerical experiments indicate that neurons based on quantum Hamiltonians can learn functions that classical neurons cannot. We further define a computational decision problem based on Fermi–Dirac neurons and prove that it is BQP-complete, providing complexity-theoretic evidence against efficient classical simulation. Finally, we generalize our approach to continuous quantum variables and sketch two different ways of composing these neurons into networks.

CONTENTS

I. Introduction	2	A. Quantizing the smooth ReLU (softplus) activation function	13
A. Background and motivation	2	B. Quantizing the sigmoid linear unit (swish) activation function	14
B. Canonical quantization of neurons	3	IV. Quantizing Gaussian activation functions	15
C. Summary of contributions	3	A. Gaussian error function (erf) activation observable	15
D. Paper organization	4	B. Gaussian-smoothed ReLU activation observable	16
II. Fermi–Dirac machines as quantizations of neurons	6	C. Gaussian error linear unit activation observable	17
A. Quantizing second-order neurons	6	D. Discussion	17
B. Fermi–Dirac objective function and its gradient	7	V. Generalization to continuous quantum variables	17
C. Hybrid quantum–classical algorithms for estimating the Fermi–Dirac objective function and its gradient	8	A. Canonical quantization of continuous neurons	17
D. Quantum algorithm for simulating the firing of a Fermi–Dirac neuron	9	B. Training and testing	18
E. Training Fermi–Dirac machines for binary classification and function approximation	10	VI. Numerical experiments	19
1. Squared-loss minimization	11	A. Data generation	19
2. Logistic-loss minimization	11	B. Models	19
3. Fermi–Dirac machines as collective measurements	13	C. Training protocol	21
III. Quantizing the rectified linear unit	13	D. Results	21
		1. Squared-loss minimization	21
		2. Logistic-loss minimization	21

E. Discussion	22	1. Proof of Theorem 8 (derivative of sigmoid linear unit function)	55
VII. Proposals for canonical quantizations of neural networks	24	2. Hybrid quantum–classical algorithms for SiLU	58
A. Review of classical neural networks	24	a. Hybrid quantum–classical algorithm for estimating gradient of SiLU	58
B. Quantum observable networks	24	b. Hybrid quantum–classical algorithm for estimating SiLU	59
C. Hybrid quantum–classical neural networks	25	3. Proof of Theorem 9 (expected value of quantum convolution and multiplication algorithm)	61
VIII. Complexity-theoretic evidence against classical simulation	26	4. Proof of Theorem 10 (correctness of Algorithm 7 for SiLU)	63
IX. Connections with quantum Boltzmann machines	26	F. Derivations for quantizing Gaussian activation functions	65
X. Lagniappe: Hybrid quantum–classical algorithm for estimating cross entropy and log-partition function	27	1. Proof of Equation (90)	65
XI. Conclusion	28	2. Gradient of expectation of Gaussian error function activation observable	66
Acknowledgments	29	3. Proof of Equation (94)	68
References	29	4. Derivative of Gaussian smoothed rectified linear unit (GReLU)	69
A. Derivations for Fermi–Dirac machines	33	5. Derivative of Gaussian error linear unit (GeLU)	72
1. Proof of Theorem 1 (derivation of gradient)	33	G. Gradient formulas for quantum observable networks	75
2. Proof of Theorem 2 (derivation of formula for the objective function)	35	1. Two-layer gradient formulas	76
3. Proof of Theorem 3 (expected value of quantum convolution algorithm)	37	2. Three-layer gradient formulas	78
4. Proof of Theorem 4 and Equation (41)	39	3. L -layer gradient formulas	80
B. Squared-loss minimization for function approximation	39	H. Proof of Theorem 11 (complexity theoretic-evidence against classical simulation)	81
C. Logistic-loss function for binary classification	41	I. Derivations for cross entropy and log partition function estimation	84
1. Derivative of matrix logistic-loss function	41	1. Proof of Theorem 12 (derivation of formula for cross entropy)	84
2. Hybrid quantum–classical algorithm for estimating derivative of matrix logistic-loss function	45	2. Hybrid quantum–classical algorithm for cross entropy and log partition function estimation	86
3. Alternative formula for logistic-loss function	45		
4. Hybrid quantum–classical algorithm for estimating logistic-loss function	48		
D. Derivations for smooth rectified linear unit (ReLU)	50		
1. Proof of Theorem 6 (derivative of smooth ReLU function)	50		
2. Hybrid quantum–classical algorithms for smooth ReLU	50		
a. Hybrid quantum–classical algorithm for estimating gradient of smooth ReLU	50		
b. Hybrid quantum–classical algorithm for estimating smooth ReLU	51		
3. Proof of Theorem 7 (correctness of Algorithm 5 for smooth ReLU)	53		
E. Derivations for sigmoid linear unit (SiLU)	55		

I. INTRODUCTION

A. Background and motivation

A key goal of quantum information science is to understand the differences between the classical and quantum theories of information, with effects like superposition, entanglement, and quantum uncertainty not being present in the classical theory, while enabling technological capabilities well beyond that of classical information processing systems [1, 2]. These differences have been explored extensively in the context of quantum computation [3], communication [4], and sensing [5], and more recently there has been a growing effort

to understand the differences between classical and quantum machine learning [6] and optimization [7].

In a recent paper [8], Fermi–Dirac machines were proposed as a method for solving semidefinite optimization problems involving quantum measurements, and they were proven to be optimal for Fermi–Dirac entropic regularizations of this task. Furthermore, hybrid quantum–classical algorithms were proposed for solving these measurement optimization problems, thus leading to a novel method for performing optimization on quantum computers that appears to resist efficient classical simulation. To review this concept briefly, let $J \in \mathbb{N}$, let (H_1, \dots, H_J) be a tuple of Hamiltonians, let $(\theta_1, \dots, \theta_J)$ be a parameter vector, and let $T > 0$ be a temperature. An important constituent of a Fermi–Dirac machine is the following measurement operator:

$$f_T(H(\theta)) := \left(e^{-H(\theta)/T} + I \right)^{-1}, \quad (1)$$

which is realized by applying the Fermi–Dirac function

$$f_T(x) := \left(e^{-x/T} + 1 \right)^{-1}, \quad (2)$$

also known as the sigmoid or logistic function [9], to the following parameterized Hamiltonian:

$$H(\theta) := \sum_{j=1}^J \theta_j H_j. \quad (3)$$

One can then evaluate the expectation of this Fermi–Dirac observable with respect to a quantum state ρ , leading to the expected value $\text{Tr}[f_T(H(\theta))\rho]$.

B. Canonical quantization of neurons

In this paper, we show how Fermi–Dirac machines admit a natural interpretation as quantizations of classical neurons, leading to a novel approach distinct from prior proposals, which we call *Fermi–Dirac neurons* [10–20]. Throughout our paper, we use the terms Fermi–Dirac machine and Fermi–Dirac neuron interchangeably. We also quantize well known neurons like the smooth rectified linear unit [21, 22] and the sigmoid linear unit [23, 24], both of which have played a key role in deep learning applications.

To gain an initial sense of our approach, recall the following basic model for a neuron [25, 26]:

$$\varphi(w^T z + b), \quad (4)$$

where $\varphi: \mathbb{R} \mapsto \mathbb{R}$ is a nonlinear activation function, $w \in \mathbb{R}^n$ is a weight vector, $z := (z_1, \dots, z_n) \in \{-1, 1\}^n$ is a vector of input spin variables, $b \in \mathbb{R}$ is a bias, and $w^T z$ is the standard inner product. The scalar function input to φ can be written as follows:

$$w^T z + b = \sum_{i=1}^n w_i z_i + b, \quad (5)$$

and thus understood as a classical noninteracting Hamiltonian over the spin variables in z .

Following the standard first quantization procedure (also known as canonical quantization) [27], we quantize the model in (4) by promoting the i th classical spin variable to a Pauli- Z observable $\sigma_Z^{(i)}$, representing the i th quantum spin in a quantum spin model. As such, the scalar function in (5) is promoted to the following parameterized Hamiltonian acting on the Hilbert space of n qubits:

$$H_C(\theta) := \sum_{i=1}^n w_i \sigma_Z^{(i)} + b I^{\otimes n}, \quad (6)$$

where $\theta := (w, b)$ and $\sigma_Z^{(i)}$ acts on the i th spin.

By the functional calculus, $\varphi(H_C(\theta))$ is itself an observable, which is a function of the observable $H_C(\theta)$. We refer to $\varphi(H_C(\theta))$ as an *activation observable* and note that its expectation can be evaluated with respect to an arbitrary input state ρ . In this case, since the Hamiltonian in (6) is classical (i.e., every term in (6) commutes), the expectation $\text{Tr}[\varphi(H_C(\theta))\rho]$ simplifies as follows:

$$\text{Tr}[\varphi(H_C(\theta))\rho] = \sum_{z \in \{-1, 1\}^n} p(z) \varphi(w^T z + b), \quad (7)$$

where $p(z) := \langle z | \rho | z \rangle$ is a probability distribution, with $|z\rangle \equiv |z_1\rangle \otimes \dots \otimes |z_n\rangle$ and $|z_i\rangle$ a ± 1 -eigenstate of $\sigma_Z^{(i)}$.

As such, in this case, the expectation $\text{Tr}[\varphi(H_C(\theta))\rho]$ reduces to that of a classical neuron; indeed, this is the same expected value that results from picking z according to the probability distribution $p(z)$ and sending the value z through the classical neuron in (4). Thus, crucially, we immediately see how our quantization $\varphi(H_C(\theta))$ reduces to a classical neuron for a classical Hamiltonian of the form in (6). Indeed, by applying the functional calculus, we find in this case that

$$\varphi(H_C(\theta)) = \sum_{z \in \{-1, 1\}^n} \varphi(w^T z + b) |z\rangle \langle z|. \quad (8)$$

C. Summary of contributions

In our paper, we generalize the approach outlined in Section IB to an arbitrary parameterized quantum Hamiltonian $H_Q(\theta)$, while also allowing for second-order interactions between the quantum spins. We also quantize a number of activation functions that have played a prominent role in deep learning. See Figure 1 for a depiction of this conceptual contribution of our paper. For example, we can set

$$H_Q(\theta) := \sum_{\alpha, \beta \in \{x, y, z\}} \sum_{i, j=1}^n \Omega_{(\alpha, i), (\beta, j)} \sigma_\alpha^{(i)} \otimes \sigma_\beta^{(j)}$$

$$+ \sum_{\alpha \in \{x,y,z\}} \sum_{i=1}^n \omega_{\alpha,i} \sigma_{\alpha}^{(i)} + bI^{\otimes n}, \quad (9)$$

where $\theta := (\Omega, \omega, b)$, $\Omega \in \mathbb{R}^{3n \times 3n}$, $\omega \in \mathbb{R}^{3n}$, and the interacting and noninteracting terms include all Pauli- X , Y , and Z observables indexed by x , y , and z . Particular examples of (9) include the transverse-field Ising model [28, Chapter 5] and Heisenberg model [29, 30] with tunable parameters.

We then construct the activation observable $\varphi(H_Q(\theta))$, where φ is a nonlinear activation function as before. The result is a quantum machine learning model that can be used for binary classification or function approximation, generalizing how single neurons can be employed for such tasks in the classical case [25, 26]. We show how both the objective function $\theta \mapsto \text{Tr}[\varphi(H_Q(\theta))\rho]$ and its gradient can be efficiently estimated by hybrid quantum-classical algorithms for various choices of φ , thus enabling efficient evaluation and training of our quantized neurons. The training algorithms involve random classical sampling, Hamiltonian simulation [33–35], and the Hadamard test [36], thus bearing a similarity to those recently proposed for training quantum Boltzmann machines [37–40]; we remark later on the duality between Fermi-Dirac and quantum Boltzmann machines. We also develop quantum algorithms for single-shot evaluation of $\text{Tr}[\varphi(H_Q(\theta))\rho]$, which rely on algorithms that we refer to as quantum convolution and multiplication and in turn build on quantum algorithms known as the power of one qumode [41] and Schrödingerization [42–44]. Table I provides a brief summary of all of the algorithms introduced in our paper.

Other contributions of our paper are as follows. We perform small-scale numerical experiments to support the case that classical neurons cannot simulate our quantized neurons. We also generalize the whole framework by quantizing neurons that have continuous inputs, by means of continuous quantum variables [45], and we outline two different ways of composing our quantized neurons to realize canonical quantizations of neural networks. Finally, with the goal of providing complexity-theoretic evidence that Fermi-Dirac machines cannot be simulated classically, we define a computational decision problem based on them and prove that it is BQP-complete, meaning that this problem can be solved efficiently using a quantum computer and every decision problem efficiently solvable by a quantum computer can be efficiently reduced to this problem.

D. Paper organization

The rest of our paper is organized as follows. In Section II, we extend the development in Section IB, by showing how to quantize second-order neurons and, more generally, by developing quantized neurons that involve arbitrary parameterized Hamiltonians (Section IIA).

Focusing specifically on Fermi-Dirac machines in Section IIB, we establish formulas for the Fermi-Dirac objective function (Theorem 2) and its gradient (Theorem 1) that are amenable to efficient estimation by means of hybrid quantum-classical algorithms. We provide detailed specifications of these algorithms in Section IIC. In applications, it is important to have an algorithm that simulates the firing of a Fermi-Dirac neuron, and we develop such an algorithm (Algorithm 4) in Section IID, which is based on a more general quantum convolution algorithm (Algorithm 3) that may be of independent interest. In Section IIE, we show how to train Fermi-Dirac neurons for binary classification and function approximation, by means of either squared-loss (Section IIE1) or logistic-loss (Section IIE2) minimization.

In Section III, we quantize neurons based on the rectified linear unit (ReLU), developing the basic models, formulas for the objective functions and gradient, and algorithms for estimating them. As mentioned previously in Section IB, ReLU-like activation functions are of particular interest, due to their usage in deep learning applications. In Section IIIA, we quantize neurons based on the smooth ReLU (also called softplus) activation function, and in Section IIIB, we quantize neurons based on the sigmoid linear unit (also called swish) activation function. Our algorithm for single-shot simulation of the sigmoid linear unit is based on a quantum convolution and multiplication algorithm (Algorithm 6), which may be of independent interest.

In Section IV, we modify all of the activation functions considered in Sections II and III to be based on the Gaussian probability density rather than the logistic probability density. This leads to activation functions called erf, Gaussian ReLU (GReLU), and Gaussian error linear unit (GeLU), which “gaussify” Fermi-Dirac, ReLU, and SiLU quantized neurons, respectively. A key practical advantage of this Gaussian approach is that the control qumode state used in Algorithms 4, 5, and 7 can be initialized to a bosonic Gaussian state, which is easier to prepare in experimental setups involving quantum-optical elements [46].

In Section V, we generalize the whole framework to continuous quantum variables, showing how to quantize neurons with continuous inputs (Section VA) and how to train and test them (Section VB). Interestingly, our hybrid quantum-classical algorithms developed for the finite-dimensional case apply nearly unchanged to the continuous-variable case.

Section VI showcases the results of numerical experiments, in which we trained and tested our quantized neurons for both binary classification and function approximation. The results reported here demonstrate, for the examples considered, that classical neurons cannot achieve the same performance as our quantized neurons do for these tasks, whenever the input data is quantum (i.e., non-orthogonal or entangled states). This indicates, consistent with prior findings

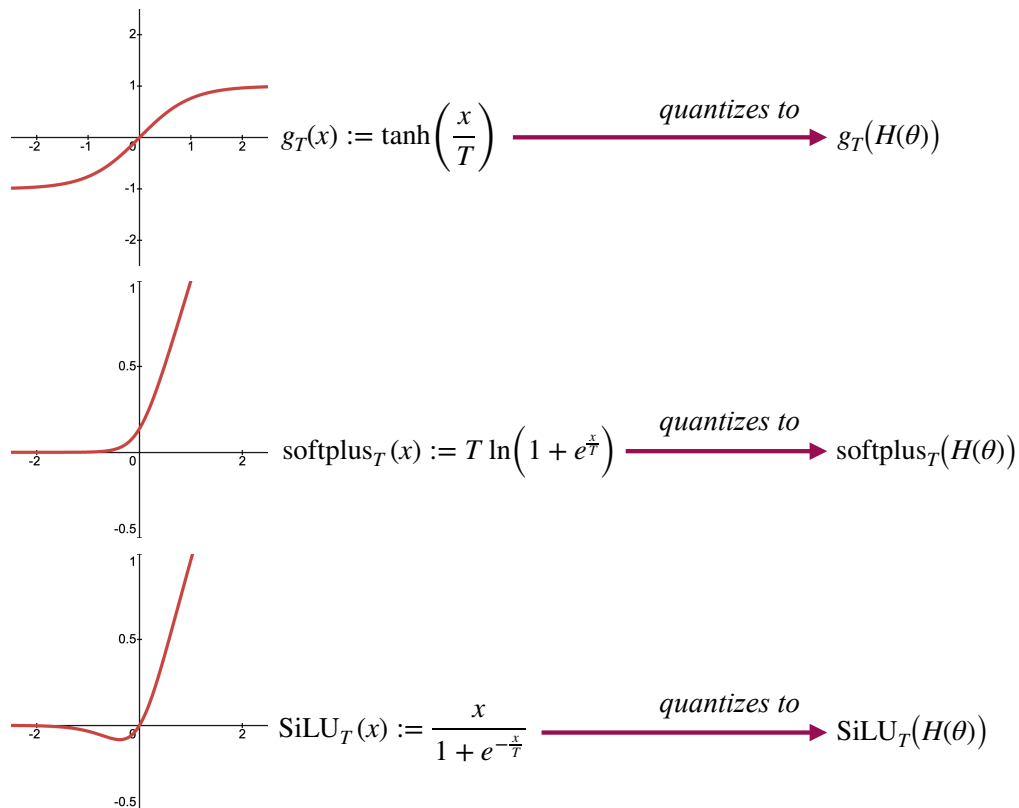


FIG. 1: This figure illustrates one of the main conceptual contributions of our paper. We quantize various common activation functions [31, 32], including hyperbolic tangent, softplus, and sigmoid linear unit (SiLU), by following the canonical quantization procedure established by the founders of quantum mechanics. Classically, an activation function $\varphi(x)$ acts on the output $x = w^T z + b$ of a classical energy function (Hamiltonian), where z is a vector input to the neuron. We replace the classical Hamiltonian with a parameterized quantum Hamiltonian $H(\theta) = \sum_j \theta_j H_j$ and subsequently apply an activation function to it, leading to an activation observable $\varphi(H(\theta))$. Some of our technical contributions include quantum algorithms for evaluating the expectation value $\text{Tr}[\varphi(H(\theta))\rho]$ and its gradient, where ρ is an input state and φ is one of the activation functions depicted.

in quantum machine learning (see, e.g., [6, Section III-B]), that our quantized neurons may demonstrate an advantage when processing quantum data. If the input data is classical in both training and testing, then our quantized neurons do not appear to provide better performance over classical neurons.

In Section VII, we provide two proposals for quantizing neural networks. In one approach, we replace every neuron in a neural network with a quantized neuron that takes in quantum states but outputs a classical variable. This allows for hybrid network, in which some of the neurons are quantized and others remain classical. This construction appears to be most effective when the first layer of a neural network consists of quantized neurons and accept quantum inputs, but neurons in other layers are classical. In another approach, we construct a quantum observable network, which consists of recursive application of activation functions and tunable weights to a parameterized Hamiltonian.

In Section VIII, we provide complexity-theoretic evidence that Fermi–Dirac neurons cannot be simulated

classically, by proving that a computational decision problem based on them is BQP-complete. Our result here relies on the guided local Hamiltonian problem [47], which is already known to be BQP-complete.

Section IX comments on connections between our quantized neurons and quantum Boltzmann machines, pinpointing a duality between these models, related to the duality between states and observables in quantum mechanics. Both approaches are Hamiltonian-based, highlighting their common foundation in fundamental quantum-physical principles.

In Section X, we show how our approach in Theorems 2, 14, and 15 and Algorithms 2, 12, and 14 can be repurposed for estimating cross entropy and the log-partition function, which are of independent interest and should find application in thermodynamics and quantum Boltzmann machine learning.

We finally conclude in Section XI by summarizing the main findings of our paper and outlining directions for future research.

Algorithm	Purpose / Output
Algorithm 1: Fermi–Dirac gradient estimation	Estimates the partial derivative $\frac{\partial}{\partial \theta_j} \text{Tr}[g_T(H(\theta))\rho]$.
Algorithm 2: Fermi–Dirac objective estimation	Estimates the expectation value $\text{Tr}[g_T(H(\theta))\rho]$.
Algorithm 3: Quantum convolution algorithm	Outputs a random variable with expected value $\text{Tr}[s(A)\rho]$, where $s = q * r$.
Algorithm 4: Fermi–Dirac neuron simulation	Simulates the activation observable $g_T(H(\theta))$ associated with a Fermi–Dirac neuron.
Algorithm 5: Smooth ReLU neuron simulation	Realizes the smooth ReLU activation observable $r_T(H(\theta))$.
Algorithm 6: Q. convolution & multiplication	Outputs a random variable with expectation value $\text{Tr}[s_1(At_1)s_2(At_2)\rho]$, where $s_i = q_i * r_i$, for $i \in \{1, 2\}$.
Algorithm 7: SiLU neuron simulation	Realizes the SiLU activation observable $\text{SiLU}_T(H(\theta))$.
Algorithm 8: Squared-loss gradient estimation	Estimates the partial derivative $\frac{\partial}{\partial \theta_j} \mathcal{L}^{(2)}(\theta)$ for the squared-loss objective.
Algorithm 9: Logistic-loss gradient estimation	Estimates the quantity ζ_j appearing in the gradient of the logistic-loss objective.
Algorithm 10: Logistic-loss objective estimation	Estimates the quantity ζ associated with the logistic-loss objective.
Algorithm 11: Smooth-ReLU gradient estimation	Estimates the quantity ζ_j appearing in the gradient of the smooth-ReLU objective.
Algorithm 12: Softplus objective estimation	Estimates the quantity ζ associated with the softplus objective function.
Algorithm 13: SiLU gradient estimation	Estimates the quantity ζ_j appearing in the gradient of the SiLU objective function.
Algorithm 14: SiLU objective estimation	Estimates the quantity ζ associated with the SiLU objective function.
Algorithm 15: Cross-entropy estimation	Estimates the cross entropy $\Xi(\eta \rho(\theta))$.

TABLE I: Summary of the hybrid quantum–classical algorithms introduced in this work.

II. FERMION–DIRAC MACHINES AS QUANTIZATIONS OF NEURONS

A. Quantizing second-order neurons

In Section IB, we already showed how to quantize neurons of the form in (4). Going beyond the model presented there, one can alternatively consider a second-order neuron [48–50], which involves quadratic interactions between the variables, via a weight matrix $W \in \mathbb{R}^{n \times n}$:

$$\varphi(z^T W z + w^T z + b), \quad (10)$$

where $z^T W z = \sum_{i,j=1}^n W_{ij} z_i z_j$. Thus, the scalar function input to φ can be written as follows:

$$z^T W z + w^T z + b = \sum_{i,j=1}^n W_{ij} z_i z_j + \sum_{i=1}^n w_i z_i + b, \quad (11)$$

and understood as a classical interaction Hamiltonian. Following the same approach as in Section IB, we quantize the model in (10)–(11) by promoting each classical spin variable to a Pauli-Z observable σ_Z . The scalar function in (11) is then promoted to a parameterized Hamiltonian of the following form:

$$H_C(\theta) := \sum_{i,j=1}^n W_{ij} \sigma_Z^{(i)} \otimes \sigma_Z^{(j)} + \sum_{i=1}^n w_i \sigma_Z^{(i)} + b I^{\otimes n}, \quad (12)$$

where $\theta := (W, w, b)$ and $\sigma_Z^{(i)}$ acts on the i th spin. Then $\varphi(H_C(\theta))$ is an activation observable, generalizing that

resulting from (6).

For the Hamiltonian in (12), all of the summands simultaneously commute, so that applying the functional calculus results in the following alternative expression for the activation observable $\varphi(H_C(\theta))$:

$$\varphi(H_C(\theta)) = \sum_{z \in \{-1,1\}^n} \varphi(z^T W z + w^T z + b) |z\rangle\langle z|. \quad (13)$$

This implies that quantization of the classical Hamiltonian in (11) does not produce any distinction between the quantum and classical cases. That is, evaluating the expectation of this observable when the system is in the classical state $|z\rangle\langle z|$ results in the value

$$\text{Tr}[\varphi(H_C(\theta)) |z\rangle\langle z|] = \varphi(z^T W z + w^T z + b). \quad (14)$$

Evaluating for a general quantum input state ρ results in the following expected value:

$$\text{Tr}[\varphi(H_C(\theta)) \rho] = \sum_{z \in \{-1,1\}^n} p(z) \varphi(z^T W z + w^T z + b), \quad (15)$$

where $p(z) := \langle z | \rho | z \rangle$.

We can realize models beyond the classical case by allowing Hamiltonians that include non-commuting terms. For example, we can set $H_Q(\theta)$ as in (9) and consider the activation observable $\varphi(H_Q(\theta))$, where φ is a nonlinear activation function as before. A key difference between the more general Hamiltonian $H_Q(\theta)$ in (9) and the classical Hamiltonian $H_C(\theta)$ in (12) is that it is no longer possible to find a simple diagonalization of

$\varphi(H_Q(\theta))$, given that the dependence of the spectrum and the eigenvectors of $H_Q(\theta)$ on θ is rather complex. However, in what follows, we show how hybrid quantum–classical algorithms can be used for efficient estimation of the expected value of $\varphi(H_Q(\theta))$ and its gradient, for certain choices of φ , thus enabling efficient evaluation and training. For this purpose, in what follows, for $J, n, k \in \mathbb{N}$, we consider a rather general parameterized Hamiltonian of the following form:

$$H(\theta) := \sum_{j=1}^J \theta_j H_j, \quad (16)$$

where $\theta_j \in \mathbb{R}$ for all $j \in [J] := \{1, \dots, J\}$ and H_j is a n -qubit Hamiltonian that acts nontrivially on k qubits, where k is a constant independent of n .

B. Fermi–Dirac objective function and its gradient

For a temperature $T > 0$ and a quantum state ρ , consider the following objective function:

$$\text{Tr}[g_T(H(\theta))\rho], \quad (17)$$

where

$$g_T(x) := \tanh\left(\frac{x}{T}\right) \quad (18)$$

and $H(\theta)$ is a parameterized Hamiltonian of the form in (16). This objective function and its gradient play an important role for training Fermi–Dirac machines for binary classification and function approximation, as detailed later in Section II E. The threshold realized by the hyperbolic tangent function becomes sharper as T decreases, and it converges to the sign function in the limit $T \rightarrow 0$. Also, note that

$$f_T(x) = \frac{1}{2} \left(1 + g_T\left(\frac{x}{2}\right)\right), \quad (19)$$

so that all of our results apply equally well to the Fermi–Dirac function $f_T(x) = (e^{-x/T} + 1)^{-1}$ defined in (2). However, as our paper focuses on spin variables taking values ± 1 , we find it more convenient to work with $g_T(x)$ instead of $f_T(x)$ and do so for the remainder of our paper. Owing to the simple relation in (19) between the Fermi–Dirac and hyperbolic tangent functions, we simply refer to quantized neurons based on $g_T(H(\theta))$ as Fermi–Dirac machines.

Our goal now is to find expressions for the gradient $\nabla_\theta \text{Tr}[g_T(H(\theta))\rho]$ and objective function $\text{Tr}[g_T(H(\theta))\rho]$ that are suitable for estimation on a quantum computer, assuming that we have sample access to the state ρ and the ability to perform Hamiltonian simulation according to $H(\theta)$. Under our assumption in (16) of a k -local Hamiltonian, standard techniques of Hamiltonian simulation are applicable [33–35].

We begin by establishing such a formula for the gradient $\nabla_\theta \text{Tr}[g_T(H(\theta))\rho]$, i.e., for each partial derivative. The expression given in Theorem 1 below follows from a novel formula for the derivative of the matrix hyperbolic tangent function, which is proven in Appendix A 1 and may be of independent interest.

Theorem 1. *Let $T > 0$ be a temperature, let $g_T(x)$ be defined as in (18), and let ρ be a quantum state. Then the following equality holds:*

$$\frac{\partial}{\partial \theta_j} \text{Tr}[g_T(H(\theta))\rho] = \frac{1}{T} \mathbb{E}_{t \sim \mu, s \sim v} \left[\Re \left[\text{Tr} \left[H_j e^{iH(\theta)t/T} \mathcal{U}_{st/T}^{H(\theta)}(\rho) \right] \right] \right], \quad (20)$$

where $\mu(t)$ is the following probability density function

$$\mu(t) := \frac{t}{2 \sinh\left(\frac{\pi t}{2}\right)}, \quad (21)$$

v is a uniform random variable over the unit interval $[0, 1]$, and $\mathcal{U}_t^{H(\theta)}$ is the following unitary quantum channel:

$$\mathcal{U}_t^{H(\theta)}(\cdot) := e^{-iH(\theta)t}(\cdot)e^{iH(\theta)t}. \quad (22)$$

Proof. See Appendix A 1. \square

Inspecting the formula in (20), we see that it is proportional to the expectation of an expression of the form $\Re[\text{Tr}[HU\sigma]]$, where H is a Hamiltonian, U is a unitary, and σ is state (to see this, set $H = H_j$, $U = e^{iH(\theta)t/T}$, and $\sigma = \mathcal{U}_{st/T}^{H(\theta)}(\rho)$). As such, we can employ random sampling, the Hadamard test, and Hamiltonian simulation to estimate this formula efficiently by means of a hybrid quantum–classical algorithm similar to those put forward in [37–39]. As T decreases (i.e., if we want a sharper threshold function), both the Hamiltonian simulation time increases and the sampling overhead does as well, the latter due to the prefactor $\frac{1}{T}$ in (20).

By employing Theorem 1 along with the fundamental theorem of calculus, we can express the objective function in (17) in terms of a telescoping sum representing integrals of its partial derivatives, leading to the following theorem:

Theorem 2. *Let $T > 0$ be a temperature, let $g_T(x)$ be as defined in (18), and let ρ be a quantum state. Then the following equality holds:*

$$\text{Tr}[g_T(H(\theta))\rho] = \frac{\|\theta\|_1}{T} \mathbb{E}_{\substack{j \sim q, \\ t \sim \mu, \\ s \sim v, \\ \lambda \sim v}} \left[\text{sgn}(\theta_j) \Re \left[\text{Tr} \left[H_j e^{iH(j,\lambda)t/T} \mathcal{U}_{st/T}^{H(j,\lambda)}(\rho) \right] \right] \right], \quad (23)$$

where $q(j)$ is the following probability distribution on $[J]$:

$$q(j) := \frac{|\theta_j|}{\|\theta\|_1}, \quad \|\theta\|_1 := \sum_{j=1}^J |\theta_j|, \quad (24)$$

μ is the probability density in (21), v is a uniform random variable over the unit interval $[0, 1]$, and

$$H(j, \lambda) \equiv H(\theta^{(j)}(\lambda)), \quad (25)$$

$$\theta^{(j)}(\lambda) := (0, \dots, 0, \lambda\theta_j, \theta_{j+1}, \dots, \theta_J), \quad (26)$$

$$H(\theta_1, \dots, \theta_J) \equiv H(\theta) = \sum_{j=1}^J \theta_j H_j. \quad (27)$$

Proof. See Appendix A 2. \square

Inspecting the formula in (23), it again is equal to the expectation of an expression of the form $\Re[\text{Tr}[HU\sigma]]$, so that the same aforementioned primitives can be used in a hybrid quantum–classical algorithm for estimating it.

C. Hybrid quantum–classical algorithms for estimating the Fermi–Dirac objective function and its gradient

Based on Theorems 1 and 2, here we delineate hybrid quantum–classical algorithms for estimating the gradient $\nabla_\theta \text{Tr}[g_T(H(\theta))\rho]$ and the objective function $\text{Tr}[g_T(H(\theta))\rho]$, which both make use of classical random sampling, Hamiltonian simulation, and the Hadamard test.

We begin with Algorithm 1 for estimating $\frac{\partial}{\partial\theta_j} \text{Tr}[g_T(H(\theta))\rho]$, which can be implemented for all $j \in [J]$ in order to estimate the gradient $\nabla_\theta \text{Tr}[g_T(H(\theta))\rho]$.

Algorithm 1. A hybrid quantum–classical algorithm for estimating the j th partial derivative $\frac{\partial}{\partial\theta_j} \text{Tr}[g_T(H(\theta))\rho]$ consists of the following steps:

1. Set $k \leftarrow 1$, and set

$$K \leftarrow O\left(\left(\frac{\|H_j\|}{T\varepsilon}\right)^2 \ln\left(\frac{1}{\delta}\right)\right), \quad (28)$$

where $\varepsilon > 0$ is the desired accuracy and $\delta \in (0, 1)$ is the desired failure probability.

2. Sample $t \sim \mu$ and $s \sim v$, where the probability densities μ and v are defined in Theorem 1.
3. Prepare the state $\mathcal{U}_{st/T}^{H(\theta)}(\rho)$ using one sample of ρ and Hamiltonian simulation to realize the unitary channel $\mathcal{U}_{st/T}^{H(\theta)}$.
4. Perform the quantum circuit depicted in Figure 2(a), with measurement outcomes $Z_k \in \{-1, 1\}$ for the σ_Z measurement and $X_k \in \text{spec}(H_j)$ for the H_j measurement. Set $Y_k \leftarrow \frac{1}{T} Z_k \cdot X_k$. Set $k \leftarrow k + 1$.
5. Repeat Steps 2–4 $K - 1$ more times. Compute the average $\bar{Y}_K := \frac{1}{K} \sum_{k=1}^K Y_k$ and output this value as an estimate of $\frac{\partial}{\partial\theta_j} \text{Tr}[g_T(H(\theta))\rho]$.

By the Hoeffding inequality [51] (e.g., in the form of [52, Theorem 1]) and Theorem 1, we are guaranteed that

$$\Pr\left[\left|\bar{Y}_K - \frac{\partial}{\partial\theta_j} \text{Tr}[g_T(H(\theta))\rho]\right| \leq \varepsilon\right] \geq 1 - \delta. \quad (29)$$

Algorithm 2 below provides a method for estimating the objective function $\text{Tr}[g_T(H(\theta))\rho]$, which makes use of the formula stated in Theorem 2.

Algorithm 2. A hybrid quantum–classical algorithm for estimating the objective function $\text{Tr}[g_T(H(\theta))\rho]$ consists of the following steps:

1. Set $k \leftarrow 1$, and set

$$K \leftarrow O\left(\left(\frac{\|\theta\|_1 \max_{j \in [J]} \|H_j\|}{T\varepsilon}\right)^2 \ln\left(\frac{1}{\delta}\right)\right), \quad (30)$$

where $\varepsilon > 0$ is the desired accuracy and $\delta \in (0, 1)$ is the desired failure probability.

2. Sample $j \sim q$, $t \sim \mu$, $s \sim v$, $\lambda \sim v$.
3. Prepare the state $\mathcal{U}_{st/T}^{H(\theta^{(j)}(\lambda))}(\rho)$ using one sample of ρ and Hamiltonian simulation to realize the unitary channel $\mathcal{U}_{st/T}^{H(\theta^{(j)}(\lambda))}$.
4. Perform the quantum circuit depicted in Figure 2(b), with measurement outcomes $Z_k \in \{-1, 1\}$ for the σ_Z measurement and $X_k \in \text{spec}(H_j)$ for the H_j measurement. Set $W_k \leftarrow \frac{\|\theta\|_1}{T} \cdot \text{sgn}(\theta_j) Z_k \cdot X_k$. Set $k \leftarrow k + 1$.
5. Repeat Steps 2–4 $K - 1$ more times. Compute the average $\bar{W}_K := \frac{1}{K} \sum_{k=1}^K W_k$ and output this value as an estimate of $\text{Tr}[g_T(H(\theta))\rho]$.

By the Hoeffding inequality, we are guaranteed that

$$\Pr\left[\left|\bar{W}_K - \text{Tr}[g_T(H(\theta))\rho]\right| \leq \varepsilon\right] \geq 1 - \delta. \quad (31)$$

Figure 2 depicts the quantum circuits used in Algorithms 1 and 2.

Let us note here that the objective function $\text{Tr}[g_T(H(\theta))\rho]$ can alternatively be estimated by means of frameworks like quantum singular value transformation [53] or Schrödingerization [42–44], which require more a complex quantum control operation in order to be realized. However, what Algorithm 2 demonstrates is that it is possible to eliminate this controlled-operation logic and instead perform a combination of classical random sampling, Hamiltonian simulation, and the Hadamard test in order to estimate $\text{Tr}[g_T(H(\theta))\rho]$. Regardless, in the next section, we show how to estimate $\text{Tr}[g_T(H(\theta))\rho]$ by means of a generalization of Schrödingerization, which we call a quantum convolution algorithm (Algorithm 3), as doing so can be useful for simulating the firing of a Fermi–Dirac neuron.

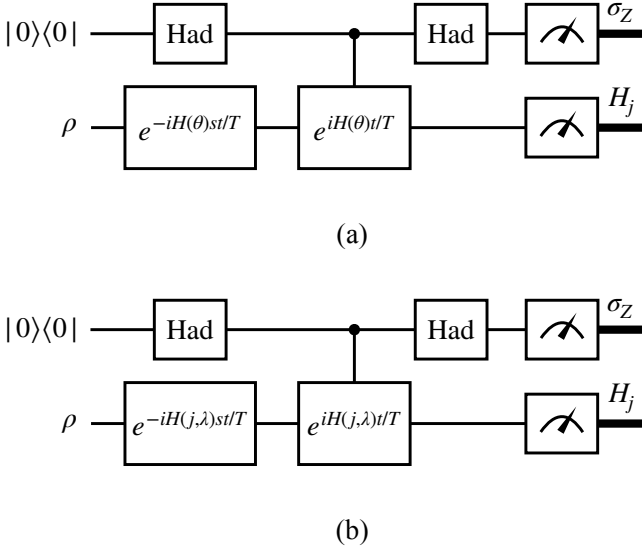


FIG. 2: (a) Quantum circuit used in Algorithm 1 for estimating the j th partial derivative $\frac{\partial}{\partial \theta_j} \text{Tr}[g_T(H(\theta))\rho]$. (b) Quantum circuit used in Algorithm 2 for estimating the objective function $\text{Tr}[g_T(H(\theta))\rho]$. The notation $H(j, \lambda)$ is defined in Theorem 2. Both circuits involve classical random sampling, Hamiltonian simulation, and the Hadamard test. “Had” denotes a single-qubit Hadamard gate.

D. Quantum algorithm for simulating the firing of a Fermi–Dirac neuron

In various applications, it is important to have a method that simulates the firing of a Fermi–Dirac neuron, i.e., when just a single sample of ρ is available. For this purpose, we develop a general quantum convolution algorithm that outputs a random variable with expected value $\text{Tr}[s(A)\rho]$, where s is equal to the convolution of an even probability density function q and another function r , the Hermitian operator A is a Hamiltonian, and ρ is an input state. This algorithm is a generalization of [8, Algorithm 19] and relies on quantum algorithmic primitives known as the power of one qumode [41] and Schrödingerization [42–44]. It may find application beyond our purposes here.

Algorithm 3 (Quantum convolution algorithm). *Let $q: \mathbb{R} \rightarrow [0, 1]$ be an even probability density function, let $r: \mathbb{R} \rightarrow \mathbb{R}$ be a measurable function such that the convolution $s = q * r$ is well defined, and let A be a Hamiltonian. The algorithm for outputting a random variable with expected value $\text{Tr}[s(A)\rho]$ proceeds as follows:*

1. Prepare a control qumode register in the state $|q\rangle\langle q|$, where

$$|q\rangle := \int_{-\infty}^{\infty} dp \sqrt{q(p)} |p\rangle \quad (32)$$

and $\{|p\rangle\}_{p \in \mathbb{R}}$ denotes the momentum quadrature basis. Prepare a data register in the state ρ .

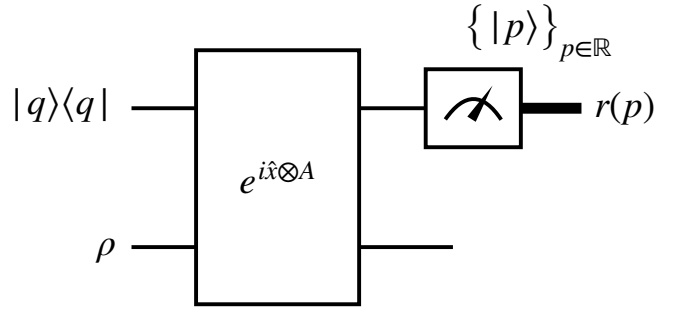


FIG. 3: Quantum circuit used in the quantum convolution algorithm (Algorithm 3). The state $|q\rangle\langle q|$ of the control qumode is defined in (32), and ρ is the input state on which we would like to perform the simulation. The measurement of the control qumode at the end is a momentum-quadrature measurement giving an outcome $p \in \mathbb{R}$. The algorithm finally outputs $r(p)$, and Theorem 3 guarantees that the expected value of the output is equal to $\text{Tr}[s(A)\rho]$, where $s = q * r$.

2. Apply the Hamiltonian evolution $e^{i\hat{x} \otimes A}$ on the control and data registers, where \hat{x} is the position quadrature operator.
3. Measure the control register in the momentum quadrature basis $\{|p\rangle\}_{p \in \mathbb{R}}$, obtaining outcome $p \in \mathbb{R}$.
4. Output $r(p)$.

Figure 3 depicts the quantum circuit used in Algorithm 3.

Theorem 3. *The expected value of the random variable output by Algorithm 3 is $\text{Tr}[s(A)\rho]$.*

Proof. See Appendix A 3. \square

We now show how to apply Algorithm 3 to simulate the firing of a Fermi–Dirac neuron. It follows from (2) and (19) that the hyperbolic tangent function g_T is related to the Fermi–Dirac function $f_{T/2}$ as follows:

$$g_T(x) = f_{T/2}(x) - (1 - f_{T/2}(x)), \quad (33)$$

which implies that

$$\begin{aligned} \text{Tr}[g_T(H(\theta))\rho] &= \\ \text{Tr}[f_{T/2}(H(\theta))\rho] - \text{Tr}[(I - f_{T/2}(H(\theta)))\rho]. \end{aligned} \quad (34)$$

Note that

$$0 \leq f_{T/2}(H(\theta)) \leq I, \quad (35)$$

so that $f_{T/2}(H(\theta))$ is a Fermi–Dirac thermal measurement operator and

$$(f_{T/2}(H(\theta)), I - f_{T/2}(H(\theta))) \quad (36)$$

is a Fermi–Dirac thermal measurement [8]. Thus, by performing the measurement in (36) on the state ρ ,

assigning the value $Z = +1$ if the outcome $f_{T/2}(H(\theta))$ occurs, and assigning the outcome $Z = -1$ if the outcome $I - f_{T/2}(H(\theta))$ occurs, we can simulate this Fermi–Dirac neuron using just a single sample of ρ . It follows from (34) that

$$\mathbb{E}[Z] = \text{Tr}[g_T(H(\theta))\rho]. \quad (37)$$

We make the following choices in Algorithm 3 to realize the outcome in (37). Set $T_1, T_2 > 0$ such that $T/2 = T_1 T_2$. Set q to be the logistic probability density function ℓ_{T_1} , where

$$\ell_{T_1}(p) := \frac{e^{p/T_1}}{T_1 (e^{p/T_1} + 1)^2} = \frac{1}{4T_1} \text{sech}^2\left(\frac{p}{2T_1}\right). \quad (38)$$

Set A to be $H(\theta)/T_2$. Set r to be the following linear combination of indicator functions:

$$r(p) = \mathbf{1}_{p \geq 0} - \mathbf{1}_{p < 0}. \quad (39)$$

For completeness, we now specialize Algorithm 3, so that it follows the choices in (38)–(39) and becomes an algorithm for simulating the firing of a Fermi–Dirac neuron using a single sample of ρ :

Algorithm 4. *The algorithm for simulating a Fermi–Dirac neuron described by the activation observable $g_T(H(\theta))$, where $T/2 = T_1 T_2$, proceeds as follows:*

1. For $T_1 > 0$, prepare a control qumode register in the state $|\ell_{T_1}\rangle\langle\ell_{T_1}|$, where

$$|\ell_{T_1}\rangle := \int_{-\infty}^{\infty} dp \sqrt{\ell_{T_1}(p)} |p\rangle, \quad (40)$$

and $\{|p\rangle\}_{p \in \mathbb{R}}$ denotes the momentum basis. Prepare a data register in the state ρ .

2. For $T_2 > 0$, apply the Hamiltonian evolution $e^{i\hat{x} \otimes H(\theta)/T_2}$ on the control and data registers, where \hat{x} is the position quadrature operator.
3. Measure the control register in the momentum basis $\{|p\rangle\}_{p \in \mathbb{R}}$, obtaining outcome $p \in \mathbb{R}$.
4. Output $Z = +1$ if $p \geq 0$ and $Z = -1$ if $p < 0$.

Theorem 4. *The expected value of the random variable output by Algorithm 4 is $\text{Tr}[g_T(H(\theta))\rho]$.*

Proof. The correctness of Algorithm 4 follows from Theorem 3 and because

$$(\ell_{T_1} * r)(p/T_2) = g_T(p), \quad (41)$$

for all $p \in \mathbb{R}$, with r set as in (39). We prove (41) in Appendix A 4. \square

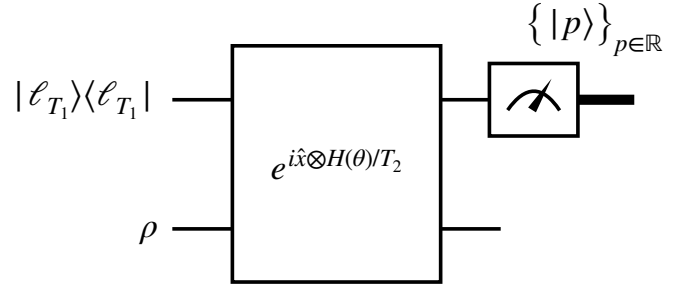


FIG. 4: Quantum circuit for simulating the firing of a Fermi–Dirac neuron using a single sample of the state ρ . The temperature $T/2 = T_1 T_2$, where $T_1, T_2 > 0$, as detailed in Algorithm 4. The state $|\ell_{T_1}\rangle\langle\ell_{T_1}|$ of the control qumode is defined in (40), and ρ is the input state on which we would like to perform the simulation. The measurement of the control qumode at the end is a momentum-quadrature measurement giving an outcome $p \in \mathbb{R}$. The algorithm finally outputs $+1$ if $p \geq 0$ and -1 otherwise.

Let us note that a sharper threshold function $g_T(p)$, with lower temperature $T > 0$, can be realized in two different ways, as discussed previously in [8, Section IV-A]. That is, Algorithm 4 contains two temperature parameters T_1 and T_2 , which allow for controlling the temperature (and thus sharpness) of the resulting Fermi–Dirac machine. In order to lower the temperature $T = T_1 T_2$ of the resulting Fermi–Dirac machine, one can choose to keep T_1 fixed while lowering T_2 , which amounts to increasing the time $t = 1/T_2$ needed for Hamiltonian evolution while keeping the input control state with fixed T_1 . This is the preferred approach, unless the coherence time of the controlled gate is smaller than $1/T_2$, such that T_2 cannot be further lowered. In cases where the coherence time of the Hamiltonian simulation cannot be increased further, one can keep T_2 fixed while lowering T_1 and instead using the input control state $|\ell_{T_1}\rangle$ with a smaller T_1 . Although $|\ell_{T_1}\rangle$ is not quite a squeezed bosonic Gaussian state of the form

$$|G_\sigma\rangle \equiv (1/(2\pi\sigma^2)^{1/4}) \int_{-\infty}^{\infty} e^{-p^2/(4\sigma^2)} |p\rangle dp, \quad (42)$$

(with squeezing $1/\sigma$ in the momentum quadrature), it can be very close to such a state. For example, with the choice $\sigma = \pi T_1/\sqrt{3}$, the quantum fidelity $\mathcal{F}(|\ell_{T_1}\rangle, |G_\sigma\rangle) \approx 0.9942$. Then decreasing T_1 means that the state is essentially more highly squeezed with respect to the momentum quadrature and requires more energy to prepare.

E. Training Fermi–Dirac machines for binary classification and function approximation

A key task for which Fermi–Dirac machines are useful is binary classification, similar to how perceptrons were originally proposed for this purpose [25]. More generally,

they can also be used for function approximation. In what follows, we focus on squared and logistic-loss functions, while noting that other quantum loss functions can be considered [54, 55].

1. Squared-loss minimization

For binary classification, we suppose that training data is available in the form of labeled quantum states, as

$$(\rho_1, y_1), \dots, (\rho_M, y_M), \quad (43)$$

where $M \in \mathbb{N}$, ρ_m is a quantum state, and $y_m \in \{-1, +1\}$ for all $m \in [M]$. For function approximation, we suppose instead that $y_m \in [-1, 1]$ for all $m \in [M]$.

Either way, for a model parameterized Hamiltonian $H(\theta)$ of the form in (16), we can employ a squared loss function of the following form:

$$\mathcal{L}^{(2)}(\theta) := \frac{1}{M} \sum_{m=1}^M (\text{Tr}[g_T(H(\theta))\rho_m] - y_m)^2, \quad (44)$$

with the goal of training being to tune the parameter vector θ in order to minimize $\mathcal{L}^{(2)}(\theta)$. In Appendix B, we show how $\mathcal{L}^{(2)}(\theta)$ can be expressed as follows:

$$\mathcal{L}^{(2)}(\theta) = \text{Tr}[\Delta^{(2)}(\theta, y)\bar{\rho}], \quad (45)$$

in terms of the following squared-loss observable:

$$\Delta^{(2)}(\theta, y) := \sum_{m=1}^M |m\rangle\langle m| \otimes (g_T(H(\theta)) - y_m I)^{\otimes 2} \quad (46)$$

and the labeled classical–quantum training state:

$$\bar{\rho} := \frac{1}{M} \sum_{m=1}^M |m\rangle\langle m| \otimes \rho_m^{\otimes 2}. \quad (47)$$

By a direct calculation, we find that

$$\begin{aligned} \frac{\partial}{\partial \theta_j} \mathcal{L}^{(2)}(\theta) &= \\ \frac{2}{M} \sum_{m=1}^M (\text{Tr}[g_T(H(\theta))\rho_m] - y_m) \frac{\partial}{\partial \theta_j} \text{Tr}[g_T(H(\theta))\rho_m], \end{aligned} \quad (48)$$

so that Algorithms 1 and 2 can be used for estimating $\frac{\partial}{\partial \theta_j} \mathcal{L}^{(2)}(\theta)$, by multiplying the corresponding estimates. The resulting estimator is a biased estimator, but it is consistent, so that it converges to $\frac{\partial}{\partial \theta_j} \mathcal{L}^{(2)}(\theta)$ if sufficiently many samples are available. If it is desired to have an unbiased estimator, the following expression for the partial derivative $\frac{\partial}{\partial \theta_j} \mathcal{L}^{(2)}(\theta)$ leads to an algorithm that lends well to sampling it in an unbiased way:

$$\begin{aligned} \frac{\partial}{\partial \theta_j} \mathcal{L}^{(2)}(\theta) &= \\ \frac{2}{M} \sum_{m=1}^M \text{Tr} \left[\left(\kappa(T, \theta, m) \otimes \frac{\partial}{\partial \theta_j} g_T(H(\theta)) \right) (\rho_m \otimes \rho_m) \right], \end{aligned} \quad (49)$$

where

$$\kappa(T, \theta, m) \equiv g_T(H(\theta)) - y_m I. \quad (50)$$

Appendix B provides a derivation of (49), an alternative formula for $\frac{\partial}{\partial \theta_j} \mathcal{L}^{(2)}(\theta)$ based on Theorems 1 and 2, and a hybrid quantum–classical algorithm for estimating $\frac{\partial}{\partial \theta_j} \mathcal{L}^{(2)}(\theta)$ in an unbiased way.

In order to train Fermi–Dirac machines for squared-loss minimization, we can employ the standard gradient descent algorithm with a learning rate $\eta > 0$. It updates the parameter vector θ according to the following rule for $p \in \mathbb{N}$:

$$\theta^{(p+1)} \leftarrow \theta^{(p)} - \eta \nabla_{\theta} \mathcal{L}^{(2)}(\theta) \Big|_{\theta=\theta^{(p)}}, \quad (51)$$

and iterates until convergence or a maximum number of iterations is reached.

2. Logistic-loss minimization

It is common to use a logistic-loss function when training a classical neuron for binary classification (see, e.g., [56]). Let us first review this concept in the classical case before moving on to the quantum case. Suppose that training data is available in the form of labeled vectors, as $(x_1, y_1), \dots, (x_M, y_M)$, where $M \in \mathbb{N}$, $x_m \in \mathbb{R}^n$, and $y_m \in \{-1, +1\}$ for all $m \in [M]$. Then the logistic-loss function is given by

$$\frac{1}{M} \sum_{m=1}^M T \ln \left(1 + e^{-y_m (w^T x_m + b)/T} \right), \quad (52)$$

where $T > 0$ controls the sharpness of the loss function and $\theta = (w, b)$, as in (4). Note that

$$\lim_{T \rightarrow 0} T \ln \left(1 + e^{-z/T} \right) = \max\{0, -z\}, \quad (53)$$

and that it is closely related to the fermionic free energy from [8, Proposition 5]. The idea behind the logistic-loss function is that there is a roughly linearly increasing penalty when the signs of y_m and $w^T x_m + b$ are mismatched (i.e., a misclassification is occurring), while there is little to no penalty if the signs match. One trains the model by minimizing the logistic-loss function by means of gradient descent, as in (51). After doing so, one can realize the function $x \mapsto f_T(w^T x + b)$ on a test data sample and then threshold this output to make a binary classification decision. Alternatively, one can

classify by outputting $+1$ with probability $f_T(w^T x + b)$ and -1 with probability $1 - f_T(w^T x + b)$.

Now suppose that training data is available in the form of labeled probability distributions

$$(p_1(x), y_1), \dots, (p_M(x), y_M), \quad (54)$$

where $M \in \mathbb{N}$, $x \in \mathbb{R}^n$ and $y_m \in \{-1, +1\}$ for all $m \in [M]$. The aforementioned deterministic case is recovered when each p_1, \dots, p_M is a degenerate probability distribution. The goal now is to use this training data in order to classify probability distributions. In this case, we can employ the following logistic-loss function:

$$\frac{1}{M} \sum_{m=1}^M \mathbb{E}_{x \sim p_m} \left[T \ln \left(1 + e^{-y_m (w^T x + b)/T} \right) \right]. \quad (55)$$

One can proceed with training by using (stochastic) gradient descent [57] on the above loss function, sampling from each probability distribution $p_m(x)$ in order to do so.

This latter case now motivates a generalization to the quantum case. Suppose that training data is available in the form of labeled quantum states, as in (43). Then, for a parameterized Hamiltonian $H(\theta)$, the logistic-loss function for this case is as follows:

$$\mathcal{L}_T^{\log}(\theta) := \frac{1}{M} \sum_{m=1}^M T \text{Tr} \left[\ln \left(I + e^{-y_m H(\theta)/T} \right) \rho_m \right]. \quad (56)$$

To have a sense of this loss function, observe that we have followed the canonical quantization procedure mentioned around (6), quantizing the energy function $w^T x + b$ in (55) by replacing it with a general parameterized Hamiltonian $H(\theta)$ and employing the following logistic-loss observable:

$$T \ln \left(I + e^{-y_m H(\theta)/T} \right). \quad (57)$$

Furthermore, consider that the Hamiltonian $H(\theta)$ can be written in terms of its spectral decomposition as

$$H(\theta) = \sum_k E_k^\theta \Pi_k^\theta, \quad (58)$$

where E_k^θ is an eigenvalue and Π_k^θ is a spectral projection. Applying the functional calculus, the following equality holds:

$$\mathcal{L}_T^{\log}(\theta) = \frac{1}{M} \sum_{m=1}^M \sum_k q_m^\theta(k) T \ln \left(1 + e^{-y_m E_k^\theta/T} \right), \quad (59)$$

where $q_m^\theta(k) := \text{Tr}[\Pi_k^\theta \rho_m]$ is a probability distribution. Thus, the classical logistic-loss function in (55) is nearly recovered when doing so, with a key difference being that the probability distribution $q_m^\theta(k)$ has a nontrivial dependence on θ .

Similar to what we did for the squared-loss function in (45), we can also rewrite the logistic-loss function $\mathcal{L}_T^{\log}(\theta)$ as follows:

$$\mathcal{L}_T^{\log}(\theta) = \text{Tr}[\Delta^{\log}(\theta, y) \bar{\rho}], \quad (60)$$

in terms of the following labeled logistic-loss observable

$$\Delta^{\log}(\theta, y) := \sum_{m=1}^M |m\rangle\langle m| \otimes T \ln \left(I + e^{-y_m H(\theta)/T} \right), \quad (61)$$

and the labeled classical-quantum training state:

$$\bar{\rho} := \frac{1}{M} \sum_{m=1}^M |m\rangle\langle m| \otimes \rho_m. \quad (62)$$

Theorem 5 below states an expression for the partial derivative $\frac{\partial}{\partial \theta_j} \mathcal{L}_T^{\log}(\theta)$, which lends well to sampling it in an unbiased way.

Theorem 5. *The following equality holds:*

$$\begin{aligned} \frac{\partial}{\partial \theta_j} \left(T \text{Tr} \left[\ln \left(I + e^{-y_m H(\theta)/T} \right) \rho_m \right] \right) \\ = -\frac{y_m}{2} \text{Tr}[H_j \rho_m] + \\ \frac{1}{2T} \|\theta\|_1 \mathbb{E}_{\substack{s \sim v, \\ k \sim q, \\ t \sim \gamma}} \left[s \Re \left[\text{Tr} \left[\text{sgn}(\theta_k) H_k H_j e^{iy_m H(\theta)t/T} \rho'_m \right] \right] \right], \end{aligned} \quad (63)$$

where

$$\rho'_m \equiv \mathcal{U}_{st/T}^{y_m H(\theta)}(\rho_m), \quad (64)$$

$y_m \in \{-1, +1\}$, $H(\theta)$ is a parameterized Hamiltonian of the form in (16), $T > 0$, $\gamma(t)$ is the following high-peak tent probability density function [37]:

$$\gamma(t) := \frac{2}{\pi} \ln \left| \coth \left(\frac{\pi t}{2} \right) \right|, \quad (65)$$

v is a uniform random variable on the unit interval $[0, 1]$, $q(k) := \frac{|\theta_k|}{\|\theta\|_1}$ is a probability distribution, and $\mathcal{U}_t^{y_m H(\theta)}$ is the following unitary quantum channel:

$$\mathcal{U}_t^{y_m H(\theta)}(\cdot) := e^{-iy_m H(\theta)t}(\cdot)e^{iy_m H(\theta)t}. \quad (66)$$

Appendix C provides a proof of Theorem 5 and develops Algorithm 9, a hybrid quantum-classical algorithm for estimating the partial derivative $\frac{\partial}{\partial \theta_j} \mathcal{L}_T^{\log}(\theta)$. In order to train this model, we can employ the standard gradient descent algorithm with a learning rate $\eta > 0$, as in (51), but using the gradient of $\mathcal{L}_T^{\log}(\theta)$ instead of that of $\mathcal{L}^{(2)}(\theta)$.

3. Fermi–Dirac machines as collective measurements

As observed in [8], we remark here that Fermi–Dirac machines, in general, realize collective measurements (also called joint measurements), meaning that they cannot be realized by performing individual measurements on each qubit, followed by post-processing, or by adaptive local measurements (see, e.g., [58]). It is well known in quantum information theory that one can have a higher performance in identifying classical messages encoded into non-orthogonal quantum states by performing collective measurements, with examples occurring in quantum optical communication [59] and qubit communication [60, 61].

Thus, this is the kind of scenario for which we expect Fermi–Dirac machines to offer an improvement in binary classification. That is, when the training data consists of non-classical states (i.e., non-orthogonal or entangled), these prior results from quantum information theory suggest that Fermi–Dirac machines should outperform classical neurons for this task, given that the measurements realized by the latter are not collective. We indeed find that Fermi–Dirac machines outperform classical neurons in the small-scale numerical simulations reported in Section VI, while we leave it open to establish theoretical evidence supporting this claim.

III. QUANTIZING THE RECTIFIED LINEAR UNIT

In this section, we quantize the rectified linear unit (ReLU) in two different ways, leading to the smooth ReLU and sigmoid linear unit (SiLU) activation observables.

ReLU is an activation function used in deep neural networks [62, 63]. Its adoption has been shown to improve optimization and alleviate the vanishing-gradient problem that can arise during training [22]. The ReLU activation function is defined as

$$\text{ReLU}(y) := y_+ := \max\{0, y\} = \begin{cases} y & : y > 0 \\ 0 & : y \leq 0 \end{cases}, \quad (67)$$

providing a simple piecewise-linear nonlinearity. Although ReLU is not differentiable at $y = 0$, several smooth approximations have been introduced and are often found to improve gradient flow and empirical training performance in deep architectures [22–24].

A. Quantizing the smooth ReLU (softplus) activation function

One smooth approximation to ReLU is the smooth ReLU (or softplus) activation function [21, 22]:

$$r_T(y) := T \ln\left(1 + e^{y/T}\right), \quad (68)$$

where $T > 0$ is a temperature parameter controlling the smoothness of the approximation. In the zero-temperature limit,

$$\lim_{T \rightarrow 0} r_T(y) = \text{ReLU}(y) \quad \forall y \in \mathbb{R}, \quad (69)$$

so that r_T interpolates smoothly between a differentiable activation and the piecewise-linear ReLU function. Moreover, r_T is closely related to the logistic-loss function already analyzed in Section II E 2. Consequently, it is also closely related to the fermionic free energy objective function studied in [8, Proposition 5].

Given a parameterized Hamiltonian $H(\theta)$, we can quantize (67) and (68) by defining the following smooth ReLU observable:

$$r_T(H(\theta)). \quad (70)$$

Its expectation with respect to an arbitrary state ρ is $\text{Tr}[r_T(H(\theta))\rho]$. In order to employ ReLU observables in quantum machine learning, we should devise methods for estimating the objective function $\text{Tr}[r_T(H(\theta))\rho]$ and its gradient $\nabla_\theta \text{Tr}[r_T(H(\theta))\rho]$.

We begin with the following theorem, which states a formula for the j th partial derivative of $\text{Tr}[r_T(H(\theta))\rho]$.

Theorem 6. *The following equality holds:*

$$\begin{aligned} \frac{\partial}{\partial \theta_j} \text{Tr}[r_T(H(\theta))\rho] &= \frac{1}{2} \text{Tr}[H_j \rho] + \\ &\frac{\|\theta\|_1}{2T} \mathbb{E}_{\substack{s \sim v, \\ k \sim q, \\ t \sim \gamma}} \left[s \Re \left[\text{Tr} \left[\text{sgn}(\theta_k) H_k H_j e^{iH(\theta)t/T} \mathcal{U}_{st/T}^{H(\theta)}(\rho) \right] \right] \right]. \end{aligned} \quad (71)$$

where $H(\theta)$ is a parameterized Hamiltonian of the form in (16), $T > 0$, $\gamma(t)$ is the probability density function defined in (65), v is a uniform random variable on the unit interval $[0, 1]$, $q(k) := \frac{|\theta_k|}{\|\theta\|_1}$ is a probability distribution, and $\mathcal{U}_t^{H(\theta)}$ is the following unitary quantum channel:

$$\mathcal{U}_t^{H(\theta)}(\cdot) := e^{-iH(\theta)t}(\cdot)e^{iH(\theta)t}. \quad (72)$$

Proof. See Appendix D 1. \square

The formula in (71) is amenable to efficient estimation on a quantum computer. In Appendix D 2, we detail hybrid quantum–classical algorithms for estimating the gradient $\nabla_\theta \text{Tr}[r_T(H(\theta))\rho]$ and the objective function $\text{Tr}[r_T(H(\theta))\rho]$.

We can also realize the expected value of the smooth ReLU observable, using just one sample of the state ρ , by means of the following special case of Algorithm 3:

Algorithm 5. *The algorithm for realizing the smooth ReLU neuron, described by the activation observable $r_T(H(\theta))$, where $T = T_1 T_2$, proceeds as follows:*

1. For $T_1 > 0$, prepare a control qumode register in the state $|\ell_{T_1}\rangle\langle\ell_{T_1}|$, defined in (40). Prepare a data register in the state ρ .
2. For $T_2 > 0$, apply the Hamiltonian evolution $e^{i\hat{x}\otimes H(\theta)/T_2}$ on the control and data registers, where \hat{x} is the position quadrature operator.
3. Measure the control register in the momentum basis $\{|p\rangle\}_{p\in\mathbb{R}}$, obtaining outcome $p \in \mathbb{R}$.
4. Output $T_2 \text{ReLU}(p) = T_2 \max\{p, 0\}$.

Theorem 7. *The expected value of the random variable output by Algorithm 5 is $\text{Tr}[r_T(H(\theta))\rho]$.*

Proof. As a consequence of Theorem 3, it suffices to prove that

$$r_T(p) = T_2 (\text{ReLU} * \ell_{T_1}) \left(\frac{p}{T_2} \right), \quad (73)$$

for all $p \in \mathbb{R}$. See Appendix D 3 for a proof of (73). \square

B. Quantizing the sigmoid linear unit (swish) activation function

Another smooth approximation to ReLU is the sigmoid linear unit (SiLU), also known as the swish activation function. It is defined as [23, 24]

$$\text{SiLU}_T(x) := \frac{x}{1 + e^{-x/T}} = x f_T(x), \quad (74)$$

where the Fermi–Dirac function $f_T(x)$ is defined in (2). Unlike ReLU, the SiLU activation is smooth and mildly non-monotonic, combining a linear response for large positive inputs with sigmoid-based gating near the origin. These properties have been observed to improve gradient flow and empirical performance in deep neural networks relative to ReLU and related piecewise-linear activations [23, 24].

Given a parameterized Hamiltonian $H(\theta)$, we can quantize (67) and (74) by defining the following SiLU observable:

$$\text{SiLU}_T(H(\theta)). \quad (75)$$

Its expectation with respect to an arbitrary state ρ is $\text{Tr}[\text{SiLU}_T(H(\theta))\rho]$. In order to employ SiLU observables in quantum machine learning, we should devise methods for estimating the objective function $\text{Tr}[\text{SiLU}_T(H(\theta))\rho]$ and its gradient $\nabla_\theta \text{Tr}[\text{SiLU}_T(H(\theta))\rho]$.

We begin by establishing a formula for the j th partial derivative of $\text{Tr}[\text{SiLU}_T(H(\theta))\rho]$, which is amenable to efficient estimation on a quantum computer:

Theorem 8. *The following equality holds:*

$$\frac{\partial}{\partial \theta_j} \text{Tr}[\text{SiLU}_T(H(\theta))\rho] = \frac{1}{2} \text{Tr}[H_j \rho] +$$

$$\frac{\|\theta\|_1}{2T} \mathbb{E}_{\substack{t \sim \xi, \\ s \sim \nu, \\ k \sim q}} \left[s \Re \left[\text{Tr} \left[\text{sgn}(\theta_k) H_k H_j e^{iH(\theta)t/(2T)} \rho' \right] \right] \right], \quad (76)$$

where

$$\rho' \equiv \mathcal{U}_{st/(2T)}^{H(\theta)}(\rho), \quad (77)$$

the objective function $\text{Tr}[\text{SiLU}_T(H(\theta))\rho]$ is defined from (74), $\xi(t)$ is the following probability density function

$$\xi(t) := \frac{\gamma(t) + \mu(t)}{2}, \quad (78)$$

$\gamma(t)$ is defined in (65), $\mu(t)$ is defined in (21), ν is a uniform random variable on the unit interval $[0, 1]$, q is the following probability distribution:

$$q(k) := \frac{|\theta_k|}{\|\theta\|_1}, \quad (79)$$

and $\mathcal{U}_t^{H(\theta)}$ is the following unitary quantum channel:

$$\mathcal{U}_t^{H(\theta)}(\cdot) := e^{-iH(\theta)t}(\cdot)e^{iH(\theta)t}. \quad (80)$$

Proof. See Appendix E 1. \square

The formula in (76) is amenable to efficient estimation on a quantum computer. In Appendix E 2, we detail hybrid quantum–classical algorithms for estimating the gradient $\nabla_\theta \text{Tr}[\text{SiLU}_T(H(\theta))\rho]$ and the objective function $\text{Tr}[\text{SiLU}_T(H(\theta))\rho]$.

In order to evaluate SiLU_T using a single sample of the state ρ , we propose the following generalization of Algorithm 3:

Algorithm 6 (Quantum convolution and multiplication algorithm). *Let $q_1, q_2: \mathbb{R} \rightarrow [0, 1]$ be even probability density functions, let $r_1, r_2: \mathbb{R} \rightarrow \mathbb{R}$ be measurable functions such that the convolutions $s_1 = q_1 * r_1$ and $s_2 = q_2 * r_2$ are well defined, let A be a Hamiltonian, and let $t_1, t_2 \geq 0$. The algorithm for outputting a random variable with expected value $\text{Tr}[s_1(At_1)s_2(At_2)\rho]$ proceeds as follows:*

1. Prepare two control qumode registers in the state $|q_1\rangle\langle q_1| \otimes |q_2\rangle\langle q_2|$, where

$$|q_i\rangle := \int_{-\infty}^{\infty} dp \sqrt{q_i(p)} |p\rangle, \quad (81)$$

for $i \in \{1, 2\}$, and $\{|p\rangle\}_{p\in\mathbb{R}}$ denotes the momentum quadrature basis. Prepare a data register in the state ρ .

2. Apply the Hamiltonian evolution $e^{i\hat{x}\otimes At_1}$ on the first control register and the data register, where \hat{x} is the position quadrature operator, and apply the Hamiltonian evolution $e^{i\hat{x}\otimes At_2}$ on the second control register and the data register.

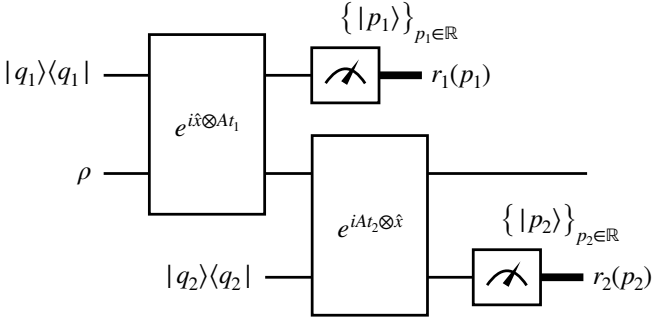


FIG. 5: Quantum circuit used in the quantum convolution and multiplication algorithm (Algorithm 6). The states $|q_1\rangle\langle q_1|$ and $|q_2\rangle\langle q_2|$ of the control qumodes are defined in (81), and ρ is the input state on which we would like to perform the simulation. The measurements of the control qumodes at the end are momentum-quadrature measurements, giving outcomes $p_1, p_2 \in \mathbb{R}$. The algorithm finally outputs $r_1(p_1)r_2(p_2)$, and Theorem 9 guarantees that the expected value of the output is equal to $\text{Tr}[s_1(At_1)s_2(At_2)\rho]$, where $s_i = q_i * r_i$, for $i \in \{1, 2\}$.

3. Measure the first and second control register in the momentum quadrature basis $\{|p\rangle\}_{p \in \mathbb{R}}$, obtaining outcomes $p_1 \in \mathbb{R}$ and $p_2 \in \mathbb{R}$.

4. Output $r_1(p_1)r_2(p_2)$.

See Figure 5 for a depiction of Algorithm 6.

Theorem 9. *The expected value of the random variable output by Algorithm 6 is $\text{Tr}[s_1(At_1)s_2(At_2)\rho]$.*

Proof. See Appendix E 3. \square

Remark 1. Algorithm 6 and Theorem 9 naturally generalize to the case of realizing the expected value $\text{Tr}[\prod_{i=1}^m s_i(At_i)\rho]$, where, for all $i \in [m]$, $q_i: \mathbb{R} \rightarrow [0, 1]$ is an even probability density function, $r_i: \mathbb{R} \rightarrow \mathbb{R}$ is a measurable function such that the convolution $s_i = q_i * r_i$ is well defined, and $t_i \geq 0$.

We can make the following choices in Algorithm 6 to realize the expected value $\text{Tr}[\text{SiLU}_T(H(\theta))\rho]$. Set $T_1, T_2 > 0$ such that $T = T_1 T_2$. Set

$$q_1(p) = \frac{e^{-p^2}}{\sqrt{\pi}}, \quad (82)$$

$$q_2 = \ell_{T_1}, \quad (83)$$

$$r_1(p_1) = p_1, \quad (84)$$

$$r_2(p_2) = \mathbf{1}_{p_2 \geq 0}. \quad (85)$$

Set $At_1 = H(\theta)$ and $At_2 = H(\theta)/T_2$. For completeness, we now specialize Algorithm 6, so that it becomes the following algorithm for realizing the SiLU neuron using a single sample of ρ :

Algorithm 7. *The algorithm for realizing the SiLU neuron, described by the activation observable $\text{SiLU}_T(H(\theta))$, where $T = T_1 T_2$, proceeds as follows:*

1. For $T_1 > 0$, prepare two control qumode registers in the state $|0\rangle\langle 0| \otimes |\ell_{T_1}\rangle\langle \ell_{T_1}|$, where $|0\rangle\langle 0|$ is the vacuum state and $|\ell_{T_1}\rangle\langle \ell_{T_1}|$ is defined in (38) and (40). Prepare a data register in the state ρ .
2. For $T_2 > 0$, apply the Hamiltonian evolution $e^{i\hat{x}\otimes H(\theta)}$ on the first control qumode register and the data register, and then apply the Hamiltonian evolution $e^{i\hat{x}\otimes H(\theta)/T_2}$ on the second control qumode register and the data register.
3. Measure the control registers in the momentum basis $\{|p\rangle\}_{p \in \mathbb{R}}$, obtaining outcomes $p_1, p_2 \in \mathbb{R}$.
4. Output $p_1 \mathbf{1}_{p_2 \geq 0}$.

Theorem 10. *The expected value of the random variable output by Algorithm 7 is $\text{Tr}[\text{SiLU}_T(H(\theta))\rho]$.*

Proof. See Appendix E 4. \square

IV. QUANTIZING GAUSSIAN ACTIVATION FUNCTIONS

In this section, we show how to quantize Gaussian activation functions, with the main idea being to replace the logistic probability density ℓ_T with the Gaussian probability density ϕ_T of mean zero and standard deviation $T > 0$, defined as

$$\phi_T(x) := \frac{1}{\sqrt{2\pi T}} \exp\left(-\frac{1}{2} \left(\frac{x}{T}\right)^2\right). \quad (86)$$

From a practical perspective, it is sensible to do so, given the ease with which experimentalists can prepare bosonic Gaussian states in the laboratory [46].

We consider Gaussian variants of Fermi–Dirac (Section II), smooth ReLU (Section III A), and SiLU (Section III B) neurons. See Figure 6 for a conceptual depiction of this section’s contribution. The result is an extension of Theorems 4, 7, and 10 and Algorithms 4, 5, and 7 to the Gaussian case. Throughout this section, we employ the standard Gaussian cumulative distribution, probability density function, and error function:

$$\Phi(x) := \frac{1}{\sqrt{2\pi}} \int_{-\infty}^x dy e^{-\frac{y^2}{2}}, \quad (87)$$

$$\phi(x) := \phi_{T=1}(x) = \frac{1}{\sqrt{2\pi}} \exp\left(-\frac{x^2}{2}\right), \quad (88)$$

$$\text{erf}(x) := \frac{2}{\sqrt{\pi}} \int_0^x dy e^{-y^2} = 2\Phi(\sqrt{2}x) - 1. \quad (89)$$

A. Gaussian error function (erf) activation observable

Let us begin by “gaussifying” Fermi–Dirac machines and the related Theorem 4 and Algorithm 4. There, the

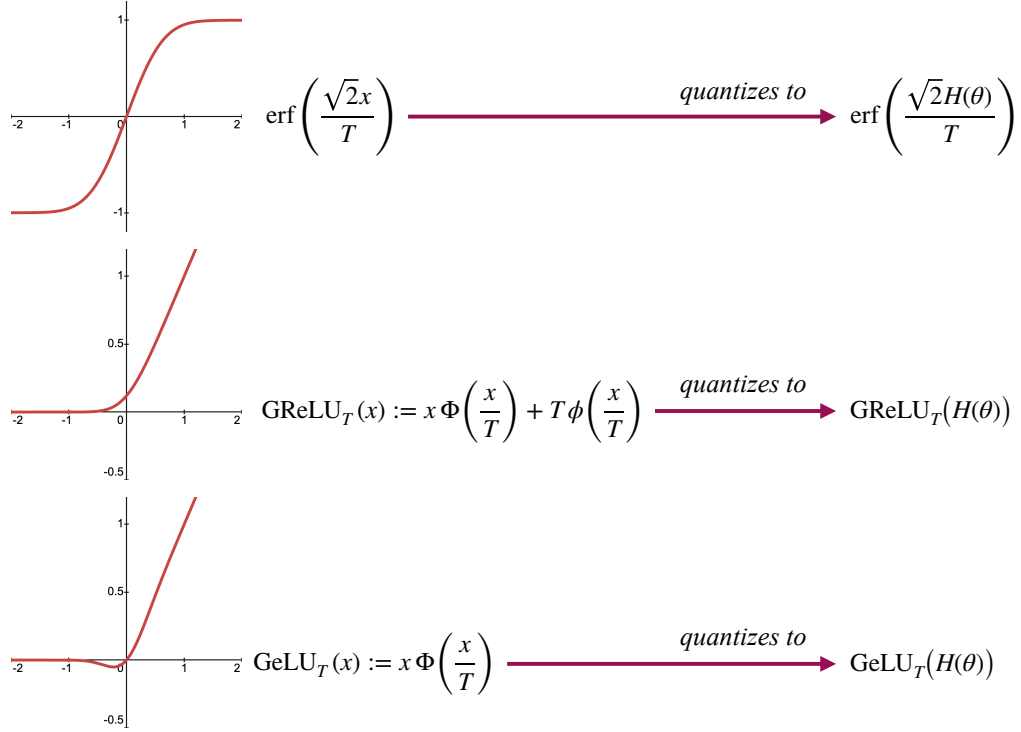


FIG. 6: This figure is similar to Figure 1, but instead showcasing the Gaussian activation functions that we quantize in Section IV, which include the Gaussian error function (erf), the Gaussian-smoothed rectified linear unit (GReLU), and the Gaussian error linear unit (GeLU).

key relation is the convolution identity in (41). If we replace ℓ_{T_1} therein with ϕ_{T_1} , we instead find that

$$(\phi_{T_1} * r)(p/T_2) = 2\Phi\left(\frac{2p}{T}\right) - 1 =: \operatorname{erf}\left(\frac{\sqrt{2}p}{T}\right), \quad (90)$$

for all $p \in \mathbb{R}$, with r set as in (39) and $T = T_1 T_2$. See Appendix F 1 for a proof of (90). Thus, the result is that the gaussified version of Algorithm 4 outputs a random variable with expected value

$$F_{\operatorname{erf}}(\theta) \equiv \operatorname{Tr}\left[\operatorname{erf}\left(\sqrt{2}H(\theta)/T\right)\rho\right]. \quad (91)$$

The error function erf can be viewed as a Gaussian approximation of the hyperbolic tangent function. For training such a neuron, we need the partial derivative $\frac{\partial}{\partial \theta_j} F_{\operatorname{erf}}(\theta)$, and employing the same proof as for Theorem 1, we find that $\mu(t)$ is replaced by a Gaussian probability density. Thus, Theorem 1 extends to the Gaussian case, as well as Algorithm 1 for estimating the partial derivative $\frac{\partial}{\partial \theta_j} F_{\operatorname{erf}}(\theta)$. See Appendix F 2 for details.

B. Gaussian-smoothed ReLU activation observable

Next we gaussify the smooth ReLU function, which we refer to as the Gaussian-smoothed ReLU (GReLU):

$$\operatorname{GReLU}_T(x) := x\Phi\left(\frac{x}{T}\right) + T\phi\left(\frac{x}{T}\right). \quad (92)$$

Note that the following identities hold:

$$\operatorname{GReLU}_T(x) = \mathbb{E}[\operatorname{ReLU}(x + TZ)] \quad (93)$$

$$= T_2(\operatorname{ReLU} * \phi_{T_1})\left(\frac{x}{T_2}\right), \quad (94)$$

where $Z \sim \mathcal{N}(0, 1)$ and $T = T_1 T_2$. Thus, GReLU arises by replacing the logistic function ℓ_{T_1} in (73) with ϕ_{T_1} in (86). See Appendix F 3 for a proof of (94). The result is that the gaussified version of Algorithm 5 outputs a random variable with expected value

$$F_{\operatorname{GReLU}_T}(\theta) \equiv \operatorname{Tr}[\operatorname{GReLU}_T(H(\theta))\rho]. \quad (95)$$

For training a GReLU neuron, we need the partial derivative $\frac{\partial}{\partial \theta_j} F_{\operatorname{GReLU}_T}(\theta)$, for which an expression is derived in Appendix F 4, making use of the following equality:

$$\frac{\partial}{\partial x} \operatorname{GReLU}_T(x) = \Phi\left(\frac{x}{T}\right). \quad (96)$$

Thus, Theorem 6 extends to the Gaussian case, as well as Algorithm 11 for estimating the partial derivative $\frac{\partial}{\partial \theta_j} F_{\operatorname{GReLU}_T}(\theta)$.

C. Gaussian error linear unit activation observable

Finally, we gaussify the sigmoid linear unit (SiLU) function, which becomes the Gaussian error linear unit (GeLU):

$$\text{GeLU}_T(x) := x\Phi\left(\frac{x}{T}\right). \quad (97)$$

The gaussified version of Algorithm 7 replaces ℓ_{T_1} with ϕ_{T_1} in the state of the control qumode. The resulting algorithm then outputs a random variable with expected value

$$F_{\text{GeLU}_T}(\theta) \equiv \text{Tr}[\text{GeLU}_T(H(\theta))\rho]. \quad (98)$$

For training such a neuron, we need the partial derivative $\frac{\partial}{\partial\theta_j} F_{\text{GeLU}_T}(\theta)$, for which an expression is derived in Appendix F 5, making use of the following equality:

$$\frac{\partial}{\partial x} \left[x\Phi\left(\frac{x}{T}\right) \right] = \frac{1}{2} + \frac{1}{2} \text{erf}\left(\frac{x}{\sqrt{2T}}\right) + \frac{x}{T}\phi\left(\frac{x}{T}\right). \quad (99)$$

Thus, Theorem 8 extends to the Gaussian case, as well as Algorithm 13 for estimating the partial derivative $\frac{\partial}{\partial\theta_j} F_{\text{GeLU}_T}(\theta)$.

D. Discussion

“Fully Gaussian” bosonic quantum computations involve the preparation of bosonic Gaussian states, evolutions according to bosonic Gaussian channels, and conclude with Gaussian measurements. Such protocols can be simulated efficiently classically [64] (see also [65]), so that one cannot expect any kind of advantage when using them. Our protocols outlined above prepare a control qumode in a bosonic Gaussian state and perform a Gaussian measurement (i.e., homodyne detection) on the control qumode. However, these protocols involve highly non-Gaussian evolutions, i.e., unitary interactions such as $e^{i\hat{x}\otimes H(\theta)t}$ or the Hadamard test, so that they fall outside the class of fully Gaussian protocols.

V. GENERALIZATION TO CONTINUOUS QUANTUM VARIABLES

In this section, we demonstrate that the whole formalism developed in previous sections extends to continuous quantum variables (see [45] for a review of this topic). In order to do so, we return to the classical second-order neuron model from (10), modify it to allow for continuous inputs, and then quantize this model.

A. Canonical quantization of continuous neurons

Let us now suppose that $x := (x_1, \dots, x_n) \in \mathbb{R}^n$ and the activation function for a classical second-order neuron

is as follows:

$$\varphi(x^T Wx + w^T x + b), \quad (100)$$

where $\varphi: \mathbb{R} \mapsto \mathbb{R}$, $W \in \mathbb{R}^{n \times n}$, $w \in \mathbb{R}^n$, and $b \in \mathbb{R}$. Noting that the input to φ is a classical Hamiltonian of the following form:

$$x^T Wx + w^T x + b = \sum_{i,j=1}^n W_{ij}x_i x_j + \sum_{i=1}^n w_i x_i + b, \quad (101)$$

we can quantize the model in (100) by employing the canonical position quadrature operators from quantum optics [45], leading to the following Hamiltonian:

$$H_C(\theta) := \sum_{i,j=1}^n W_{ij}\hat{x}_i \otimes \hat{x}_j + \sum_{i=1}^n w_i \hat{x}_i + bI^{\otimes n}, \quad (102)$$

which acts on n bosonic modes, with \hat{x}_i being a position quadrature operator acting on the i th bosonic mode. Then the activation observable in this case is

$$\varphi(H_C(\theta)). \quad (103)$$

Using the spectral representation of each position quadrature operator as $\hat{x}_i = \int_{\mathbb{R}} dx_i x_i |x_i\rangle\langle x_i|$, where $|x_i\rangle$ is a position quadrature eigenstate, and employing the functional calculus, we can write

$$\varphi(H_C(\theta)) = \int_{\mathbb{R}^n} dx \varphi(x^T Wx + w^T x + b) |x\rangle\langle x|, \quad (104)$$

where $|x\rangle \equiv |x_1\rangle \otimes \dots \otimes |x_n\rangle$. It then follows that the expectation of $\varphi(H_C(\theta))$ with respect to an n -mode state ρ is as follows:

$$\text{Tr}[\varphi(H_C(\theta))\rho] = \int_{\mathbb{R}^n} dx p(x) \varphi(x^T Wx + w^T x + b), \quad (105)$$

where $p(x) := \langle x|\rho|x\rangle$ is a probability density function. As such, this model does not go beyond the classical case, similar to what happened in (12)–(15).

To go beyond the classical case, we can employ the canonical quadrature operators for n bosonic modes [45, Chapter 3], which we denote by

$$(\hat{r}_1, \dots, \hat{r}_{2n}) := (\hat{x}_1, \hat{p}_1, \dots, \hat{x}_n, \hat{p}_n), \quad (106)$$

where \hat{p}_i is a momentum quadrature operator for all $i \in [n]$. The quadrature operators are subject to the canonical commutation relations:

$$[\hat{x}_j, \hat{p}_k] = i\delta_{jk}I, \quad (107)$$

holding for all $j, k \in [n]$. We can then write a general parameterized (quadratic) quantum Hamiltonian as follows:

$$H_Q(\theta) := \sum_{i,j=1}^{2n} \Omega_{i,j} \hat{r}_i \otimes \hat{r}_j + \sum_{i=1}^n \omega_i \hat{r}_i + bI^{\otimes n}, \quad (108)$$

where $\theta := (\Omega, \omega, b)$, $\Omega \in \mathbb{R}^{2n \times 2n}$, $\omega \in \mathbb{R}^{2n}$, and $b \in \mathbb{R}$. A signature of the Hamiltonian $H_Q(\theta)$ is that its summands need not commute, thus going beyond the classical case in (102).

Applying the activation function φ to $H_Q(\theta)$ then leads to the activation observable $\varphi(H_Q(\theta))$. In the case that the weight matrix Ω is positive definite, the Hamiltonian $H_Q(\theta)$ simplifies and admits a normal-mode decomposition along the lines discussed in [45, Chapter 3]. However, if this is not the case, then $H_Q(\theta)$ no longer admits this simple decomposition and its structure is more complex. More generally, we can consider k -local bosonic Hamiltonians of the form in (16), denoted by $H_Q(\theta)$, but with each H_j being a tensor product of quadrature operators that act nontrivially on k modes or even being a degree- k polynomial of the quadrature operators. Indeed, we can extend the continuous-variable setting to higher-order neurons [50], by performing the same canonical quantization procedure on the following cubic-order neuron:

$$\varphi \left(\sum_{i,j,k} V_{ijk} x_i x_j x_k + \sum_{i,j} W_{ij} x_i x_j + \sum_i w_i x_i + b \right), \quad (109)$$

or higher-order versions.

While it is known that having only Gaussian quadrature operators in the Hamiltonian $H_Q(\theta)$ can imply that simulating $\exp(iH_Q(\theta)t)$ classically is efficient [64], this statement does not apply to these continuous-variable Fermi–Dirac neurons. Indeed, while $H_Q(\theta)$ may only contain Gaussian terms, the activation observable $\varphi(H_Q(\theta))$ certainly is not limited to Gaussian operators. In fact, the expansion $\tanh(x) = x - x^3/3 + 2x^5/15 + O(x^7)$ means that high-degree non-Gaussian observables are being simulated. However, a finite-order polynomial cut-off may be sufficient if one works in an energy-limited subspace.

B. Training and testing

In order to train and test canonical quantizations of neurons based on bosonic Hamiltonians, we need quantum algorithms for estimating the objective function $\text{Tr}[\varphi(H_Q(\theta))\rho]$ and its gradient. Interestingly, many of our algorithms can be used essentially unchanged for this purpose, whenever the state ρ has bounded energy or a bounded higher moment of the photon number operator; i.e., $\text{Tr}[\hat{N}^k \rho] < +\infty$ for some $k \in \mathbb{N}$, where $\hat{N} := \sum_{i=1}^n \hat{n}_i$ is the total photon number operator and $\hat{n}_i := \frac{1}{2}(\hat{x}_i^2 + \hat{p}_i^2 - 1)$ (the case of bounded energy corresponds to $k = 1$). This includes Algorithm 4 for Fermi–Dirac neurons, Algorithm 5 for smooth ReLU, and Algorithm 7 for SiLU. Here, one needs to use Hamiltonian simulation algorithms suitable for bosonic systems [66, 67].

Many of our estimation guarantees in the finite-dimensional, qubit case are based on the Hoeffding

inequality (see, e.g., (29)). A desirable feature of the Hoeffding inequality is that it implies that the sample complexity needed to obtain an ε -accurate estimate with failure probability $\leq \delta$ is $O\left(\left(\frac{M}{\varepsilon}\right)^2 \ln\left(\frac{1}{\delta}\right)\right)$, where M is the size of the interval in which the random variable being estimated takes values.

In the continuous-variable case, we are no longer guaranteed that the random variable being estimated takes values in a bounded interval. However, we often have a guarantee that the state being used in an experiment has finite energy or finite higher moments of the total photon number operator. As a consequence of the Chebyshev inequality, estimating the mean of a random variable X with finite variance σ^2 to accuracy ε and failure probability δ requires $n \geq O\left(\left(\frac{\sigma}{\varepsilon}\right)^2 \frac{1}{\delta}\right)$ samples, when using the sample mean as an estimator. This dependence of the sample complexity on δ is less favorable when compared to the guarantees from the Hoeffding inequality. Interestingly, the median-of-means estimator essentially restores the favorable dependence of the sample complexity on δ to be like that from the Hoeffding inequality; indeed, the median-of-means estimator requires only $O\left(\left(\frac{\sigma}{\varepsilon}\right)^2 \ln\left(\frac{1}{\delta}\right)\right)$ samples [68, Theorem 2], thus having a dramatic improvement in its dependence on δ .

If we want to estimate $\text{Tr}[O\rho]$, where O is an observable, then we require the condition $\text{Tr}[O^2\rho] < \infty$ to hold in order to invoke the sample complexity guarantees from the Chebyshev inequality or the median-of-means estimator. Suppose now that we use $H_Q(\theta)$ of the form in (108). Algorithms 1 and 2 for Fermi–Dirac neurons aim to estimate a quantity of the form $\Re[\text{Tr}[H_j U \mathcal{V}(\rho)]]$, where H_j is one of the terms in (108), U is a unitary, and \mathcal{V} is a unitary channel applied to ρ . Such a quantity can be estimated by the same Hadamard test used in Algorithms 1 and 2, but instead using homodyne detection at the end to measure H_j . Here, one needs to use Hamiltonian simulation algorithms suitable for bosonic systems [66, 67], and given that Algorithms 1 and 2 require a control qubit, we need to use methods for interacting qubit and bosonic systems [69]. Since each H_j term in (108) is quadratic in the quadrature operators, we thus require that the input state ρ satisfies $\text{Tr}[\hat{N}^2 \rho] < \infty$ in order to estimate $\Re[\text{Tr}[H_j U \mathcal{V}(\rho)]]$ reliably using either the sample mean or the median-of-means estimators.

Algorithms 11 and 12 for smooth ReLU neurons and Algorithms 13 and 14 for SiLU neurons aim to estimate a quantity of the form $\Re[\text{Tr}[H_j H_k U \mathcal{V}(\rho)]]$. To estimate these quantities in the qubit case, we assumed that each H_k is a Pauli operator, implying that one can incorporate it into a controlled unitary interaction to perform the estimation task. For the Hamiltonian in (108), this assumption of H_k being unitary no longer holds. However, the form of the Hamiltonian in (108) implies that the products $H_j H_k$ are linear combinations of terms of the form $\hat{r}_i \hat{r}_j \hat{r}_k \hat{r}_\ell$, each of

which can be measured by homodyne detection, after performing algebraic manipulations of the quadrature operators based on (107). This special structure implies that we can again employ a Hadamard test circuit similar to that in Figure 2, but we use homodyne detection to measure $H_j H_k$ at the end of the circuit. Since each H_j term in (108) is at most quadratic in the quadrature operators, the term $H_j H_k$ is at most quartic, and we thus require that the input state ρ satisfies $\text{Tr}[\hat{N}^4 \rho] < \infty$, a stronger assumption than before, in order to estimate $\Re[\text{Tr}[H_j H_k U \mathcal{V}(\rho)]]$ reliably using either the sample mean or the median-of-means estimators.

VI. NUMERICAL EXPERIMENTS

In this section, we report the results of numerical experiments, comparing classical neurons to our quantized neurons for binary classification and function approximation tasks, using squared-loss and logistic-loss minimization for training, respectively. We restricted our experiments to Hamiltonians involving just a few qubits (ranging from two to seven), leaving it open to scale up these simulations to much larger numbers of qubits. Across all experiments, the results indicate that our quantized neurons outperform classical neurons for learning functions generated by quantum data. The code used to perform our experiments is publicly available [70].

A. Data generation

All of our experiments began by generating training data as follows. We assumed a target Hamiltonian $H^* \equiv H^*(\zeta)$ of the form in (9) with a parameter vector $\zeta \in \mathbb{R}^J$ selected at random, and we selected a set of quantum states

$$\rho_1, \dots, \rho_M, \quad (110)$$

where $M \in \mathbb{N}$. Then, for a fixed activation function φ , we set $z_m \leftarrow \text{Tr}[\varphi(H^*)\rho_m]$, for all $m \in [M]$. If the goal was binary classification and $\varphi = g_T$, then we set $y_m \leftarrow \text{sgn}(z_m)$. If instead the goal was function approximation, then we set $y_m \leftarrow z_m$. This procedure generated the labeled training data

$$(\rho_1, y_1), \dots, (\rho_M, y_M), \quad (111)$$

which we used for training via squared-loss or logistic-loss minimization.

For binary classification, we also tested the performance of the trained model, using the following method. For $L \in \mathbb{N}$, we selected a separate set of quantum states

$$\rho_{M+1}, \dots, \rho_{M+L}, \quad (112)$$

for validation. For the same activation function φ used in training, we set $y_m \leftarrow \text{sgn}(\text{Tr}[\varphi(H^*)\rho_m])$ as the ground

truth. Then, we compared the output of the trained models to the ground truth and computed the validation accuracy based on this.

B. Models

Next, we selected a Hamiltonian $H_Q(\theta)$ of the form in (9). We then picked a Hamiltonian $H_C(\theta)$ of the same form, but with every coefficient labeled by $\alpha, \beta \in \{x, y\}$ set to zero. Thus, $H_C(\theta)$ is a classical Hamiltonian featuring only σ_Z terms, and it has a straightforward diagonalization as in (13). We then trained both $H_Q(\theta)$ and $H_C(\theta)$ on the training set $(\rho_1, y_1), \dots, (\rho_M, y_M)$, using the gradient-descent algorithm outlined in (51), until convergence or a maximum number of iterations was reached. For binary classification, we finally tested the trained models $H_Q(\theta)$ and $H_C(\theta)$ on the validation set $(\rho_{M+1}, y_{M+1}), \dots, (\rho_{M+L}, y_{M+L})$, and we computed both $\text{Tr}[\varphi(H_Q(\theta))\rho_m]$ and $\text{Tr}[\varphi(H_C(\theta))\rho_m]$ and compared them to the true values y_{M+1}, \dots, y_{M+L} .

For squared-loss minimization, we used the transverse-field Ising model $H_{\text{TFIM}}(\theta)$ for both $H^*(\zeta)$ and $H_Q(\theta)$ and the classical Ising model $H_{\text{IM}}(\theta)$ for $H_C(\theta)$. Specifically, setting $\theta \equiv (W, w, b)$, the n -qubit Hamiltonians H_{TFIM} and H_{IM} are specified by

$$H_{\text{TFIM}}(\theta) := \sum_{i=1}^{n-1} W_i \sigma_Z^{(i)} \otimes \sigma_Z^{(i+1)} + \sum_{i=1}^n w_i \sigma_X^{(i)} + b I^{\otimes n}, \quad (113)$$

$$H_{\text{IM}}(\theta) := \sum_{i=1}^{n-1} W_i \sigma_Z^{(i)} \otimes \sigma_Z^{(i+1)} + \sum_{i=1}^n w_i \sigma_Z^{(i)} + b I^{\otimes n}, \quad (114)$$

with the key difference between the models being in the second sum in each expression above. Observe that the number of parameters are the same for both the quantum model H_{TFIM} and the classical model H_{IM} .

For logistic-loss minimization, we used the quantum Heisenberg model for both $H^*(\zeta)$ and $H_Q(\theta)$, which has the following form:

$$H_{\text{Heis}}(\theta) := \sum_{\alpha \in \{x, y, z\}} \sum_{i=1}^{n-1} W_{i, \alpha} \sigma_\alpha^{(i)} \otimes \sigma_\alpha^{(i+1)} + \sum_{\alpha \in \{x, y, z\}} \sum_{i=1}^n w_{i, \alpha} \sigma_\alpha^{(i)}. \quad (115)$$

The number of parameters for $H_{\text{Heis}}(\theta)$ is $6n - 3$. For the classical model $H_C(\theta)$, we used the fully-connected Ising Model $H_{\text{FCIM}}(\theta)$, which includes $\sigma_Z^{(i)} \otimes \sigma_Z^{(j)}$ interactions on every pair of qubits. It is specified by

$$H_{\text{FCIM}}(\theta) := \sum_{i, j=1}^n W_{i, j} \sigma_Z^{(i)} \otimes \sigma_Z^{(j)} + \sum_{i=1}^n w_i \sigma_Z^{(i)}. \quad (116)$$

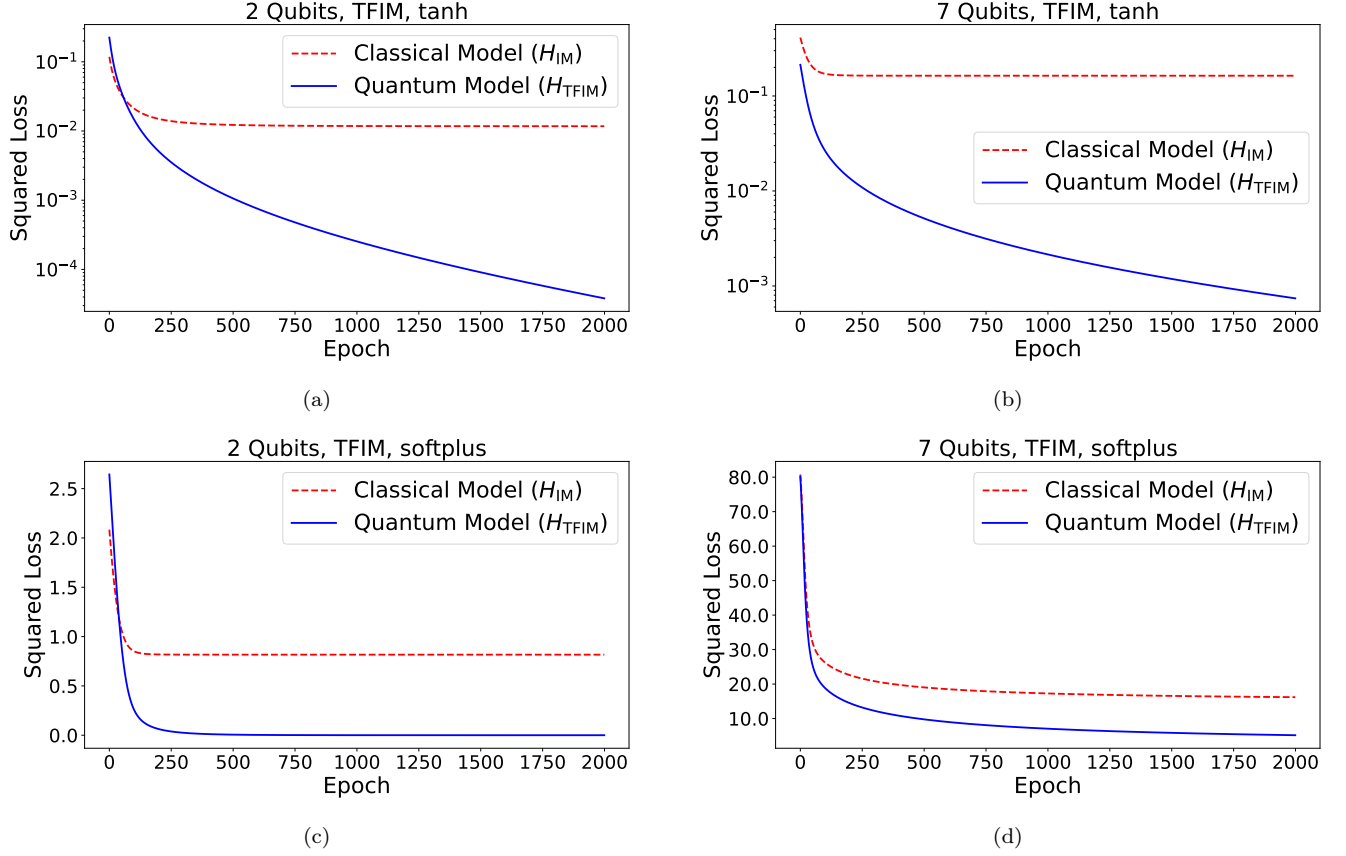


FIG. 7: Results of function-approximation experiments for training using squared-loss minimization. The quantum Hamiltonian is the transverse-field Ising model (TFIM) and the classical Hamiltonian is the classical Ising model (IM). We conducted experiments using both tanh and softplus as activation observables for systems of two and seven qubits.

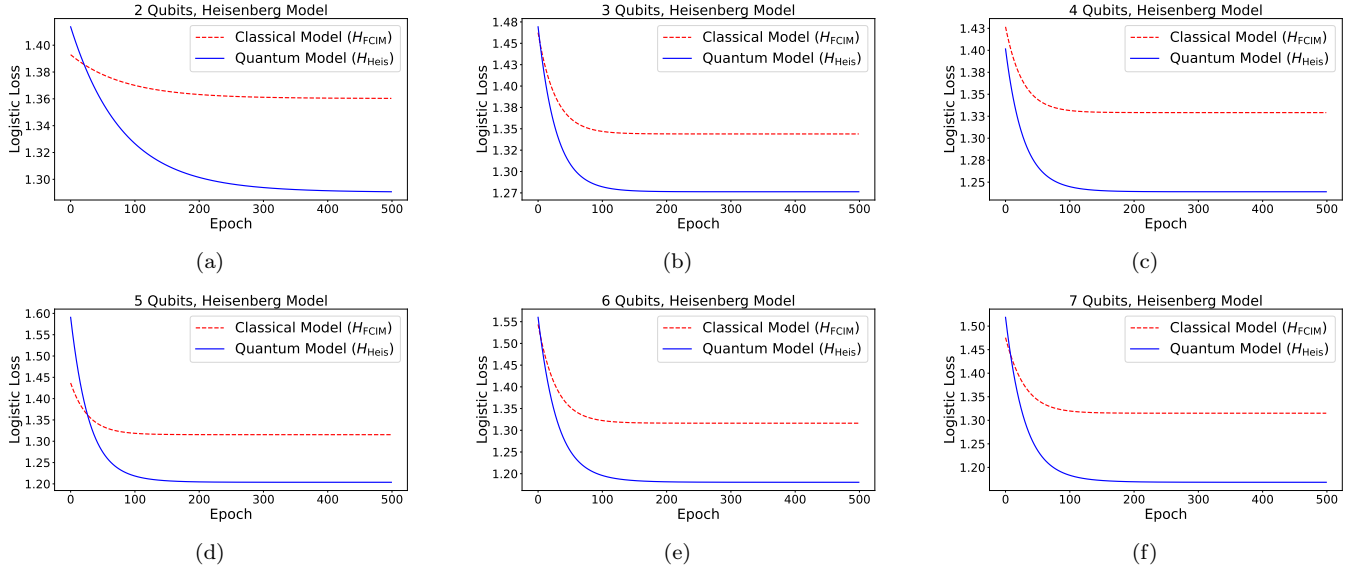


FIG. 8: Results of binary-classification experiments for training using logistic-loss minimization. The quantum Hamiltonian is the Heisenberg model (Heis), while the classical model is the fully-connected Ising model (FCIM). We conducted experiments using systems of 2-7 qubits.

The number of parameters for $H_{\text{FCIM}}(\theta)$ is $\frac{n(n+1)}{2}$. Thus, the number of parameters in the classical model $H_{\text{FCIM}}(\theta)$ is roughly comparable to that of the quantum model H_{Heis} for moderate values of n . Note that the identity terms have been removed in both models; the justification for this choice is discussed in Section VID.

C. Training protocol

We proceeded with training according to the following steps:

1. Select a learning rate $\eta = 1/10$ and temperature $T = 2$.
2. Initialize $H_Q(\theta^q)$ and $H_C(\theta^c)$ with random choices of θ^q and θ^c .
3. For each training state ρ_m , calculate $f_q(\theta^q, \rho_m)$ and $f_c(\theta^c, \rho_m)$, where

$$f_q(\theta^q, \rho) := \text{Tr}[\varphi(H_Q(\theta^q))\rho], \quad (117)$$

$$f_c(\theta^c, \rho) := \text{Tr}[\varphi(H_C(\theta^c))\rho], \quad (118)$$

and evaluate the squared (or logistic) losses $\mathcal{L}_q(\theta^q)$ and $\mathcal{L}_c(\theta^c)$, making use of each true value $f(\rho_m) = \text{Tr}[\varphi(H^*)\rho_m]$ to calculate both.

4. For $i \in [\text{dim } \theta]$ and $k \in \{q, c\}$, calculate $\left. \frac{\partial}{\partial \theta_i} \mathcal{L}_k(\theta) \right|_{\theta=\theta^k}$ and perform the update:

$$\theta^k \leftarrow \theta^k - \eta \nabla_{\theta} \mathcal{L}_k(\theta) \Big|_{\theta=\theta^k}. \quad (119)$$

5. Repeat steps 3-4 until convergence or a maximum number of iterations is reached.

D. Results

1. Squared-loss minimization

In our experiments for squared-loss minimization, we set the target Hamiltonian $H^* \equiv H^*(\zeta)$ to be a transverse-field Ising model of the form in (113), by sampling each entry of ζ uniformly at random from the interval $[-2, 2]$. The target function to learn is

$$f(\rho) := \text{Tr}[\varphi(H^*)\rho]. \quad (120)$$

We set the model quantum Hamiltonian $H_Q(\theta)$ to be of the form in (113) and the model classical Hamiltonian $H_C(\theta)$ to be of the form in (114).

We performed training using various combinations of the following state vectors: computational basis states (built from $|0\rangle$ and $|1\rangle$), Hadamard basis states (built from $|+\rangle$ and $|-\rangle$), Bell basis states $|\Phi^+\rangle$, $|\Phi^-\rangle$, $|\Psi^+\rangle$, $|\Psi^-\rangle$, GHZ states, and $\sqrt{p}|00\rangle + \sqrt{1-p}|11\rangle$, for various choices of $p \in (0, 1)$. We also incorporated the maximally

Qubit Count	Quantum Accuracy	Classical Accuracy
2	95.2%	64.0%
3	97.6%	65.8%
4	96.8%	68.6%
5	92.2%	63.8%
6	91.2%	73.6%
7	91.0%	69.6%

TABLE II: Results of binary classification with logistic-loss minimization on randomly generated datasets of 500 states.

mixed state $I/2^n$ into training, where n is the number of qubits. We then generated the training data by calculating $y_m = f(\rho_m)$ for every training state ρ_m .

Figure 7 depicts the performance of training for squared-loss minimization. The experiments included learning using both tanh and softplus for two and seven-qubit systems. They indicate that activation observables built from quantum Hamiltonians outperform those built from classical Hamiltonians.

2. Logistic-loss minimization

We conducted similar experiments for logistic-loss minimization, but with $H^* \equiv H^*(\zeta)$ and $H_Q(\theta)$ set to be Heisenberg models of the form in (115), $H_C(\theta)$ set to be the fully-connected Ising model of the form in (116), in both cases using the logistic-loss function in (56). We excluded identity terms from both Hamiltonians, since we observed that including them led to an excessive weighting on the constant offset, causing the optimization to prioritize this term rather than learning meaningful structure in the remaining parameters. Incorporating regularization terms into the loss function may mitigate this issue in future experiments to penalize the excessive weighting. Since the target Hamiltonian additionally contains σ_Y terms, the training states were expanded to also include σ_Y -basis states (generated by $|+i\rangle_Y$ and $|-i\rangle_Y$). The training labels were generated by calculating $y_m = \text{sgn}(f(\rho_m))$ for every training state ρ_m . The validation set was generated by picking 500 Haar-random pure states.

The results of training are plotted in Figure 8. The validation accuracies for binary classification are shown in Table II. At all qubit numbers, there is a significant separation in the losses between the quantum and classical models. Since the classical model has access to σ_Z interactions only, the training states in the σ_X and σ_Y bases have expectation value equal to zero, so that the model is effectively insensitive to these states. This effect is most pronounced in our current selection of training states, which has σ_Z -, σ_X -, and σ_Y - basis states chosen in equal part. Indeed, when we train on only σ_Z and σ_X states, the separation between the quantum and classical models is less pronounced. Thus, we again find

that quantum Hamiltonians outperform classical ones for training for binary classification.

E. Discussion

Across all experiments, the results indicate that noncommuting Hamiltonian models provide a consistent advantage over commuting (diagonal) models when learning observables generated by nonlinear functions of quantum Hamiltonians. This suggests that the expressive power of the underlying operator algebra plays a central role in the learnability of quantum-induced functions in this setting. On one level, it is not difficult to understand why the noncommuting Hamiltonian model should offer more expressivity, since the Hamiltonian itself contains directions that are not contained in the commuting case. For example, while H_{TFIM} contains σ_X terms, H_{IM} does not, and so one would not expect H_{IM} to learn states in the σ_X eigenbasis well. This explains the simulation result that a separation between the classical and the quantum linear model $\text{Tr}[H(\theta)\rho]$ is present, as depicted in Figure 9. However, from the same figure, the Fermi–Dirac neuron appears to learn much better than $\text{Tr}[H(\theta)\rho]$ (we will come back to an exception for the two-qubit Heisenberg model case later). We will see that this better performance arises directly from the noncommutativity of the individual terms in the Hamiltonian itself.

There is an intuitive way to understand the importance of this noncommutativity. We can first consider high-temperature expansions of the Fermi–Dirac neuron ($\|H(\theta)\|/T \ll 1$) with $H(\theta) = \sum_{j=1}^J \theta_j H_j$:

$$\text{Tr} \left[\tanh \left(\frac{H(\theta)}{T} \right) \rho \right] \approx \frac{1}{2T} \text{Tr}[H(\theta)\rho] - \frac{1}{24T^3} \text{Tr}[H(\theta)^3\rho] + O(T^{-5}). \quad (121)$$

If we only keep the term linear in $1/T$ (for very high temperatures), then the neuron can be mapped directly into a quantum kernel model with corresponding feature map vectors with components $\text{Tr}[H_j\rho]$, and here the role of noncommutativity between the H_j operators themselves do not yet appear. However, for lower temperatures where $1/T^3$ and higher orders are required, it is clear where the power of Fermi–Dirac neurons comes from: it can learn higher-order features like $\Re[\text{Tr}[H_j H_k H_\ell \rho]]$. If the elements from the original set $\{H_j\}_j$ of Hamiltonians do not commute, then these higher-order terms like $H_j H_k H_\ell$ can generate a greater diversity of new terms not in the original set. In fact, the lower the temperature, the Fermi–Dirac neuron might be expected to be more powerful, since it can capture patterns depending on even higher-order terms. However, as we will later see, beyond a certain critical temperature, its power might not increase further. Figure 9 supports this reasoning.

This advantage from noncommutativity only happens beyond single-qubit cases. In single-qubit cases, for instance, if one chooses the original set $\{H_1 = I, H_2 = \sigma_X, H_3 = \sigma_Z\}$, then $\tanh(H(\theta))$ only contains terms in the span of $\{I, \sigma_X, \sigma_Z\}$. However, for our two-qubit example using the transverse-field Ising model, we chose the noncommuting original set $\{H_1 = \sigma_X^{(1)}, H_2 = \sigma_X^{(2)}, H_3 = \sigma_Z^{(1)} \otimes \sigma_Z^{(2)}\}$. Then $H(\theta)^3$ already contains new terms like $\sigma_Y^{(1)} \otimes \sigma_Y^{(2)}$, where no σ_Y Hamiltonian appeared in the original set. This can explain why there are certain features in this example (i.e., those that correspond to σ_Y directions) that a Fermi–Dirac neuron can learn, but the corresponding classical classifier, which depends only on a commuting Hamiltonian set, is not capable of learning. This inability is reflected in our simulation results. In this particular case, since higher-order terms like $H(\theta)^5$ do not generate new types of terms since the algebra closes, then it appears that it is sufficient to have a relatively high temperature Fermi–Dirac neuron, where higher-temperature versions could be more experimentally accessible; see the discussion, for example, in Section IID.

However, as we increase the number of qubits, the algebra does not close at such low-order polynomials, and lower temperature limits are necessary. In the transverse-field Ising model, the original Hamiltonian set includes $\{I, \sigma_X^{(i)}, \sigma_Z^{(i)} \otimes \sigma_Z^{(i+1)}\}$. In this case, for n qubits, each polynomial $H(\theta)^{2n-1} \supset \sigma_Y^{(1)} \otimes \sigma_X^{(2)} \otimes \dots \otimes \sigma_X^{(n-1)} \otimes \sigma_Y^{(n)}$; thus, we see that higher powers generate new features and long-range Pauli strings that are missed by low-degree truncations. In the presence of long-range phenomena, the Fermi–Dirac neuron therefore allows the exploration of all the higher-order features by a single training procedure without explicit estimation of these higher-order features themselves.

For finite-dimensional systems, the algebra always closes at a finite polynomial order. More precisely, from the Cayley–Hamilton theorem, for a d -dimensional Hamiltonian $H(\theta)$ with D distinct eigenvalues, $H(\theta)^D$ can already be expressed in terms of a linear sum of lower-order polynomials of H , where $D_{\text{max}} = d = 2^n$ for n -qubit systems. This means that only terms up to but not including $\text{Tr}[H(\theta)^D \rho]/T^D$ need to be kept. Thus a full exploration of the possible features generated by powers of $H(\theta)$ is only possible if the temperature T is low enough, so that the corresponding term is not negligible. This can be considered like a critical temperature, since no features appear if the temperature is further lowered.

For highly structured $H(\theta)$, generally D is much smaller than 2^n . Here it is expected that using Fermi–Dirac neurons is still more efficient, since with J Hamiltonian terms in the original set for the Fermi–Dirac neuron, there are only J free parameters to learn. On the other hand, if one were to separately learn the higher-order polynomial terms in $H(\theta)$, there are generally many more parameters to learn, in cases where $J \ll D$.

Not only are Fermi–Dirac neurons advantageous in

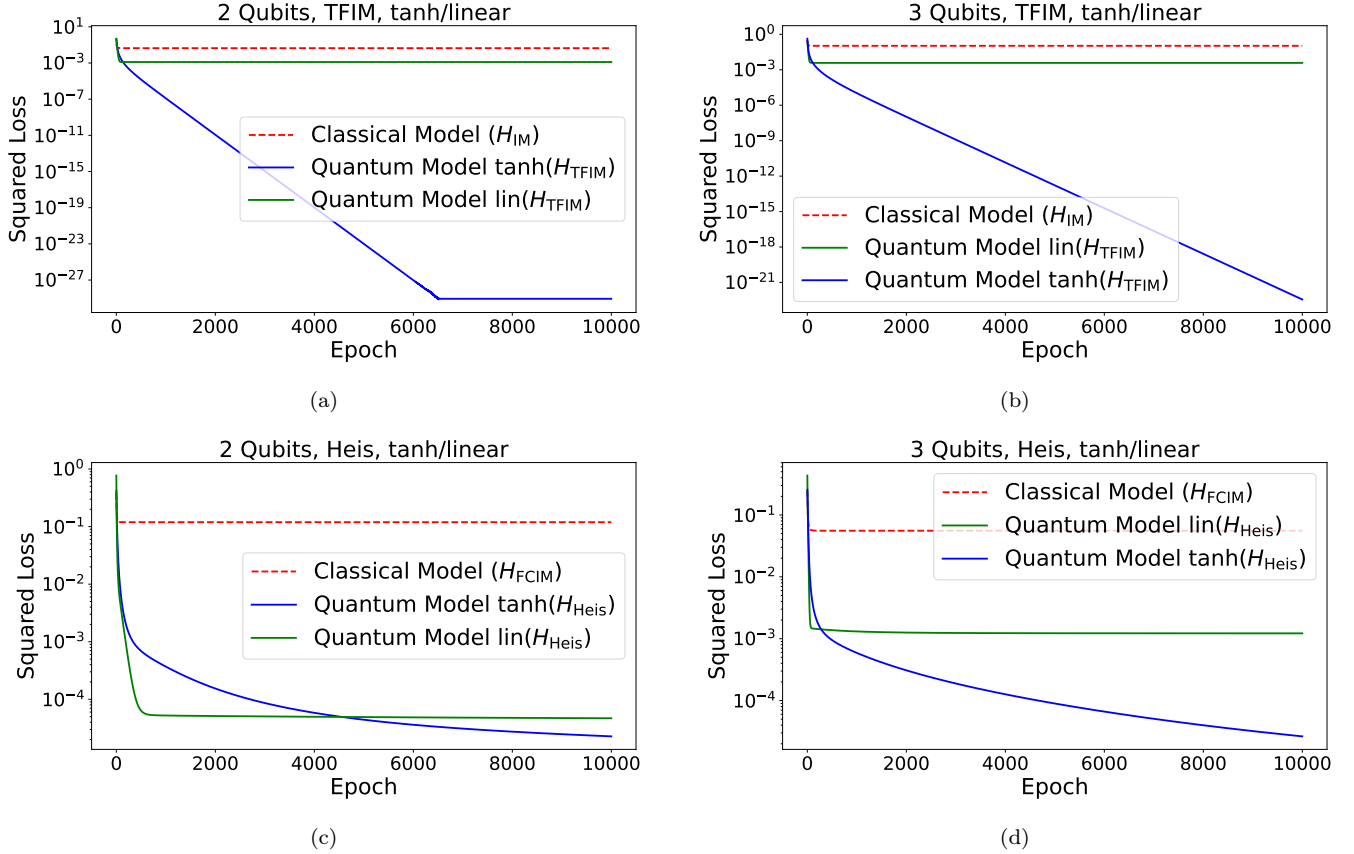


FIG. 9: Comparison of classical, quantum linear, and quantum nonlinear models for function approximation. Quantum linear models have expected value $\text{Tr}[H_{TFIM}(\theta)\rho_m]$, and quantum nonlinear models have expected value $\text{Tr}[\tanh(H_{TFIM}(\theta)/T)\rho_m]$. The plots depict the results of training for squared-loss minimization. The quantum Hamiltonian is the transverse-field Ising model (TFIM) and the classical Hamiltonian is the classical Ising model (IM). We conducted experiments using tanh as an activation observable for systems of two and three qubits.

requiring less parameters, the fact that the coefficients corresponding to different Hamiltonian terms in the $\tanh(H(\theta))$ expansion are coupled to each other means that it is possible for the neuron to be sensitive to directions that are not present in the original training data. For instance, in the two-qubit transverse-field Ising model simulation, even though states sensitive to σ_Y are not included in the original training data, the quantum model learns these states (which are not learned by the classical model). This can be explained as the coefficient in front of $\sigma_Y^{(1)} \otimes \sigma_Y^{(2)}$ is coupled to coefficients in the other directions that are included in the training data, and thus cannot be zero.

We can also look at the case of the Heisenberg model, where the original Hamiltonian set includes $\{\sigma_X^{(i)} \otimes \sigma_X^{(i+1)}, \sigma_Y^{(i)} \otimes \sigma_Y^{(i+1)}, \sigma_Z^{(i)} \otimes \sigma_Z^{(i+1)}, \sigma_X^{(i)}, \sigma_Y^{(i)}, \sigma_Z^{(i)}\}$. For two-qubit cases, the $\tanh(H(\theta))$ expansion does not introduce any new terms to the original set. This means that any quantum advantage that we see mostly arises from including both σ_X and σ_Y directions in the original Hamiltonian, which is absent in the corresponding classical model that contains only σ_Z terms. This means

that we do not expect a large difference between the Fermi–Dirac neuron and the linear model for the two-qubit case, and this is verified by Figure 9. However, for three qubits we again see a separation between the linear model and the Fermi–Dirac neuron, as with the transverse-Ising model. This is because for three qubits, $H(\theta)^3$ is sufficient to generate new terms belonging to the set $\mathcal{S}_{13} = \{\sigma_X^{(1)} \otimes \sigma_X^{(3)}, \sigma_Y^{(1)} \otimes \sigma_Y^{(3)}, \sigma_Z^{(1)} \otimes \sigma_Z^{(3)}\}$ (while $H(\theta)^5$ and higher polynomials generate no extra features), hence generating features on next-nearest neighbors that are not present in the original Hamiltonian. For larger numbers of qubits, longer-range two-qubit exchange terms are present, containing terms in \mathcal{S}_{ij} such that $2 < |i - j| < n$, as well as genuine n -body Pauli strings. Thus the Fermi–Dirac neuron with Heisenberg model selected as the Hamiltonian is expected to learn genuine n -body correlations better than the corresponding linear model.

VII. PROPOSALS FOR CANONICAL QUANTIZATIONS OF NEURAL NETWORKS

A. Review of classical neural networks

Composing classical neurons into multilayer neural networks leads to powerful computational capabilities. We can express this composition mathematically as follows. To begin with, recall from (4) that a single neuron acting on $z \in \{-1, +1\}^n$ has the following form:

$$\varphi\left(\sum_{i=1}^n w_i z_i + b\right). \quad (122)$$

In what follows, we consider fully connected feedforward neural networks. Let $L \in \mathbb{N}$, $\ell \in [L]$, and $J_\ell \in \mathbb{N}$. Suppose that we have L layers of neurons, with layer ℓ consisting of J_ℓ neurons. Then, letting $a_i^{(\ell)}$ denote the output of neuron i in layer ℓ , its dependence on the previous layer is given by

$$a_i^{(\ell)} = \varphi_\ell\left(\sum_{j=1}^{J_{\ell-1}} w_{ij}^{(\ell)} a_j^{(\ell-1)} + b_i^{(\ell)}\right), \quad (123)$$

where $w_{ij}^{(\ell)} \in \mathbb{R}$ denotes the weight from neuron j in layer $\ell - 1$ to neuron i in layer ℓ and $b_i^{(\ell)}$ denotes the bias of neuron i in layer ℓ . The full network is defined by initializing

$$a_j^{(0)} = z_j, \quad (124)$$

and recursively defining $a_i^{(\ell)}$ as in (123), with the final output being

$$F(z) = \left(a_1^{(L)}, \dots, a_{J_L}^{(L)}\right). \quad (125)$$

Thus, the network output $F(z) \in \mathbb{R}^{J_L}$.

For a two-layer network, the general development above reduces to

$$a_j^{(1)} = \varphi_1\left(\sum_{i=1}^{J_0} w_{ji}^{(1)} z_i + b_j^{(1)}\right), \quad (126)$$

$$F_k(z) = a_k^{(2)} \quad (127)$$

$$= \varphi_2\left(\sum_{j=1}^{J_1} w_{kj}^{(2)} a_j^{(1)} + b_k^{(2)}\right) \quad (128)$$

$$= \varphi_2\left(\sum_{j=1}^{J_1} w_{kj}^{(2)} \varphi_1\left(\sum_{i=1}^{J_0} w_{ji}^{(1)} z_i + b_j^{(1)}\right) + b_k^{(2)}\right). \quad (129)$$

In preparation for our quantum generalization in Section VIII B, let us simplify the notation somewhat. A

single neuron can be written more generally as

$$\varphi\left(\sum_{j=1}^J \theta_j h_j(z)\right), \quad (130)$$

where each $\theta_j \in \mathbb{R}$ and $h_j(z)$ is an energy function (classical Hamiltonian) interacting just a few of the variables in z (e.g., as in (5) or (11)). We recover (122) by setting $J = n + 1$, $\theta_j = w_j$ and $h_j(z) = z_j$ for all $j \in [n]$, $\theta_{n+1} = b$, and $h_{n+1}(z) = 1$. As before, suppose that we have L layers of neurons, with layer ℓ consisting of J_ℓ neurons. Then, letting $a_i^{(\ell)}$ denote the output of neuron i in layer ℓ , its dependence on the previous layer is given by

$$a_i^{(\ell)} = \varphi_\ell\left(\sum_{j=1}^{J_{\ell-1}} \theta_{ij}^{(\ell)} a_j^{(\ell-1)}\right), \quad (131)$$

where $\theta_{ij}^{(\ell)} \in \mathbb{R}$ denotes the parameter from neuron j in layer $\ell - 1$ to neuron i in layer ℓ . The full network is defined by initializing

$$a_j^{(0)} = h_j(z), \quad (132)$$

and recursively defining $a_i^{(\ell)}$ as in (131), with the final output being

$$F(z) = \left(a_1^{(L)}, \dots, a_{J_L}^{(L)}\right). \quad (133)$$

For a two-layer network, the general development above reduces to

$$a_j^{(1)} = \varphi_1\left(\sum_{i=1}^{J_0} \theta_{ji}^{(1)} h_i(z)\right), \quad (134)$$

$$F_k(z) = a_k^{(2)} \quad (135)$$

$$= \varphi_2\left(\sum_{j=1}^{J_1} \theta_{kj}^{(2)} a_j^{(1)}\right) \quad (136)$$

$$= \varphi_2\left(\sum_{j=1}^{J_1} \theta_{kj}^{(2)} \varphi_1\left(\sum_{i=1}^{J_0} \theta_{ji}^{(1)} h_i(z)\right)\right). \quad (137)$$

B. Quantum observable networks

Extending the development in (130)–(137) to the quantum case, we quantize each variable $a_i^{(\ell)}$ by replacing it with an observable $A_i^{(\ell)}$, and then we construct a *quantum observable network*, as defined below.

To begin with, recall from Section IC that the activation observable corresponding to a single neuron can be written as

$$\varphi\left(\sum_{j=1}^J \theta_j H_j\right), \quad (138)$$

where each $\theta_j \in \mathbb{R}$ and H_j is a Hamiltonian acting nontrivially on just k qubits, while $\sum_{j=1}^J \theta_j H_j$ acts on n qubits. As before, here and in what follows, the activation function φ maps $\mathbb{R} \rightarrow \mathbb{R}$, so that $\varphi\left(\sum_j \theta_j H_j\right)$ is a Hermitian operator. Although the Hamiltonian $\sum_{j=1}^J \theta_j H_j$ is k -local, the activation observable $\varphi\left(\sum_j \theta_j H_j\right)$ need not be.

Suppose that we have L layers of neurons, with layer ℓ consisting of J_ℓ neurons. Then, letting $A_i^{(\ell)}$ denote the observable associated with neuron i in layer ℓ , its dependence on the previous layer is given by

$$A_i^{(\ell)} = \varphi_\ell\left(B_i^{(\ell)}\right), \quad (139)$$

$$B_i^{(\ell)} := \sum_{j=1}^{J_{\ell-1}} \theta_{ij}^{(\ell)} A_j^{(\ell-1)}, \quad (140)$$

where $\theta_{ij}^{(\ell)} \in \mathbb{R}$ denotes the parameter from neuron j in layer $\ell - 1$ to neuron i in layer ℓ and the activation function φ_ℓ acts via functional calculus to produce the activation observable $A_i^{(\ell)}$. Since each $A_j^{(\ell-1)}$ is Hermitian and each $\theta_{ij}^{(\ell)} \in \mathbb{R}$, the functional calculus defining the action of φ_ℓ is well defined at every layer. The full quantum observable network is defined by initializing

$$A_j^{(0)} = H_j, \quad (141)$$

and recursively defining $A_i^{(\ell)}$ as in (139), with the final tuple of activation observables being

$$F \equiv \left(A_1^{(L)}, \dots, A_{J_L}^{(L)}\right). \quad (142)$$

Thus, the quantum observable network produces J_L observables, each of which acts on n qubits.

For a two-layer network, the general development above reduces to

$$A_j^{(1)} = \varphi_1\left(\sum_{i=1}^{J_0} \theta_{ji}^{(1)} H_i\right), \quad (143)$$

$$F_k = A_k^{(2)} \quad (144)$$

$$= \varphi_2\left(\sum_{j=1}^{J_1} \theta_{kj}^{(2)} A_j^{(1)}\right) \quad (145)$$

$$= \varphi_2\left(\sum_{j=1}^{J_1} \theta_{kj}^{(2)} \varphi_1\left(\sum_{i=1}^{J_0} \theta_{ji}^{(1)} H_i\right)\right). \quad (146)$$

The expectation of each observable in F with respect to a state ρ is as follows:

$$\text{Tr}\left[A_k^{(L)} \rho\right]. \quad (147)$$

Evaluating the quantum observable network on an input state ρ then amounts to estimating this expectation, and one can train it by using labeled training data of the form in (43). For example, the squared-loss function is as follows:

$$\mathcal{L}_k^{(2)}(\theta) := \frac{1}{M} \sum_{m=1}^M \left(\text{Tr}\left[A_k^{(L)} \rho_m\right] - y_m\right)^2, \quad (148)$$

where θ is a parameter vector containing all of the parameters defined in (139). Alternatively, the logistic loss function is as follows:

$$\mathcal{L}_{T,k}^{\text{log}}(\theta) := \frac{1}{M} \sum_{m=1}^M T \text{Tr}\left[\ln\left(I + e^{-y_m A_k^{(L)}/T}\right) \rho_m\right]. \quad (149)$$

In order to train the model, we require the gradient of these functions with respect to θ . For the case of squared-loss minimization in (148), calculating the gradient reduces to calculating the gradient $\nabla_\theta \text{Tr}[A_k^{(L)} \rho_m]$. In Appendix G, we establish formulas for the gradient of a general L -layer network, after presenting the simpler cases of two- and three-layer networks. The derived formulas can be expressed in terms of a backpropagation rule similar to the well known one from [71, 72]. However, we leave it open to determine if there is an efficient quantum algorithm that generalizes the backpropagation algorithm [71, 72] to quantum observable networks, while noting that there have been difficulties in extending it to other quantum machine learning models [73].

C. Hybrid quantum–classical neural networks

Another neural-network architecture consists of a hybrid quantum–classical format, in which some of the neurons are quantized while others are classical. Perhaps the most interesting such instantiation is one in which the input data is quantum, the first layer consists of quantized neurons, and all subsequent layers are classical. This model extends the single-neuron setup studied in Sections II–VI of our paper, and it seems reasonable that it might have enhanced performance for classification and function approximation tasks.

The basic idea behind this approach is that it is indeed a hybrid of the networks proposed in Sections VII A and VII B. The first layer consists of the following J_1 activation observables:

$$A_i^{(1)} = \varphi_1\left(\sum_{j=1}^{J_0} \theta_{ij}^{(1)} H_j\right). \quad (150)$$

However, in distinction to the proposal in Section VII B, each of these observables is measured with respect to an input state ρ , leading to an activation variable $a_i^{(1)}$. Each activation variable $a_i^{(1)}$ is then fed into the second layer,

leading to

$$a_i^{(2)} = \varphi_2 \left(\sum_{j=1}^{J_1} \theta_{ij}^{(2)} a_j^{(1)} \right). \quad (151)$$

After that, the rest of the network continues as in (131) and (133).

There are at least two ways in which we can measure each activation observable $A_i^{(1)}$ in the first layer. If the input state is ρ , one can prepare it and perform one of our single-shot algorithms (i.e., Algorithms 4, 5, or 7) that outputs a random variable $a_i^{(1)}$ with expected value $\text{Tr}[A_i^{(1)}\rho]$. Each random variable $a_i^{(1)}$ would then be fed into the second layer. Alternatively, one could perform repeated sampling, followed by averaging, to form an estimate $\tilde{a}_i^{(1)}$ of the expected value $\text{Tr}[A_i^{(1)}\rho]$, and then one could feed each estimate $\tilde{a}_i^{(1)}$ into the second layer. The single-shot approach thus induces stochastic activation variables, analogous to stochastic neural networks in classical machine learning [74, 75].

The hybrid quantum–classical architecture seems like a practical method for incorporating quantum algorithms into neural networks. That is, the classical network reviewed in Section VII A does not benefit from quantum processing, while the quantum observable network proposed in Section VII B might be too difficult to realize in the near term. So this hybrid architecture represents a compromise between the two approaches, while also extending the capabilities of a single quantized neuron.

Additionally, for training these hybrid networks according to squared- or logistic-loss minimization, one can take advantage of our hybrid quantum–classical algorithms for gradient estimation, as well as the standard backpropagation algorithm [71, 72], due to the hybrid nature of the network. We leave it open to future work to simulate the performance and training of hybrid quantum–classical neural networks.

VIII. COMPLEXITY-THEORETIC EVIDENCE AGAINST CLASSICAL SIMULATION

In this section, we provide complexity-theoretic evidence that Fermi–Dirac machines can efficiently solve problems that classical computers cannot. To begin with, consider the following computational decision problem based on Fermi–Dirac machines, recalling the definition of g_T in (18):

Problem 1. Let $H = \sum_{j=1}^J H_j$ be a k -local Hamiltonian such that $\|H_j\| \leq 1$ for all $j \in [J]$, let ρ be a state preparable by a quantum circuit, and let $T > 0$ be a temperature. Given real numbers α and β such that $-1 \leq \beta < \alpha \leq 1$, decide which of the following holds:

$$\text{YES : } \quad \text{Tr}[g_T(H)\rho] \geq \alpha, \quad (152)$$

$$\text{NO : } \quad \text{Tr}[g_T(H)\rho] \leq \beta, \quad (153)$$

under the promise that one of the two cases is true.

We now state our main complexity-theoretic result:

Theorem 11. *Let n be the number of bits needed to specify H , the circuit that generates ρ , the temperature T , and the thresholds α and β . Then Problem 1 is BQP-complete for $k \geq 5$ under polynomial-time reductions, for inverse polynomial temperature $T = \frac{1}{\text{poly}(n)}$, provided that the promise gap satisfies $\alpha - \beta \geq \frac{1}{\text{poly}(n)}$.*

Proof. See Appendix H. \square

Let us summarize the reasoning why Theorem 11 holds. Containment in BQP follows by applying Algorithm 2 to estimate $\text{Tr}[g_T(H)\rho]$ to inverse polynomial additive accuracy.

Hardness follows by employing the same reasoning used in the proof of [47, Proposition 7], which established BQP hardness for the guided local Hamiltonian problem. A critical aspect of this approach, relevant for Problem 1, is that a general BQP computation is encoded entirely in the Hamiltonian H , via the standard Feynman–Kitaev circuit-to-Hamiltonian construction [76, 77] (see also [78, 79]), while the state ρ is a state that is independent of the computation (e.g., a simple computational basis state tensored with a uniform superposition state of the clock register). Thus, this approach illustrates that it is the activation observable $g_T(H)$ underlying the computational power of Fermi–Dirac machines. By choosing $T = \frac{1}{\text{poly}(n)}$, the function $g_T(x) = \tanh(x/T)$ acts as a smooth approximation to the sign function, sharply distinguishing positive from negative eigenvalues of H . As a result, $\text{Tr}[g_T(H)\rho]$ encodes the acceptance probability of the underlying BQP computation, up to inverse polynomial accuracy. This establishes BQP-hardness.

IX. CONNECTIONS WITH QUANTUM BOLTZMANN MACHINES

A central feature of our construction is that quantized neurons are defined by applying an activation function φ to a parameterized Hamiltonian $H(\theta)$ of the form in (9), producing an activation observable $\varphi(H(\theta))$. This viewpoint places our framework within a broader class of Hamiltonian-based quantum machine learning models, where nonlinearities are induced via functional calculus on operators. A particularly relevant choice is when φ is the Fermi–Dirac function in (2). The resulting activation observable is a measurement operator, as introduced in [8] and explored in more detail in the present paper. As mentioned in Section IB, the notion of an activation observable distinguishes our approach to quantizing neurons from all prior proposals [10–20].

Quantum Boltzmann machines (QBMs) provide another prominent example of Hamiltonian-based learning models [80–82], being realized by applying

the exponential function to the Hamiltonian $H(\theta)$ and normalizing the resulting operator, leading to a parameterized thermal state of the form $e^{-H(\theta)}/\text{Tr}[e^{-H(\theta)}]$. As in the classical case, the exponential function induces nonlinearity at the level of the induced probability distribution, rather than producing an observable-valued activation.

From this perspective, both frameworks employ a Hamiltonian $H(\theta)$ followed by a nonlinear functional transformation; in fact, by consulting Eqs. (1), (2), (9), and (12) of [80], one can see that the way in which we quantized neurons in Sections IB and IIA here is similar to the way in which the authors of [80] quantized Boltzmann machines. However, our quantized neurons and QBMs differ in the type of object produced. QBMs map Hamiltonians to quantum states (density operators), whereas quantized neurons map Hamiltonians to activation observables. This distinction can be interpreted through the standard state–observable duality of quantum mechanics, where expectation values take the form $\text{Tr}[A\rho]$ for an observable A and a state ρ .

The particular nonlinear functions arising for both quantum Boltzmann machines and Fermi–Dirac machines are not arbitrary, but instead arise from well motivated free-energy minimization problems; see, e.g., [40, 83] and [8, 83], respectively. Indeed, the nonlinear function

$$H \mapsto e^{-H/T} / \text{Tr}[e^{-H/T}] \quad (154)$$

for quantum Boltzmann machines arises by optimizing a semidefinite program over the set of density operators after augmenting the objective with a free-energy term involving the von Neumann entropy scaled by a temperature $T > 0$. The nonlinear function

$$H \mapsto (e^{-H/T} + I)^{-1} \quad (155)$$

for Fermi–Dirac machines arises instead by optimizing a semidefinite program over the set of measurement operators after augmenting the objective with a free-energy term involving the Fermi–Dirac entropy scaled by T . Thus, the two nonlinearities arise from parallel variational principles defined on different convex sets: the set of density operators in one case and the operator interval $0 \leq M \leq I$ in the other. Moreover, the two nonlinear maps inherit the geometric constraints of their respective feasible sets: the thermal map in (154) is normalized to have unit trace because it produces density operators, whereas the Fermi–Dirac map in (155) satisfies $0 < (e^{-H/T} + I)^{-1} < I$, making it naturally observable-valued as a measurement operator. In this sense, Fermi–Dirac machines are a natural counterpart to quantum Boltzmann machines, reflecting the broader duality between states and observables in quantum mechanics.

The structural analogy relating the approaches is reflected in training algorithms. That is, our algorithms for training Fermi–Dirac and other quantized neurons

are broadly similar to the algorithms from [37–40] for training quantum Boltzmann machines. In both cases, the training algorithms are used to tune the values in the parameter vector θ and their core constituents include classical random sampling, Hamiltonian simulation, and the Hadamard test, due to the common form of the gradients in both cases. The main distinction lies in the particular classical random sampling conducted and in the state input to the quantum circuit. The circuits used to train our quantized neurons take quantum training data as input, while the circuits used for training quantum Boltzmann machines require parameterized thermal states as input. Thus, training quantum Boltzmann machines requires quantum algorithms for thermal state preparation (see, e.g., [84] and references therein), while our algorithms for training quantized neurons do not. This difference leads to a potential computational advantage of quantized neurons in quantum learning settings, as it removes the need for thermal state preparation while retaining a Hamiltonian-based nonlinear learning model.

X. LAGNIAPPE: HYBRID QUANTUM–CLASSICAL ALGORITHM FOR ESTIMATING CROSS ENTROPY AND LOG-PARTITION FUNCTION

As an offshoot of our findings in this paper, we note here that our approach in Theorems 2, 14, and 15 and Algorithms 2, 12, and 14 can be repurposed for estimating cross entropy and the log-partition function. That is, these theorems and algorithms all have to do with methods for estimating $\text{Tr}[\varphi(H(\theta))\rho]$ that are derived from the fundamental theorem of calculus and expressions for the gradient $\nabla_{\theta} \text{Tr}[\varphi(H(\theta))\rho]$, and the same idea can be used for the aforementioned purposes, which are relevant for quantum Boltzmann machine learning [82, 85] and quantum thermodynamics more broadly.

To see this, let $H(\theta)$ be a parameterized Hamiltonian of the form in (12), and define the parameterized thermal state $\rho(\theta)$ as follows:

$$\rho(\theta) := \frac{e^{-H(\theta)}}{Z(\theta)}, \quad (156)$$

$$Z(\theta) := \text{Tr}[e^{-H(\theta)}]. \quad (157)$$

Let η be a quantum state to which we have sample access. The quantum relative entropy is defined as [86]

$$D(\eta||\rho(\theta)) := \text{Tr}[\eta(\ln \eta - \ln \rho(\theta))] \quad (158)$$

and is a standard measure of distinguishability well motivated in quantum information theory [87, 88]. The cross entropy corresponds to the second term in (158) and is defined as follows:

$$\Xi(\eta||\rho(\theta)) := -\text{Tr}[\eta \ln \rho(\theta)] \quad (159)$$

$$= \langle H(\theta) \rangle_\eta + \ln Z(\theta). \quad (160)$$

The following expression for the j th partial derivative of $\Xi(\eta||\rho(\theta))$ is known [82, Eq. (4)]:

$$\frac{\partial}{\partial \theta_j} \Xi(\eta||\rho(\theta)) = \langle H_j \rangle_\eta - \langle H_j \rangle_{\rho(\theta)}, \quad (161)$$

following from basic calculus and the fact that

$$\frac{\partial}{\partial \theta_j} Z(\theta) = -\text{Tr} \left[H_j e^{-H(\theta)} \right]. \quad (162)$$

Theorem 12. *The following equality holds:*

$$\begin{aligned} & \Xi(\eta||\rho(\theta)) - \ln d \\ &= \langle H(\theta) \rangle_\eta - \|\theta\|_1 \mathbb{E}_{j \sim q, \lambda \sim \nu} \left[\text{sgn}(\theta_j) \langle H_j \rangle_{\rho(\theta^{(j)}(\lambda))} \right] \end{aligned} \quad (163)$$

$$= \|\theta\|_1 \mathbb{E}_{j \sim q, \lambda \sim \nu} \left[\text{sgn}(\theta_j) \left(\langle H_j \rangle_\eta - \langle H_j \rangle_{\rho(\theta^{(j)}(\lambda))} \right) \right], \quad (164)$$

where $q(j) := \frac{|\theta_j|}{\|\theta\|_1}$ is a probability distribution, ν is a uniform random variable over the unit interval $[0, 1]$, and

$$H(\theta_1, \dots, \theta_J) \equiv H(\theta) = \sum_{j=1}^J \theta_j H_j, \quad (165)$$

$$\theta^{(j)}(\lambda) := (0, \dots, 0, \lambda \theta_j, \theta_{j+1}, \dots, \theta_J), \quad (166)$$

$$\rho(\theta^{(j)}(\lambda)) := \frac{e^{-H(\theta^{(j)}(\lambda))}}{Z(\theta^{(j)}(\lambda))}, \quad (167)$$

$$Z(\theta^{(j)}(\lambda)) := \text{Tr} \left[e^{-H(\theta^{(j)}(\lambda))} \right]. \quad (168)$$

Proof. See Appendix I 1. \square

In Appendix I 2, we use the formula in (164) to delineate a hybrid quantum–classical algorithm for estimating the cross entropy $\Xi(\eta||\rho(\theta))$. Note that it requires methods for thermal state preparation (see, e.g., [84] and references therein for such methods).

By combining (160) and (163), we arrive at the following formula for the log-partition function:

Corollary 1. *Using the same notation as in Theorem 12, the following equality holds:*

$$\ln Z(\theta) = \ln d - \|\theta\|_1 \mathbb{E}_{j \sim q, \lambda \sim \nu} \left[\text{sgn}(\theta_j) \langle H_j \rangle_{\rho(\theta^{(j)}(\lambda))} \right]. \quad (169)$$

In Appendix I 2, we use the formula in (169) to delineate a hybrid quantum–classical algorithm for estimating the log-partition function $\ln Z(\theta)$.

XI. CONCLUSION

In conclusion, the main conceptual contribution of our paper is a novel method for quantizing neurons, rooted

in canonical quantization. Indeed, by viewing a classical neuron as an activation function applied to an energy function (classical Hamiltonian), we quantize this model by replacing the classical Hamiltonian with a quantum Hamiltonian. Applying the activation function to the quantum Hamiltonian results in an activation observable.

Our technical contributions demonstrate how to train and evaluate these quantized neurons for many key examples of activation functions, which include the Fermi–Dirac (sigmoid), hyperbolic tangent, smooth rectified linear unit (ReLU), sigmoid linear unit (SiLU), Gaussian error function (erf), Gaussian-smoothed ReLU, and Gaussian error linear unit (GeLU). For all of these activation functions, we developed methods for single-shot evaluation of them based on quantum convolution algorithms (Algorithms 3 and 6), and we developed formulas for their gradients that lead to hybrid quantum–classical algorithms for efficiently training them.

We generalized the whole framework from finite-dimensional to continuous-variable quantum systems, and we performed numerical experiments that support a separation between the performance of classical neurons and our quantized neurons for binary classification and function approximation. Finally, we proposed canonical quantizations of neural networks based on our quantized neurons, and we proved that a computational decision problem based on Fermi–Dirac neurons is BQP-complete, thus providing complexity-theoretic evidence that they cannot be efficiently simulated classically.

We believe our contributions here lead to many fruitful directions for future research. First, further work is needed to explore the performance of our quantized neurons in a neural network architecture. As mentioned, what seems promising is a hybrid architecture in which the first layer consists of quantized neurons that accept quantum data as inputs and output classical variables, while neurons in later layers are classical and produce classical values at the output of the final layer. It would also certainly be interesting to conduct more numerical experiments that incorporate the effects of finite sampling and scale to larger systems. Our algorithms that realize single-shot evaluation of our quantized neurons all rely on having a control qumode that is prepared and measured and interacts with the data register via controlled Hamiltonian evolution; it is possible to discretize these algorithms based on the methods of [89–91], and it would be interesting to provide a detailed analysis of performance when doing so.

There are many more questions of interest for applications, including a better understanding of which target observables can be efficiently captured by a relatively small number of Fermi–Dirac neurons. This could be of particular interest to condensed-matter physics with many-body observables, for example, in order-parameter discovery and phase classification. This Hamiltonian-based framework lends itself readily to more interpretable learning that additionally includes inductive bias like symmetries. It is also important

to know whether or not there are vanishing-gradient problems [92, 93] or barren-plateau problems [94, 95] in relevant settings for applications. Different activation observables also have different expansions, and the differences in learning can be investigated from the viewpoint of approximation theory. While very high-temperature limits of Fermi–Dirac neurons are expected to be less powerful than low-temperature limits (analogously to how high-temperature quantum thermal states are classically simulable but low temperatures ones need not be), more remains to be understood how this power changes as a function of temperature and whether there are deeper insights that can emerge from

thermodynamical analogies.

ACKNOWLEDGMENTS

NL acknowledges funding from the Science and Technology Commission of Shanghai Municipality (STCSM) grant no. 24LZ1401200 (21JC1402900), NSFC grants no. 12471411 and no. 12341104, the Shanghai Jiao Tong University 2030 Initiative, the Shanghai Pilot Program for Basic Research, and the Fundamental Research Funds for the Central Universities. MMW acknowledges support from the National Science Foundation under grant no. 2329662.

-
- [1] G.-L. Long, Progress in quantum information, *National Science Review* **12**, nwaf289 (2025).
- [2] D. D. Awschalom, H. Bernien, R. Hanson, W. D. Oliver, and J. Vučković, Challenges and opportunities for quantum information hardware, *Science* **390**, 1004 (2025).
- [3] A. M. Dalzell, S. McArdle, M. Berta, P. Bienias, C.-F. Chen, A. Gilyén, C. T. Hann, M. J. Kastoryano, E. T. Khabiboulline, A. Kubica, G. Salton, S. Wang, and F. G. S. L. Brandão, *Quantum Algorithms: A Survey of Applications and End-to-end Complexities* (Cambridge University Press, 2025).
- [4] N. Gisin and R. Thew, Quantum communication, *Nature Photonics* **1**, 165 (2007).
- [5] C. L. Degen, F. Reinhard, and P. Cappellaro, Quantum sensing, *Reviews of Modern Physics* **89**, 035002 (2017).
- [6] S. Y. Chang and M. Cerezo, *A primer on quantum machine learning* (2025), [arXiv:2511.15969v1](https://arxiv.org/abs/2511.15969v1) [quant-ph].
- [7] A. Abbas, A. Ambainis, B. Augustino, A. Bärtschi, H. Buhrman, C. Coffrin, G. Cortiana, V. Dunjko, D. J. Egger, B. G. Elmegreen, N. Franco, F. Fratini, B. Fuller, J. Gacon, C. Gondiulea, S. Gribling, S. Gupta, S. Hadfield, R. Heese, G. Kircher, T. Kleinert, T. Koch, G. Korpas, S. Lenk, J. Marecek, V. Markov, G. Mazzola, S. Mensa, N. Mohseni, G. Nannicini, C. O’Meara, E. P. Tapia, S. Pokutta, M. Proissl, P. Rebentrost, E. Sahin, B. C. B. Symons, S. Tornow, V. Valls, S. Woerner, M. L. Wolf-Bauwens, J. Yard, S. Yarkoni, D. Zechiel, S. Zhuk, and C. Zoufal, Challenges and opportunities in quantum optimization, *Nature Reviews Physics* **6**, 718 (2024).
- [8] N. Liu and M. M. Wilde, *Fermi–Dirac thermal measurements: A framework for quantum hypothesis testing and semidefinite optimization* (2026), [arXiv:2603.04061v1](https://arxiv.org/abs/2603.04061v1) [quant-ph].
- [9] T. Hastie, R. Tibshirani, and J. Friedman, *The Elements of Statistical Learning: Data Mining, Inference, and Prediction*, 2nd ed., Springer Series in Statistics (Springer, New York, NY, 2009).
- [10] A. Kapoor, N. Wiebe, and K. Svore, Quantum perceptron models, in *Advances in Neural Information Processing Systems*, Vol. 29, edited by D. Lee, M. Sugiyama, U. Luxburg, I. Guyon, and R. Garnett (Curran Associates, Inc., 2016) [arXiv:1602.04799](https://arxiv.org/abs/1602.04799) [quant-ph].
- [11] Y. Cao, G. G. Guerreschi, and A. Aspuru-Guzik, *Quantum neuron: an elementary building block for machine learning on quantum computers* (2017), [arXiv:1711.11240](https://arxiv.org/abs/1711.11240) [quant-ph].
- [12] K. H. Wan, O. Dahlsten, H. Kristjánsson, R. Gardner, and M. S. Kim, Quantum generalisation of feedforward neural networks, *npj Quantum Information* **3**, 36 (2017).
- [13] W. Hu, Towards a real quantum neuron, *Natural Science* **10**, 99 (2018).
- [14] N. Killoran, T. R. Bromley, J. M. Arrazola, M. Schuld, N. Quesada, and S. Lloyd, Continuous-variable quantum neural networks, *Physical Review Research* **1**, 033063 (2019).
- [15] S. Yan, H. Qi, and W. Cui, Nonlinear quantum neuron: A fundamental building block for quantum neural networks, *Physical Review A* **102**, 052421 (2020).
- [16] L. B. Kristensen, M. Degroote, P. Wittek, A. Aspuru-Guzik, and N. T. Zinner, An artificial spiking quantum neuron, *npj Quantum Information* **7**, 59 (2021).
- [17] C. A. Monteiro, G. I. S. Filho, M. H. J. Costa, F. M. de Paula Neto, and W. R. de Oliveira, Quantum neuron with real weights, *Neural Networks* **143**, 698 (2021).
- [18] U. Singh, A. Z. Goldberg, and K. Heshami, Coherent feed-forward quantum neural network, *Quantum Machine Intelligence* **6**, 89 (2024).
- [19] R. Barney, D. Lakhdar-Hamina, and V. Galitski, *Natural quantization of neural networks* (2025), [arXiv:2503.15482](https://arxiv.org/abs/2503.15482) [quant-ph].
- [20] S. Roncallo, A. R. Morgillo, C. Macchiavello, L. Maccone, and S. Lloyd, Quantum optical classifier with superexponential speedup, *Communications Physics* **8**, 147 (2025).
- [21] C. Dugas, Y. Bengio, F. Bélisle, C. Nadeau, and R. Garcia, Incorporating second-order functional knowledge for better option pricing, in *Advances in Neural Information Processing Systems*, Vol. 13, edited by T. Leen, T. Dietterich, and V. Tresp (MIT Press, 2000).
- [22] X. Glorot, A. Bordes, and Y. Bengio, Deep sparse rectifier neural networks, in *Proceedings of*

- the Fourteenth International Conference on Artificial Intelligence and Statistics*, Proceedings of Machine Learning Research, Vol. 15, edited by G. Gordon, D. Dunson, and M. Dudík (PMLR, Fort Lauderdale, FL, USA, 2011) pp. 315–323.
- [23] S. Elfving, E. Uchibe, and K. Doya, Sigmoid-weighted linear units for neural network function approximation in reinforcement learning, *Neural Networks* **107**, 3 (2018), special issue on deep reinforcement learning, arXiv:1702.03118 [cs.LG].
- [24] P. Ramachandran, B. Zoph, and Q. V. Le, *Searching for activation functions* (2017), arXiv:1710.05941 [cs.NE].
- [25] F. Rosenblatt, The perceptron: A probabilistic model for information storage and organization in the brain, *Psychological Review* **65**, 386 (1958).
- [26] P. J. Werbos, *Beyond Regression: New Tools for Prediction and Analysis in the Behavioral Sciences*, Ph.D. thesis, Harvard University (1974).
- [27] R. Shankar, *Principles of Quantum Mechanics* (Springer, 1994).
- [28] S. Sachdev, *Quantum Phase Transitions*, 2nd ed. (Cambridge University Press, 2011).
- [29] D. C. Mattis, *The Theory of Magnetism Made Simple* (World Scientific, 2006).
- [30] C. Goldschmidt, D. Ueltschi, and P. Windridge, Entropy and the quantum II, *Contemporary Mathematics* (2011) Chap. Quantum Heisenberg models and their probabilistic representations, pp. 177–224, arXiv:1104.0983 [math-ph].
- [31] J. Lederer, *Activation functions in artificial neural networks: A systematic overview* (2021), arXiv:2101.09957 [cs.LG].
- [32] S. R. Dubey, S. K. Singh, and B. B. Chaudhuri, Activation functions in deep learning: A comprehensive survey and benchmark, *Neurocomputing* **503**, 92 (2022).
- [33] S. Lloyd, Universal quantum simulators, *Science* **273**, 1073 (1996).
- [34] A. M. Childs, D. Maslov, Y. Nam, N. J. Ross, and Y. Su, Toward the first quantum simulation with quantum speedup, *Proceedings of the National Academy of Sciences* **115**, 9456 (2018).
- [35] M. Motta and J. E. Rice, Emerging quantum computing algorithms for quantum chemistry, *WIREs Computational Molecular Science* **12**, e1580 (2022).
- [36] R. Cleve, A. Ekert, C. Macchiavello, and M. Mosca, Quantum algorithms revisited, *Proceedings of the Royal Society A* **454**, 339 (1998).
- [37] D. Patel, D. Koch, S. Patel, and M. M. Wilde, *Quantum Boltzmann machine learning of ground-state energies* (2025), arXiv:2410.12935 [quant-ph].
- [38] D. Patel and M. M. Wilde, Natural gradient and parameter estimation for quantum Boltzmann machines, *Physical Review A* **112**, 052421 (2025).
- [39] M. Minervini, D. Patel, and M. M. Wilde, Evolved quantum Boltzmann machines, *Physical Review A* **113**, 032427 (2026).
- [40] N. Liu, M. Minervini, D. Patel, and M. M. Wilde, *Quantum thermodynamics and semi-definite optimization* (2025), arXiv:2505.04514 [quant-ph].
- [41] N. Liu, J. Thompson, C. Weedbrook, S. Lloyd, V. Vedral, M. Gu, and K. Modi, Power of one qumode for quantum computation, *Physical Review A* **93**, 052304 (2016).
- [42] S. Jin and N. Liu, Analog quantum simulation of partial differential equations, *Quantum Science and Technology* **9**, 035047 (2024).
- [43] S. Jin, N. Liu, and Y. Yu, Quantum simulation of partial differential equations: Applications and detailed analysis, *Physical Review A* **108**, 032603 (2023).
- [44] S. Jin, N. Liu, and Y. Yu, Quantum simulation of partial differential equations via Schrödingerization, *Physical Review Letters* **133**, 230602 (2024).
- [45] A. Serafini, *Quantum Continuous Variables: A Primer of Theoretical Methods*, 2nd ed. (CRC Press, 2023).
- [46] U. L. Andersen, G. Leuchs, and C. Silberhorn, Continuous-variable quantum information processing, *Laser & Photonics Reviews* **4**, 337 (2010), arXiv:1008.3468 [quant-ph].
- [47] C. Cade, M. Folkertsma, S. Gharibian, R. Hayakawa, F. Le Gall, T. Morimae, and J. Weggemans, Improved hardness results for the guided local Hamiltonian problem, in *50th International Colloquium on Automata, Languages, and Programming (ICALP 2023)*, Leibniz International Proceedings in Informatics (LIPIcs), Vol. 261, edited by K. Etessami, U. Feige, and G. Puppis (Schloss Dagstuhl – Leibniz-Zentrum für Informatik, Dagstuhl, Germany, 2023) pp. 32:1–32:19.
- [48] A. G. Ivakhnenko, Polynomial theory of complex systems, *IEEE Transactions on Systems, Man, and Cybernetics SMC-1*, 364 (1971).
- [49] D. E. Rumelhart, J. L. McClelland, and the PDP Research Group, *Parallel Distributed Processing: Explorations in the Microstructure of Cognition, Volume 1: Foundations* (MIT Press, 1986).
- [50] C. L. Giles and T. Maxwell, Learning, invariance, and generalization in high-order neural networks, *Applied Optics* **26**, 4972 (1987).
- [51] W. Hoeffding, Probability inequalities for sums of bounded random variables, *Journal of the American Statistical Association* **58**, 13 (1963).
- [52] R. Bandyopadhyay, A. H. Rubin, M. Radulaski, and M. M. Wilde, Efficient quantum algorithms for testing symmetries of open quantum systems, *Open Systems & Information Dynamics* **30**, 2350017 (2023).
- [53] A. Gilyén, Y. Su, G. H. Low, and N. Wiebe, Quantum singular value transformation and beyond: exponential improvements for quantum matrix arithmetics, in *Proceedings of the 51st Annual ACM SIGACT Symposium on Theory of Computing*, STOC 2019 (Association for Computing Machinery, New York, NY, USA, 2019) p. 193–204, arXiv:1806.01838.
- [54] Y. Qiu, L. Pira, and P. Reberntrost, *Quantum learning with tunable loss functions* (2025), arXiv:2508.21369 [quant-ph].
- [55] Y. Qiu, J. Lumberras, X. Li, and P. Reberntrost, *Quantum tilted loss in variational optimization: Theory and applications* (2026), arXiv:2605.02850 [quant-ph].
- [56] Z. Zhang, L. Shi, and D.-X. Zhou, Classification with deep neural networks and logistic loss, *Journal of Machine Learning Research* **25**, 1 (2024).
- [57] L. Bottou, F. E. Curtis, and J. Nocedal, Optimization methods for large-scale machine learning, *SIAM Review* **60**, 223 (2018).
- [58] B. L. Higgins, A. C. Doherty, S. D. Bartlett, G. J. Pryde, and H. M. Wiseman, Multiple-copy state discrimination: Thinking globally, acting locally, *Physical Review A* **83**, 052314 (2011).

- [59] V. Giovannetti, S. Guha, S. Lloyd, L. Maccone, J. H. Shapiro, and H. P. Yuen, Classical capacity of the lossy bosonic channel: The exact solution, *Physical Review Letters* **92**, 027902 (2004).
- [60] C. A. Fuchs, Nonorthogonal quantum states maximize classical information capacity, *Physical Review Letters* **79**, 1162 (1997).
- [61] C. King, M. Nathanson, and M. B. Ruskai, Qubit channels can require more than two inputs to achieve capacity, *Physical Review Letters* **88**, 057901 (2002).
- [62] K. Jarrett, K. Kavukcuoglu, M. Ranzato, and Y. LeCun, What is the best multi-stage architecture for object recognition?, in *2009 IEEE 12th International Conference on Computer Vision* (2009) pp. 2146–2153.
- [63] V. Nair and G. E. Hinton, Rectified linear units improve restricted Boltzmann machines, in *Proceedings of the 27th International Conference on Machine Learning (ICML)* (2010) pp. 807–814.
- [64] S. D. Bartlett, B. C. Sanders, S. L. Braunstein, and K. Nemoto, Efficient classical simulation of continuous variable quantum information processes, *Physical Review Letters* **88**, 097904 (2002).
- [65] V. Veitch, N. Wiebe, C. Ferrie, and J. Emerson, Efficient simulation scheme for a class of quantum optics experiments with non-negative Wigner representation, *New Journal of Physics* **15**, 013037 (2013).
- [66] B. Peng, Y. Su, D. Claudino, K. Kowalski, G. Hao Low, and M. Roetteler, Quantum simulation of boson-related Hamiltonians: techniques, effective Hamiltonian construction, and error analysis, *Quantum Science and Technology* **10**, 023002 (2025).
- [67] S. Becker, N. Galke, L. van Luijk, and R. Salzmann, Convergence rates for the Trotter splitting for unbounded operators, *Foundations of Computational Mathematics* [10.1007/s10208-025-09730-w](https://doi.org/10.1007/s10208-025-09730-w) (2025).
- [68] G. Lugosi and S. Mendelson, Mean estimation and regression under heavy-tailed distributions: A survey, *Foundations of Computational Mathematics* **19**, 1145 (2019), [arXiv:1906.04280 \[math.ST\]](https://arxiv.org/abs/1906.04280).
- [69] Y. Liu, S. Singh, K. C. Smith, E. Crane, J. M. Martyn, A. Eickbusch, A. Schuckert, R. D. Li, J. Sinanan-Singh, M. B. Soley, T. Tsunoda, I. L. Chuang, N. Wiebe, and S. M. Girvin, Hybrid oscillator-qubit quantum processors: Instruction set architectures, abstract machine models, and applications, *PRX Quantum* **7**, 010201 (2026).
- [70] A. He, Code for “Fermi–Dirac machines as quantizations of neurons”, <https://github.com/Alexheeeee/quantized-neurons> (2026), gitHub repository, accessed 2026-05-21.
- [71] D. E. Rumelhart, G. E. Hinton, and R. J. Williams, Learning internal representations by error propagation, in *Parallel Distributed Processing: Explorations in the Microstructure of Cognition, Volume 1: Foundations*, edited by D. E. Rumelhart, J. L. McClelland, and the PDP Research Group (MIT Press, Cambridge, MA, 1986) pp. 318–362.
- [72] D. E. Rumelhart, G. E. Hinton, and R. J. Williams, Learning representations by back-propagating errors, *Nature* **323**, 533 (1986).
- [73] A. Abbas, R. King, H.-Y. Huang, W. J. Huggins, R. Movassagh, D. Gilboa, and J. R. McClean, On quantum backpropagation, information reuse, and cheating measurement collapse, in *Thirty-seventh Conference on Neural Information Processing Systems* (2023).
- [74] B. Müller, J. Reinhardt, and M. T. Strickland, Stochastic neurons, in *Neural Networks: An Introduction* (Springer Berlin Heidelberg, Berlin, Heidelberg, 1995) pp. 38–45.
- [75] C. Turchetti, *Stochastic Models of Neural Networks* (IOS Press, Amsterdam, 2004).
- [76] A. Y. Kitaev, A. H. Shen, and M. N. Vyalıy, *Classical and Quantum Computation*, Graduate Studies in Mathematics, Vol. 47 (American Mathematical Society, 2002).
- [77] R. P. Feynman, Quantum mechanical computers, *Optics News* **11**, 11 (1985).
- [78] D. Aharonov, W. van Dam, J. Kempe, Z. Landau, S. Lloyd, and O. Regev, Adiabatic quantum computation is equivalent to standard quantum computation, *SIAM Journal on Computing* **37**, 166 (2007).
- [79] S. Gharibian, *Approximation, proof systems, and correlations in a quantum world* (2013), [arXiv:1301.2632 \[quant-ph\]](https://arxiv.org/abs/1301.2632).
- [80] M. H. Amin, E. Andriyash, J. Rolfe, B. Kulchytskyy, and R. Melko, Quantum Boltzmann machine, *Physical Review X* **8**, 021050 (2018).
- [81] M. Benedetti, J. Realpe-Gómez, R. Biswas, and A. Perdomo-Ortiz, Quantum-assisted learning of hardware-embedded probabilistic graphical models, *Physical Review X* **7**, 041052 (2017).
- [82] M. Kieferova and N. Wiebe, Tomography and generative data modeling via quantum Boltzmann training, *Physical Review A* **96**, 062327 (2017), [arXiv:1612.05204 \[quant-ph\]](https://arxiv.org/abs/1612.05204).
- [83] M. Lindsey, *Fast randomized entropically regularized semidefinite programming* (2023), [arXiv:2303.12133v1 \[math.OC\]](https://arxiv.org/abs/2303.12133v1).
- [84] C.-F. Chen, M. Kastoryano, F. G. S. L. Brandão, and A. Gilyén, Efficient quantum thermal simulation, *Nature* **646**, 561 (2025).
- [85] L. Coopmans and M. Benedetti, On the sample complexity of quantum Boltzmann machine learning, *Communications Physics* **7**, 274 (2024).
- [86] H. Umegaki, Conditional expectation in an operator algebra, IV (entropy and information), *Kodai Mathematical Journal* **14**, 59 (1962).
- [87] F. Hiai and D. Petz, The proper formula for relative entropy and its asymptotics in quantum probability, *Communications in Mathematical Physics* **143**, 99 (1991).
- [88] T. Ogawa and H. Nagaoka, Strong converse and Stein’s lemma in quantum hypothesis testing, *IEEE Transactions on Information Theory* **46**, 2428 (2000).
- [89] S. McArdle, A. Gilyén, and M. Berta, *Quantum state preparation without coherent arithmetic* (2025), [arXiv:2210.14892 \[quant-ph\]](https://arxiv.org/abs/2210.14892).
- [90] N. Guseynov and N. Liu, Efficient explicit circuit for quantum state preparation of piecewise continuous functions, *Physical Review A* **113**, 012604 (2026).
- [91] B. Claudon, A. Lucas, J.-P. Piquemal, C. Feniou, and J. Zylberman, *Logarithmic-depth quantum state preparation of polynomials* (2026), [arXiv:2603.16527 \[quant-ph\]](https://arxiv.org/abs/2603.16527).
- [92] S. Hochreiter, The vanishing gradient problem during learning recurrent neural nets and problem solutions,

- International Journal of Uncertainty, Fuzziness and Knowledge-Based Systems **6**, 107 (1998).
- [93] I. Goodfellow, Y. Bengio, and A. Courville, *Deep Learning* (MIT Press, Cambridge, MA, 2016).
- [94] J. R. McClean, S. Boixo, V. N. Smelyanskiy, R. Babbush, and H. Neven, Barren plateaus in quantum neural network training landscapes, *Nature Communications* **9**, 4812 (2018).
- [95] M. Larocca, S. Thanasilp, S. Wang, K. Sharma, J. Biamonte, P. J. Coles, L. Cincio, J. R. McClean, Z. Holmes, and M. Cerezo, Barren plateaus in variational quantum computing, *Nature Reviews Physics* **7**, 174 (2025).
- [96] M. M. Wilde, Quantum Fisher information matrices from Rényi relative entropies (2025), arXiv:2510.02218 [quant-ph].
- [97] F. X. Kaertner, Ultrafast optics, appendix: Sech algebra, [https://eng.libretexts.org/Bookshelves/Electrical_Engineering/Electro-Optics/Ultrafast_Optics_\(Kaertner\)/03:_Nonlinear_Pulse_Propagation/3.08:_Appendix-_Sech-Algebra](https://eng.libretexts.org/Bookshelves/Electrical_Engineering/Electro-Optics/Ultrafast_Optics_(Kaertner)/03:_Nonlinear_Pulse_Propagation/3.08:_Appendix-_Sech-Algebra) (2005), mIT OpenCourseWare / LibreTexts, Accessed: 2026-04-23.
- [98] R. Coleman, Differentiation, in *Calculus on Normed Vector Spaces* (Springer New York, New York, NY, 2012) pp. 35–60.
- [99] S. Ejima and Y. Ogata, Perturbation theory of KMS states, *Annales Henri Poincaré* **20**, 2971 (2019).
- [100] A. Anshu, S. Arunachalam, T. Kuwahara, and M. Soleimanifar, Sample-efficient learning of interacting quantum systems, *Nature Physics* **17**, 931 (2021).

Appendix A: Derivations for Fermi–Dirac machines

1. Proof of Theorem 1 (derivation of gradient)

In this appendix, we derive a formula for the gradient that is useful for estimation on quantum computers. We begin by deriving a novel formula for the derivative of the matrix hyperbolic tangent function.

Lemma 1. *Let $x \in \mathbb{R}$, and let $x \mapsto A(x)$ be a Hermitian-valued function. Then the following equality holds:*

$$\frac{\partial}{\partial x} \tanh(A(x)) = \int_{-\infty}^{\infty} dt \mu(t) \int_0^1 ds e^{itsA(x)} \left(\frac{\partial}{\partial x} A(x) \right) e^{it(1-s)A(x)}, \quad (\text{A1})$$

where $\mu(t)$ is the following probability density function:

$$\mu(t) := \frac{t}{2 \sinh\left(\frac{\pi t}{2}\right)}. \quad (\text{A2})$$

Proof. To begin with, let

$$A(x) = \sum_k \lambda_k \Pi_k \quad (\text{A3})$$

be a spectral decomposition of $A(x)$, where we have omitted the dependence on x in the eigenvalues and eigenprojections. Consider that the derivative of the matrix hyperbolic tangent function is given by

$$\frac{\partial}{\partial x} \tanh(A(x)) = \sum_{k,\ell} f_{\tanh}^{[1]}(\lambda_k, \lambda_\ell) \Pi_k \left(\frac{\partial}{\partial x} A(x) \right) \Pi_\ell, \quad (\text{A4})$$

where $f_{\tanh}^{[1]}$ is the first divided difference of the hyperbolic tangent function, defined as

$$f_{\tanh}^{[1]}(y_1, y_2) := \begin{cases} \frac{\tanh(y_1) - \tanh(y_2)}{y_1 - y_2} & : y_1 \neq y_2 \\ \operatorname{sech}^2(y_1) & : y_1 = y_2 \end{cases}, \quad (\text{A5})$$

where we used the fact that $\frac{\partial}{\partial x} \tanh(x) = \operatorname{sech}^2(x)$ (see, e.g., [96, Theorem 42] for a proof of (A4)). Now observe that an alternative expression for $f_{\tanh}^{[1]}$ is as follows:

$$f_{\tanh}^{[1]}(y_1, y_2) = \int_0^1 ds \operatorname{sech}^2(sy_1 + (1-s)y_2), \quad (\text{A6})$$

as a consequence of the fundamental theorem of calculus and that

$$\frac{d}{ds} \tanh(sy_1 + (1-s)y_2) = \operatorname{sech}^2(sy_1 + (1-s)y_2) (y_1 - y_2). \quad (\text{A7})$$

Then it follows that

$$\frac{\partial}{\partial x} \tanh(A(x)) = \sum_{k,\ell} \int_0^1 ds \operatorname{sech}^2(s\lambda_k + (1-s)\lambda_\ell) \Pi_k \left(\frac{\partial}{\partial x} A(x) \right) \Pi_\ell. \quad (\text{A8})$$

Now consider that the Fourier transform of $\text{sech}^2(x)$ is as follows [97]:

$$\text{sech}^2(x) = \int_{-\infty}^{\infty} dt \mu(t) e^{itx}, \quad (\text{A9})$$

where $\mu(t)$ is the following probability density function:

$$\mu(t) := \frac{t}{2 \sinh\left(\frac{\pi t}{2}\right)}. \quad (\text{A10})$$

Then it follows that

$$\frac{\partial}{\partial x} \tanh(A(x)) = \sum_{k,\ell} \int_0^1 ds \int_{-\infty}^{\infty} dt \mu(t) e^{it(s\lambda_k + (1-s)\lambda_\ell)} \Pi_k \left(\frac{\partial}{\partial x} A(x) \right) \Pi_\ell \quad (\text{A11})$$

$$= \int_{-\infty}^{\infty} dt \mu(t) \int_0^1 ds \sum_{k,\ell} e^{it(s\lambda_k + (1-s)\lambda_\ell)} \Pi_k \left(\frac{\partial}{\partial x} A(x) \right) \Pi_\ell \quad (\text{A12})$$

$$= \int_{-\infty}^{\infty} dt \mu(t) \int_0^1 ds \left(\sum_k e^{its\lambda_k} \Pi_k \right) \left(\frac{\partial}{\partial x} A(x) \right) \sum_\ell e^{it(1-s)\lambda_\ell} \Pi_\ell \quad (\text{A13})$$

$$= \int_{-\infty}^{\infty} dt \mu(t) \int_0^1 ds e^{itsA(x)} \left(\frac{\partial}{\partial x} A(x) \right) e^{it(1-s)A(x)}, \quad (\text{A14})$$

thus concluding the proof. \square

Remark 2. For Hermitian matrices A and H , we can write the Fréchet derivative [98] of $\tanh(A)$ at H as follows:

$$D \tanh(A)[H] = \int_{-\infty}^{\infty} dt \mu(t) \int_0^1 ds e^{itsA} H e^{it(1-s)A}. \quad (\text{A15})$$

Theorem (Restatement of Theorem 1). *The following equality holds:*

$$\frac{\partial}{\partial \theta_j} \text{Tr}[g_T(H(\theta))\rho] = \frac{1}{T} \mathbb{E}_{t \sim \mu, s \sim v} \left[\Re \left[\text{Tr} \left[H_j e^{iH(\theta)t/T} \mathcal{U}_{st/T}^{H(\theta)}(\rho) \right] \right] \right], \quad (\text{A16})$$

where the objective function $\text{Tr}[g_T(H(\theta))\rho]$ is defined in (17), $\mu(t)$ is the probability density function defined in (A2), v is a uniform random variable on the unit interval $[0, 1]$, and $\mathcal{U}_t^{H(\theta)}$ is the following unitary quantum channel:

$$\mathcal{U}_t^{H(\theta)}(\cdot) := e^{-iH(\theta)t}(\cdot)e^{iH(\theta)t}, \quad (\text{A17})$$

Proof of Theorem 1. Consider that

$$\frac{\partial}{\partial \theta_j} \text{Tr}[g_T(H(\theta))\rho] = \text{Tr} \left[\left(\frac{\partial}{\partial \theta_j} g_T(H(\theta)) \right) \rho \right] \quad (\text{A18})$$

$$= \int_{-\infty}^{\infty} dt \mu(t) \int_0^1 ds \text{Tr} \left[e^{itsH(\theta)/T} \left(\frac{\partial}{\partial \theta_j} \frac{H(\theta)}{T} \right) e^{it(1-s)H(\theta)/T} \rho \right] \quad (\text{A19})$$

$$= \frac{1}{T} \int_{-\infty}^{\infty} dt \mu(t) \int_0^1 ds \text{Tr} \left[e^{itsH(\theta)/T} H_j e^{it(1-s)H(\theta)/T} \rho \right] \quad (\text{A20})$$

$$= \frac{1}{T} \int_{-\infty}^{\infty} dt \mu(t) \int_0^1 ds \text{Tr} \left[H_j e^{it(1-s)H(\theta)/T} \rho e^{itsH(\theta)/T} \right]. \quad (\text{A21})$$

Using the conventions in the statement of the lemma, we can rewrite the expression once more as follows:

$$\frac{\partial}{\partial \theta_j} \text{Tr}[g_T(H(\theta))\rho] = \frac{1}{T} \mathbb{E}_{t \sim \mu, s \sim \nu} \left[\text{Tr} \left[H_j e^{iH(\theta)t/T} \mathcal{U}_{ts/T}^{H(\theta)}(\rho) \right] \right]. \quad (\text{A22})$$

We can now observe that $\frac{\partial}{\partial \theta_j} g_T(H(\theta))$ is a Hermitian matrix. Indeed, this is a consequence of the fact that $H(\theta)$ is a Hermitian matrix and from the limit definition of the derivative as a limit of a divided difference. Given that ρ is Hermitian, we conclude that $\frac{\partial}{\partial \theta_j} \text{Tr}[g_T(H(\theta))\rho]$ is real. So then it follows that

$$\frac{\partial}{\partial \theta_j} \text{Tr}[g_T(H(\theta))\rho] = \Re \left[\frac{\partial}{\partial \theta_j} \text{Tr}[g_T(H(\theta))\rho] \right] \quad (\text{A23})$$

$$= \frac{1}{T} \Re \left[\mathbb{E}_{t \sim \mu, s \sim \nu} \left[\text{Tr} \left[H_j e^{iH(\theta)t/T} \mathcal{U}_{ts/T}^{H(\theta)}(\rho) \right] \right] \right] \quad (\text{A24})$$

$$= \frac{1}{T} \mathbb{E}_{t \sim \mu, s \sim \nu} \left[\Re \left[\text{Tr} \left[H_j e^{iH(\theta)t/T} \mathcal{U}_{ts/T}^{H(\theta)}(\rho) \right] \right] \right], \quad (\text{A25})$$

where the last equality follows because the expectations are over probability density functions, which are in turn real-valued. \square

2. Proof of Theorem 2 (derivation of formula for the objective function)

We can also rewrite the objective function itself in terms of its partial derivatives, by employing Theorem 1 and the fundamental theorem of calculus, leading to the following theorem.

Theorem (Restatement of Theorem 2). *The following equality holds:*

$$\text{Tr}[g_T(H(\theta))\rho] = \frac{\|\theta\|_1}{T} \mathbb{E}_{\substack{j \sim q, t \sim \mu, \\ s \sim \nu, \lambda \sim \nu}} \left[\text{sgn}(\theta_j) \Re \left[\text{Tr} \left[H_j e^{iH(\theta^{(j)}(\lambda))t/T} \mathcal{U}_{ts/T}^{H(\theta^{(j)}(\lambda))}(\rho) \right] \right] \right], \quad (\text{A26})$$

where $q(j) := \frac{|\theta_j|}{\|\theta\|_1}$ is a probability distribution, and

$$H(\theta_1, \dots, \theta_J) \equiv H(\theta) = \sum_{j=1}^J \theta_j H_j, \quad (\text{A27})$$

$$\theta^{(j)}(\lambda) := (0, \dots, 0, \lambda \theta_j, \theta_{j+1}, \dots, \theta_J). \quad (\text{A28})$$

Proof of Theorem 2. Consider that

$$\begin{aligned} & \text{Tr}[g_T(H(\theta))\rho] - \text{Tr}[g_T(H(0, \theta_2, \dots, \theta_J))\rho] \\ &= \text{Tr}[g_T(H(\theta_1, \theta_2, \dots, \theta_J))\rho] - \text{Tr}[g_T(H(0, \theta_2, \dots, \theta_J))\rho] \end{aligned} \quad (\text{A29})$$

$$= \text{Tr}[g_T(H(\theta^{(1)}(1)))\rho] - \text{Tr}[g_T(H(\theta^{(1)}(0)))\rho] \quad (\text{A30})$$

$$= \int_0^1 d\lambda_1 \frac{\partial}{\partial \lambda_1} \text{Tr}[g_T(H(\theta^{(1)}(\lambda_1)))\rho] \quad (\text{A31})$$

$$= \int_0^1 d\lambda_1 \frac{\theta_1}{T} \mathbb{E}_{t \sim \mu, s \sim \nu} \left[\Re \left[\text{Tr} \left[H_1 e^{iH(\theta^{(1)}(\lambda_1))t/T} \mathcal{U}_{ts/T}^{H(\theta^{(1)}(\lambda_1))}(\rho) \right] \right] \right] \quad (\text{A32})$$

$$= \frac{\theta_1}{T} \mathbb{E}_{t \sim \mu, s \sim \nu, \lambda_1 \sim \nu} \left[\Re \left[\text{Tr} \left[H_1 e^{iH(\theta^{(1)}(\lambda_1))t/T} \mathcal{U}_{ts/T}^{H(\theta^{(1)}(\lambda_1))}(\rho) \right] \right] \right]. \quad (\text{A33})$$

The penultimate equality follows from an application of Theorem 1, while accounting for the fact that

$$\frac{\partial}{\partial \lambda_1} H(\theta^{(1)}(\lambda_1)) = \theta_1 H_1. \quad (\text{A34})$$

Additionally,

$$\begin{aligned} & \text{Tr}[g_T(H(0, \theta_2, \dots, \theta_J))\rho] - \text{Tr}[g_T(H(0, 0, \theta_3, \dots, \theta_J))\rho] \\ &= \text{Tr}[g_T(H(\theta^{(2)}(1)))\rho] - \text{Tr}[g_T(H(\theta^{(2)}(0)))\rho] \end{aligned} \quad (\text{A35})$$

$$= \int_0^1 d\lambda_2 \frac{\partial}{\partial \lambda_2} \text{Tr}[g_T(H(\theta^{(2)}(\lambda_2)))\rho] \quad (\text{A36})$$

$$= \int_0^1 d\lambda_2 \frac{\theta_2}{T} \mathbb{E}_{t \sim \mu, s \sim \nu} \left[\Re \left[\text{Tr} \left[H_2 e^{iH(\theta^{(2)}(\lambda_2))t/T} \mathcal{U}_{ts/T}^{H(\theta^{(2)}(\lambda_2))}(\rho) \right] \right] \right] \quad (\text{A37})$$

$$= \frac{\theta_2}{T} \mathbb{E}_{t \sim \mu, s \sim \nu, \lambda_2 \sim \nu} \left[\Re \left[\text{Tr} \left[H_2 e^{iH(\theta^{(2)}(\lambda_2))t/T} \mathcal{U}_{ts/T}^{H(\theta^{(2)}(\lambda_2))}(\rho) \right] \right] \right]. \quad (\text{A38})$$

We continue iteratively along these lines and find that the last term is given by

$$\begin{aligned} & \text{Tr}[g_T(H(0, \dots, 0, \theta_J))\rho] \\ &= \text{Tr}[g_T(H(0, \dots, 0, \theta_J))\rho] - \text{Tr}[g_T(H(0, \dots, 0, 0))\rho] \end{aligned} \quad (\text{A39})$$

$$= \text{Tr}[g_T(H(\theta^{(J)}(1)))\rho] - \text{Tr}[g_T(H(\theta^{(J)}(0)))\rho] \quad (\text{A40})$$

$$= \frac{\theta_J}{T} \mathbb{E}_{t \sim \mu, s \sim \nu, \lambda_J \sim \nu} \left[\Re \left[\text{Tr} \left[H_J e^{iH(\theta^{(J)}(\lambda_J))t/T} \mathcal{U}_{ts/T}^{H(\theta^{(J)}(\lambda_J))}(\rho) \right] \right] \right], \quad (\text{A41})$$

where we used the fact that

$$g_T(H(\theta^{(J)}(0))) = g_T(H(0, \dots, 0)) = g_T(0) = 0, \quad (\text{A42})$$

given that $\tanh(0) = 0$. So then we form a telescoping sum and conclude that

$$\begin{aligned} \text{Tr}[g_T(H(\theta))\rho] &= \text{Tr}[g_T(H(\theta))\rho] - \text{Tr}[g_T(H(0, \theta_2, \dots, \theta_J))\rho] \\ &\quad + \text{Tr}[g_T(H(0, \theta_2, \dots, \theta_J))\rho] - \text{Tr}[g_T(H(0, 0, \theta_3, \dots, \theta_J))\rho] \\ &\quad + \dots + \text{Tr}[g_T(H(0, \dots, 0, \theta_J))\rho] - \text{Tr}[g_T(H(0, \dots, 0, 0))\rho] \end{aligned} \quad (\text{A43})$$

$$\begin{aligned} &= \frac{\theta_1}{T} \mathbb{E}_{t \sim \mu, s \sim \nu, \lambda_1 \sim \nu} \left[\Re \left[\text{Tr} \left[H_1 e^{iH(\theta^{(1)}(\lambda_1))t/T} \mathcal{U}_{ts/T}^{H(\theta^{(1)}(\lambda_1))}(\rho) \right] \right] \right] \\ &\quad + \frac{\theta_2}{T} \mathbb{E}_{t \sim \mu, s \sim \nu, \lambda_2 \sim \nu} \left[\Re \left[\text{Tr} \left[H_2 e^{iH(\theta^{(2)}(\lambda_2))t/T} \mathcal{U}_{ts/T}^{H(\theta^{(2)}(\lambda_2))}(\rho) \right] \right] \right] \\ &\quad + \frac{\theta_3}{T} \mathbb{E}_{t \sim \mu, s \sim \nu, \lambda_3 \sim \nu} \left[\Re \left[\text{Tr} \left[H_3 e^{iH(\theta^{(3)}(\lambda_3))t/T} \mathcal{U}_{ts/T}^{H(\theta^{(3)}(\lambda_3))}(\rho) \right] \right] \right] \\ &\quad + \dots + \frac{\theta_J}{T} \mathbb{E}_{t \sim \mu, s \sim \nu, \lambda_J \sim \nu} \left[\Re \left[\text{Tr} \left[H_J e^{iH(\theta^{(J)}(\lambda_J))t/T} \mathcal{U}_{ts/T}^{H(\theta^{(J)}(\lambda_J))}(\rho) \right] \right] \right] \end{aligned} \quad (\text{A44})$$

$$= \sum_{j=1}^J \frac{\theta_j}{T} \mathbb{E}_{t \sim \mu, s \sim \nu, \lambda_j \sim \nu} \left[\Re \left[\text{Tr} \left[H_j e^{iH(\theta^{(j)}(\lambda_j))t/T} \mathcal{U}_{ts/T}^{H(\theta^{(j)}(\lambda_j))}(\rho) \right] \right] \right] \quad (\text{A45})$$

$$= \sum_{j=1}^J \frac{\theta_j}{T} \mathbb{E}_{t \sim \mu, s \sim \nu, \lambda \sim \nu} \left[\Re \left[\text{Tr} \left[H_j e^{iH(\theta^{(j)}(\lambda))t/T} \mathcal{U}_{ts/T}^{H(\theta^{(j)}(\lambda))}(\rho) \right] \right] \right] \quad (\text{A46})$$

$$= \frac{\|\theta\|_1}{T} \sum_{j=1}^J \frac{|\theta_j|}{\|\theta\|_1} \mathbb{E}_{t \sim \mu, s \sim \nu, \lambda \sim \nu} \left[\text{sgn}(\theta_j) \Re \left[\text{Tr} \left[H_j e^{iH(\theta^{(j)}(\lambda))t/T} \mathcal{U}_{ts/T}^{H(\theta^{(j)}(\lambda))}(\rho) \right] \right] \right], \quad (\text{A47})$$

$$= \frac{\|\theta\|_1}{T} \mathbb{E}_{\substack{j \sim q, t \sim \mu, \\ s \sim \nu, \lambda \sim \nu}} \left[\text{sgn}(\theta_j) \Re \left[\text{Tr} \left[H_j e^{iH(\theta^{(j)}(\lambda))t/T} \mathcal{U}_{ts/T}^{H(\theta^{(j)}(\lambda))}(\rho) \right] \right] \right], \quad (\text{A48})$$

thus completing the proof. \square

3. Proof of Theorem 3 (expected value of quantum convolution algorithm)

If q is a probability density, then $|q\rangle$ is a state vector because

$$\langle q|q\rangle = \left(\int_{-\infty}^{\infty} dp' \sqrt{q(p')} \langle p'| \right) \left(\int_{-\infty}^{\infty} dp \sqrt{q(p)} |p\rangle \right) \quad (\text{A49})$$

$$= \int_{-\infty}^{\infty} dp' \int_{-\infty}^{\infty} dp \sqrt{q(p')q(p)} \langle p'|p\rangle \quad (\text{A50})$$

$$= \int_{-\infty}^{\infty} dp' \int_{-\infty}^{\infty} dp \sqrt{q(p')q(p)} \delta(p - p') \quad (\text{A51})$$

$$= \int_{-\infty}^{\infty} dp q(p) \quad (\text{A52})$$

$$= 1. \quad (\text{A53})$$

Let us first suppose that the state of the data register is pure and given by $|\varphi\rangle\langle\varphi|$, where $|\varphi\rangle$ is a state vector. Suppose that a spectral decomposition of A is given by

$$A = \sum_i a_i |i\rangle\langle i|. \quad (\text{A54})$$

This implies that

$$e^{i\hat{x}\otimes A} = \sum_i \int_{-\infty}^{\infty} dx e^{ixa_i} |x\rangle\langle x| \otimes |i\rangle\langle i|. \quad (\text{A55})$$

The probability density that Step 3 of Algorithm 3 outputs $p \in \mathbb{R}$ is equal to

$$\|(\langle p| \otimes I) e^{i\hat{x}\otimes A} (|q\rangle \otimes |\varphi\rangle)\|^2. \quad (\text{A56})$$

Thus, the expected value of the output of Algorithm 3 is

$$\int_{-\infty}^{\infty} dp r(p) \|(\langle p| \otimes I) e^{i\hat{x}\otimes A} (|q\rangle \otimes |\varphi\rangle)\|^2. \quad (\text{A57})$$

Consider that

$$\begin{aligned} & (\langle p| \otimes I) e^{i\hat{x}\otimes A} (|q\rangle \otimes |\varphi\rangle) \\ &= (\langle p| \otimes I) \left(\sum_i \int_{-\infty}^{\infty} dx e^{ixa_i} |x\rangle\langle x| \otimes |i\rangle\langle i| \right) \left(\int_{-\infty}^{\infty} dp' \sqrt{q(p')} |p'\rangle \otimes |\varphi\rangle \right) \end{aligned} \quad (\text{A58})$$

$$= \sum_i \int_{-\infty}^{\infty} dp' \int_{-\infty}^{\infty} dx e^{ixa_i} \langle p|x\rangle \langle x|p'\rangle \sqrt{q(p')} |i\rangle\langle i| |\varphi\rangle \quad (\text{A59})$$

$$= \sum_i \int_{-\infty}^{\infty} dp' \delta(p' - p + a_i) \sqrt{q(p')} |i\rangle\langle i| \varphi \rangle \quad (\text{A60})$$

$$= \sum_i \sqrt{q(p - a_i)} |i\rangle\langle i| \varphi \rangle \quad (\text{A61})$$

$$= \sum_i \sqrt{q(a_i - p)} |i\rangle\langle i| \varphi \rangle \quad (\text{A62})$$

where the third equality follows because

$$\int_{-\infty}^{\infty} dx e^{ix a_i} \langle p|x\rangle \langle x|p'\rangle = \frac{1}{2\pi} \int_{-\infty}^{\infty} dx e^{ix a_i} e^{-ipx} e^{ip'x} \quad (\text{A63})$$

$$= \frac{1}{2\pi} \int_{-\infty}^{\infty} dx e^{i(p'+a_i-p)x} \quad (\text{A64})$$

$$= \delta(p' - p + a_i), \quad (\text{A65})$$

and the last equality from the assumption that q is even. So then

$$\|(\langle p| \otimes I) e^{i\hat{x} \otimes A} (|q\rangle \otimes |\varphi\rangle)\|^2 = \left\| \sum_i \sqrt{q(a_i - p)} |i\rangle\langle i| \varphi \rangle \right\|^2 \quad (\text{A66})$$

$$= \langle \varphi | \left(\sum_i q(a_i - p) |i\rangle\langle i| \right) | \varphi \rangle. \quad (\text{A67})$$

Then we conclude that the expected value is given by

$$\int_{-\infty}^{\infty} dp r(p) \|(\langle p| \otimes I) e^{i\hat{x} \otimes A} (|q\rangle \otimes |\varphi\rangle)\|^2 = \int_{-\infty}^{\infty} dp r(p) \langle \varphi | \left(\sum_i q(a_i - p) |i\rangle\langle i| \right) | \varphi \rangle \quad (\text{A68})$$

$$= \langle \varphi | \left(\sum_i \int_{-\infty}^{\infty} dp r(p) q(a_i - p) |i\rangle\langle i| \right) | \varphi \rangle \quad (\text{A69})$$

$$= \langle \varphi | \left(\sum_i s(a_i) |i\rangle\langle i| \right) | \varphi \rangle \quad (\text{A70})$$

$$= \langle \varphi | s(A) | \varphi \rangle. \quad (\text{A71})$$

The result generalizes to an arbitrary state ρ because every such state can be written as a convex combination of pure states as

$$\rho = \sum_z t(z) |\varphi_z\rangle\langle \varphi_z|, \quad (\text{A72})$$

so that

$$\begin{aligned} & \int_{-\infty}^{\infty} dp r(p) \text{Tr}[(|p\rangle\langle p| \otimes I) e^{i\hat{x} \otimes A} (|q\rangle\langle q| \otimes \rho) e^{-i\hat{x} \otimes A}] \\ &= \sum_z t(z) \int_{-\infty}^{\infty} dp r(p) \text{Tr}[(|p\rangle\langle p| \otimes I) e^{i\hat{x} \otimes A} (|q\rangle\langle q| \otimes |\varphi_z\rangle\langle \varphi_z|) e^{-i\hat{x} \otimes A}] \end{aligned} \quad (\text{A73})$$

$$= \sum_z t(z) \int_{-\infty}^{\infty} dp r(p) \|(\langle p| \otimes I) e^{i\hat{x} \otimes A} (|q\rangle \otimes |\varphi_z\rangle)\|^2 \quad (\text{A74})$$

$$= \sum_z t(z) \text{Tr}[s(A)|\varphi_z\rangle\langle\varphi_z|] \quad (\text{A75})$$

$$= \text{Tr}[s(A)\rho], \quad (\text{A76})$$

where the penultimate equality follows from (A71).

4. Proof of Theorem 4 and Equation (41)

Recall that $T_1, T_2 > 0$ such that $T/2 = T_1 T_2$,

$$\ell_{T_1}(p) := \frac{e^{p/T_1}}{T_1 (e^{p/T_1} + 1)^2}, \quad (\text{A77})$$

$$r(p) = \mathbf{1}_{p \geq 0} - \mathbf{1}_{p < 0}, \quad (\text{A78})$$

and observe that

$$\frac{d}{dp} f_{T_1}(p) = \ell_{T_1}(p), \quad (\text{A79})$$

where $f_{T_1}(p) = (e^{-p/T_1} + 1)^{-1}$ is the Fermi–Dirac function defined in (2). Consider that

$$(\ell_{T_1} * r)(p/T_2) = (\ell_{T_1} * \mathbf{1}_{p \geq 0})(p/T_2) - (\ell_{T_1} * \mathbf{1}_{p < 0})(p/T_2) \quad (\text{A80})$$

$$= \int_{-\infty}^{\infty} dp' \mathbf{1}_{p' \geq 0} \ell_{T_1}(p/T_2 - p') - \int_{-\infty}^{\infty} dp' \mathbf{1}_{p' < 0} \ell_{T_1}(p/T_2 - p') \quad (\text{A81})$$

$$= \int_0^{\infty} dp' \ell_{T_1}(p/T_2 - p') - \int_{-\infty}^0 dp' \ell_{T_1}(p/T_2 - p') \quad (\text{A82})$$

$$= \int_0^{\infty} dp' \ell_{T_1}(p' - p/T_2) - \int_{-\infty}^0 dp' \ell_{T_1}(p' - p/T_2) \quad (\text{A83})$$

$$= \int_{-p/T_2}^{\infty} dp' \ell_{T_1}(p') - \int_{-\infty}^{-p/T_2} dp' \ell_{T_1}(p') \quad (\text{A84})$$

$$= \int_{-p/T_2}^{\infty} dp' \frac{d}{dp'} f_{T_1}(p') - \int_{-\infty}^{-p/T_2} dp' \frac{d}{dp'} f_{T_1}(p') \quad (\text{A85})$$

$$= f_{T_1}(\infty) - f_{T_1}(-p/T_2) - f_{T_1}(-p/T_2) + f_{T_1}(-\infty) \quad (\text{A86})$$

$$= 1 - f_{T_1 T_2}(-p) - f_{T_1 T_2}(-p) \quad (\text{A87})$$

$$= 1 - f_{T/2}(-p) - f_{T/2}(-p) \quad (\text{A88})$$

$$= f_{T/2}(p) - (1 - f_{T/2}(p)) \quad (\text{A89})$$

$$= g_T(p). \quad (\text{A90})$$

The fourth equality follows because ℓ_{T_1} is an even function.

Appendix B: Squared-loss minimization for function approximation

We first prove (44). Consider that

$$\frac{1}{M} \sum_{m=1}^M (\text{Tr}[g_T(H(\theta))\rho_m] - y_m)^2 = \frac{1}{M} \sum_{m=1}^M (\text{Tr}[(g_T(H(\theta)) - y_m I) \rho_m])^2 \quad (\text{B1})$$

$$= \frac{1}{M} \sum_{m=1}^M \text{Tr}[(g_T(H(\theta)) - y_m I)^{\otimes 2} \rho_m^{\otimes 2}] \quad (\text{B2})$$

$$= \text{Tr}[\Delta^{(2)}(\theta, y)\bar{\rho}], \quad (\text{B3})$$

where the squared-loss observable is defined in (46) and the labeled classical–quantum training state $\bar{\rho}$ in (47).

Corollary 2. *For the squared-loss function $\mathcal{L}^{(2)}(\theta)$ defined in (44), for $j \in [J]$, the j th partial derivative can be expressed as follows:*

$$\frac{\partial}{\partial \theta_j} \mathcal{L}^{(2)}(\theta) = \frac{2 \|\theta\|_1}{T^2} \mathbb{E}_{\substack{k \sim q, t_1, t_2 \sim \mu, \\ s_1, s_2, \lambda \sim \nu, \\ m \sim [M]}} \left[\text{sgn}(\theta_k) \Re \left[\text{Tr} \left[\left((H_k - y_m I) \otimes H_j \right) \left(e^{iH(k, \lambda)t_1/T} \otimes e^{iH(\theta)t_2/T} \right) \times \right. \right. \right. \\ \left. \left. \left. \left(\mathcal{U}_{s_1 t_1/T}^{H(k, \lambda)} \otimes \mathcal{U}_{s_2 t_2/T}^{H(\theta)} \right) (\rho_m \otimes \rho_m) \right) \right] \right]. \quad (\text{B4})$$

Proof. Consider that

$$\frac{\partial}{\partial \theta_j} \mathcal{L}^{(2)}(\theta) = \frac{2}{M} \sum_{m=1}^M (\text{Tr}[g_T(H(\theta))\rho_m] - y_m) \frac{\partial}{\partial \theta_j} \text{Tr}[g_T(H(\theta))\rho_m] \quad (\text{B5})$$

$$= \frac{2}{M} \sum_{m=1}^M (\text{Tr}[(g_T(H(\theta)) - y_m I) \rho_m]) \text{Tr} \left[\frac{\partial}{\partial \theta_j} g_T(H(\theta)) \rho_m \right] \quad (\text{B6})$$

$$= \frac{2}{M} \sum_{m=1}^M \left(\text{Tr} \left[\left((g_T(H(\theta)) - y_m I) \otimes \frac{\partial}{\partial \theta_j} g_T(H(\theta)) \right) (\rho_m \otimes \rho_m) \right] \right). \quad (\text{B7})$$

By substituting the expressions stated in Theorems 1 and 2, we conclude the proof. \square

We can then use the expression in (B4) to develop the following hybrid quantum–classical algorithm for estimating $\frac{\partial}{\partial \theta_j} \mathcal{L}^{(2)}(\theta)$:

Algorithm 8. *A hybrid quantum–classical algorithm for estimating the j th partial derivative $\frac{\partial}{\partial \theta_j} \mathcal{L}^{(2)}(\theta)$ consists of the following steps:*

1. Set $\ell \leftarrow 1$, and set

$$L \leftarrow O \left(\left(\frac{\|\theta\|_1 (H_{\max} + y_{\max}) H_{\max}}{T^2 \varepsilon} \right)^2 \ln \left(\frac{1}{\delta} \right) \right), \quad (\text{B8})$$

where $H_{\max} := \max_{j \in [J]} \|H_j\|$, $y_{\max} := \max_{m \in [M]} |y_m|$, $\varepsilon > 0$ is the desired accuracy, and $\delta \in (0, 1)$ is the desired failure probability.

2. Sample $t_1, t_2 \sim \mu$, $s_1, s_2 \sim \nu$, $k \sim q$, $\lambda \sim \nu$, and $m \sim [M]$, where the probability densities μ and ν are defined in Theorem 1, q is defined in Theorem 2, and $m \sim [M]$ indicates that m is selected uniformly at random from $[M]$.

3. Prepare the states $\mathcal{U}_{s_1 t_1/T}^{H(k, \lambda)}(\rho_m)$ and $\mathcal{U}_{s_2 t_2/T}^{H(\theta)}(\rho_m)$ using two samples of ρ_m and Hamiltonian simulation to realize the unitary channels $\mathcal{U}_{s_1 t_1/T}^{H(k, \lambda)}$ and $\mathcal{U}_{s_2 t_2/T}^{H(\theta)}$.

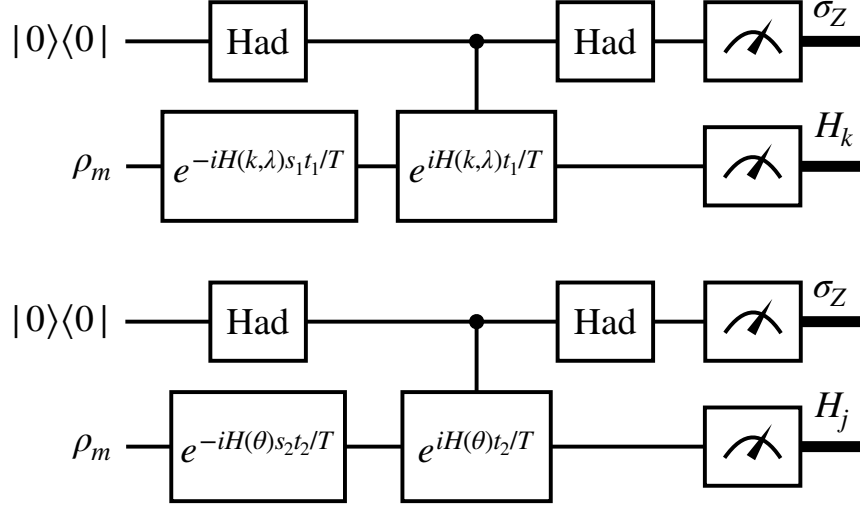


FIG. 10: Quantum circuit used in Algorithm 8 for estimating the j th partial derivative $\frac{\partial}{\partial \theta_j} \mathcal{L}^{(2)}(\theta)$. The notation $H(k, \lambda)$ is defined in Theorem 2. The circuit involves random classical sampling, Hamiltonian simulation, and the Hadamard test.

4. Perform the quantum circuit depicted in Figure 10, with measurement outcomes $Z_\ell^{(1)}, Z_\ell^{(2)} \in \{-1, 1\}$ for the σ_Z measurements, $X_\ell^{(1)} \in \text{spec}(H_k)$ for the H_k measurement, and $X_\ell^{(2)} \in \text{spec}(H_j)$ for the H_j measurement. Set

$$Y_\ell \leftarrow \frac{2 \|\theta\|_1}{T^2} \text{sgn}(\theta_k) \left(X_\ell^{(1)} - y_m \right) \cdot X_\ell^{(2)} \cdot Z_\ell^{(1)} \cdot Z_\ell^{(2)}. \quad (\text{B9})$$

Set $\ell \leftarrow \ell + 1$.

5. Repeat Steps 2-4 $L - 1$ more times. Compute the average $\bar{Y}_L := \frac{1}{L} \sum_{\ell=1}^L Y_\ell$ and output this value as an estimate of $\frac{\partial}{\partial \theta_j} \mathcal{L}(\theta)$.

Figure 10 depicts the quantum circuit used in Algorithm 8. By the Hoeffding inequality, we are guaranteed that

$$\Pr \left[\left| \bar{Y}_L - \frac{\partial}{\partial \theta_j} \mathcal{L}^{(2)}(\theta) \right| \leq \varepsilon \right] \geq 1 - \delta. \quad (\text{B10})$$

Appendix C: Logistic-loss function for binary classification

1. Derivative of matrix logistic-loss function

We begin by deriving a novel formula for the derivative of the matrix logistic-loss function $A \mapsto \ln(1 + e^{-A})$, where A is a Hermitian matrix.

Lemma 2. *Let $x \in \mathbb{R}$, and let $x \mapsto A(x)$ be a Hermitian-valued function. Then the following equality holds:*

$$\frac{\partial}{\partial x} \ln(I + e^{-A(x)}) = -\frac{1}{2} \frac{\partial}{\partial x} A(x) + \frac{1}{2} \mathbb{E}_{s \sim \nu, t \sim \gamma} \left[s \Re \left[A(x) e^{-iA(x)st} \left(\frac{\partial}{\partial x} A(x) \right) e^{-iA(x)(1-s)t} \right] \right], \quad (\text{C1})$$

where the high-peak-tent probability density $\gamma(t)$ is defined as

$$\gamma(t) := \frac{2}{\pi} \ln \left| \coth \left(\frac{\pi t}{2} \right) \right|. \quad (\text{C2})$$

Proof. To begin with, let

$$A(x) = \sum_k \lambda_k \Pi_k \quad (\text{C3})$$

be a spectral decomposition of $A(x)$, where we have omitted the dependence on x in the eigenvalues and eigenprojections. Defining

$$\text{logloss}(y) := \ln(1 + e^{-y}), \quad (\text{C4})$$

consider that the derivative of the matrix logistic-loss function is given by

$$\frac{\partial}{\partial x} \ln(I + e^{-A(x)}) = \sum_{k,\ell} f_{\text{logloss}}^{[1]}(\lambda_k, \lambda_\ell) \Pi_k \left(\frac{\partial}{\partial x} A(x) \right) \Pi_\ell, \quad (\text{C5})$$

where $f_{\text{logloss}}^{[1]}$ is the first divided difference of the logistic-loss function, defined as

$$f_{\text{logloss}}^{[1]}(y_1, y_2) := \begin{cases} \frac{\text{logloss}(y_1) - \text{logloss}(y_2)}{y_1 - y_2} & : y_1 \neq y_2 \\ \frac{1}{2} \left(\tanh\left(\frac{y_1}{2}\right) - 1 \right) & : y_1 = y_2 \end{cases}, \quad (\text{C6})$$

where we used the fact that

$$\frac{\partial}{\partial x} \text{logloss}(x) = -\frac{e^{-x}}{1 + e^{-x}} = -(1 + e^x)^{-1} = \frac{1}{2} \left(-1 + \tanh\left(\frac{x}{2}\right) \right). \quad (\text{C7})$$

(see, e.g., [96, Theorem 42] for a proof of (C5)). Now observe that an alternative expression for $f_{\text{logloss}}^{[1]}$ is as follows:

$$f_{\text{logloss}}^{[1]}(y_1, y_2) = \int_0^1 ds \frac{1}{2} \left(-1 + \tanh\left(\frac{sy_1 + (1-s)y_2}{2}\right) \right) \quad (\text{C8})$$

$$= -\frac{1}{2} + \frac{1}{2} \int_0^1 ds \tanh\left(\frac{sy_1 + (1-s)y_2}{2}\right), \quad (\text{C9})$$

as a consequence of the fundamental theorem of calculus and that

$$\frac{d}{ds} \text{logloss}(sy_1 + (1-s)y_2) = \left(-\frac{1}{2} + \frac{1}{2} \int_0^1 ds \tanh\left(\frac{sy_1 + (1-s)y_2}{2}\right) \right) (y_1 - y_2). \quad (\text{C10})$$

Then it follows that

$$\frac{\partial}{\partial x} \tanh(A(x)) = \sum_{k,\ell} \left[-\frac{1}{2} + \frac{1}{2} \int_0^1 ds \tanh\left(\frac{sy_1 + (1-s)y_2}{2}\right) \right] \Pi_k \left(\frac{\partial}{\partial x} A(x) \right) \Pi_\ell. \quad (\text{C11})$$

$$\begin{aligned} &= -\frac{1}{2} \sum_{k,\ell} \Pi_k \left(\frac{\partial}{\partial x} A(x) \right) \Pi_\ell \\ &\quad + \frac{1}{2} \sum_{k,\ell} \int_0^1 ds \tanh\left(\frac{s\lambda_k + (1-s)\lambda_\ell}{2}\right) \Pi_k \left(\frac{\partial}{\partial x} A(x) \right) \Pi_\ell \end{aligned} \quad (\text{C12})$$

$$\begin{aligned} &= -\frac{1}{2} \frac{\partial}{\partial x} A(x) \\ &\quad + \frac{1}{2} \sum_{k,\ell} \int_0^1 ds \left(\frac{s\lambda_k + (1-s)\lambda_\ell}{2} \right) \frac{\tanh\left(\frac{s\lambda_k + (1-s)\lambda_\ell}{2}\right)}{\frac{s\lambda_k + (1-s)\lambda_\ell}{2}} \Pi_k \left(\frac{\partial}{\partial x} A(x) \right) \Pi_\ell. \end{aligned} \quad (\text{C13})$$

Now consider that the Fourier transform of $\omega \mapsto \frac{\tanh(\omega/2)}{\omega/2}$ is as follows [37, 99, 100]:

$$\int_{-\infty}^{\infty} dt \gamma(t) e^{-i\omega t} = \frac{\tanh(\omega/2)}{\omega/2}. \quad (\text{C14})$$

Substituting (C14) into the second term of (C13), we find that

$$\begin{aligned} & \frac{1}{2} \sum_{k,\ell} \int_0^1 ds \left(\frac{s\lambda_k + (1-s)\lambda_\ell}{2} \right) \frac{\tanh\left(\frac{s\lambda_k + (1-s)\lambda_\ell}{2}\right)}{\frac{s\lambda_k + (1-s)\lambda_\ell}{2}} \Pi_k \left(\frac{\partial}{\partial x} A(x) \right) \Pi_\ell \\ &= \frac{1}{4} \sum_{k,\ell} \int_0^1 ds (s\lambda_k + (1-s)\lambda_\ell) \int_{-\infty}^{\infty} dt \gamma(t) e^{-i(s\lambda_k + (1-s)\lambda_\ell)t} \Pi_k \left(\frac{\partial}{\partial x} A(x) \right) \Pi_\ell \end{aligned} \quad (\text{C15})$$

$$= \frac{1}{4} \int_0^1 ds \int_{-\infty}^{\infty} dt \gamma(t) \sum_{k,\ell} (s\lambda_k + (1-s)\lambda_\ell) e^{-i(s\lambda_k + (1-s)\lambda_\ell)t} \Pi_k \left(\frac{\partial}{\partial x} A(x) \right) \Pi_\ell \quad (\text{C16})$$

$$= \frac{1}{4} \int_0^1 ds \int_{-\infty}^{\infty} dt \gamma(t) \sum_{k,\ell} (s\lambda_k + (1-s)\lambda_\ell) e^{-is\lambda_k t} \Pi_k \left(\frac{\partial}{\partial x} A(x) \right) e^{-i(1-s)\lambda_\ell t} \Pi_\ell \quad (\text{C17})$$

$$\begin{aligned} &= \frac{1}{4} \int_0^1 ds s \int_{-\infty}^{\infty} dt \gamma(t) \sum_{k,\ell} \lambda_k e^{-is\lambda_k t} \Pi_k \left(\frac{\partial}{\partial x} A(x) \right) e^{-i(1-s)\lambda_\ell t} \Pi_\ell \\ &\quad + \frac{1}{4} \int_0^1 ds (1-s) \int_{-\infty}^{\infty} dt \gamma(t) \sum_{k,\ell} e^{-is\lambda_k t} \Pi_k \left(\frac{\partial}{\partial x} A(x) \right) \lambda_\ell e^{-i(1-s)\lambda_\ell t} \Pi_\ell \end{aligned} \quad (\text{C18})$$

$$\begin{aligned} &= \frac{1}{4} \int_0^1 ds s \int_{-\infty}^{\infty} dt \gamma(t) \left(\sum_k \lambda_k e^{-is\lambda_k t} \Pi_k \right) \left(\frac{\partial}{\partial x} A(x) \right) \left(\sum_\ell e^{-i(1-s)\lambda_\ell t} \Pi_\ell \right) \\ &\quad + \frac{1}{4} \int_0^1 ds (1-s) \int_{-\infty}^{\infty} dt \gamma(t) \left(\sum_k e^{-is\lambda_k t} \Pi_k \right) \left(\frac{\partial}{\partial x} A(x) \right) \left(\sum_\ell \lambda_\ell e^{-i(1-s)\lambda_\ell t} \Pi_\ell \right) \end{aligned} \quad (\text{C19})$$

$$\begin{aligned} &= \frac{1}{4} \int_0^1 ds s \int_{-\infty}^{\infty} dt \gamma(t) A(x) e^{-iA(x)st} \left(\frac{\partial}{\partial x} A(x) \right) e^{-iA(x)(1-s)t} \\ &\quad + \frac{1}{4} \int_0^1 ds (1-s) \int_{-\infty}^{\infty} dt \gamma(t) e^{-iA(x)st} \left(\frac{\partial}{\partial x} A(x) \right) e^{-iA(x)(1-s)t} A(x) \end{aligned} \quad (\text{C20})$$

$$\stackrel{(a)}{=} \frac{1}{4} \int_0^1 ds s \int_{-\infty}^{\infty} dt \gamma(t) A(x) e^{-iA(x)st} \left(\frac{\partial}{\partial x} A(x) \right) e^{-iA(x)(1-s)t} \quad (\text{C21})$$

$$+ \frac{1}{4} \int_0^1 ds s \int_{-\infty}^{\infty} dt \gamma(t) e^{-iA(x)(1-s)t} \left(\frac{\partial}{\partial x} A(x) \right) e^{-iA(x)st} A(x) \quad (\text{C22})$$

$$\stackrel{(b)}{=} \frac{1}{4} \int_0^1 ds s \int_{-\infty}^{\infty} dt \gamma(t) A(x) e^{-iA(x)st} \left(\frac{\partial}{\partial x} A(x) \right) e^{-iA(x)(1-s)t} \quad (\text{C23})$$

$$+ \frac{1}{4} \int_0^1 ds s \int_{-\infty}^{\infty} dt \gamma(t) e^{iA(x)(1-s)t} \left(\frac{\partial}{\partial x} A(x) \right) e^{iA(x)st} A(x) \quad (\text{C24})$$

$$= \frac{1}{2} \int_0^1 ds s \int_{-\infty}^{\infty} dt \gamma(t) \Re \left[A(x) e^{-iA(x)st} \left(\frac{\partial}{\partial x} A(x) \right) e^{-iA(x)(1-s)t} \right]. \quad (\text{C25})$$

The equality (a) follows from the substitution $s \rightarrow 1-s$, and the equality (b) follows from the

substitution $t \rightarrow -t$, given that $\gamma(t)$ is an even function. The final equality follows from the definition $\Re[B] = (B + B^\dagger) / 2$. \square

Remark 3. For Hermitian matrices A and H , we can write the Fréchet derivative [98] of $\ln(I + e^{-A})$ at H as follows:

$$D \ln(I + e^{-A}) [H] = -\frac{1}{2}H + \frac{1}{2} \mathbb{E}_{s \sim v, t \sim \gamma} [s \Re [A e^{-iA s t} H e^{-iA(1-s)t}]]. \quad (\text{C26})$$

Theorem (Restatement of Theorem 5). *The following equality holds:*

$$\begin{aligned} \frac{\partial}{\partial \theta_j} T \text{Tr} [\ln(I + e^{-y_m H(\theta)/T}) \rho_m] &= -\frac{y_m}{2} \text{Tr} [H_j \rho_m] + \\ &\quad \frac{1}{2T} \|\theta\|_1 \mathbb{E}_{\substack{s \sim v, \\ k \sim q, \\ t \sim \gamma}} [s \Re [\text{Tr} [\text{sgn}(\theta_k) H_k H_j e^{iy_m H(\theta)t/T} \mathcal{U}_{st/T}^{y_m H(\theta)}(\rho_m)]]]. \end{aligned} \quad (\text{C27})$$

where $y_m \in \{-1, +1\}$, $H(\theta)$ is a parameterized Hamiltonian of the form in (16), $T > 0$, $\gamma(t)$ is the probability density function defined in (C2), v is a uniform random variable on the unit interval $[0, 1]$, $q(k) := \frac{|\theta_k|}{\|\theta\|_1}$ is a probability distribution, and $\mathcal{U}_t^{y_m H(\theta)}$ is the following unitary quantum channel:

$$\mathcal{U}_t^{y_m H(\theta)}(\cdot) := e^{-iy_m H(\theta)t}(\cdot)e^{iy_m H(\theta)t}. \quad (\text{C28})$$

Proof. Consider that

$$\begin{aligned} &\frac{\partial}{\partial \theta_j} T \text{Tr} [\ln(I + e^{-y_m H(\theta)/T}) \rho_m] \\ &= T \text{Tr} \left[\left(\frac{\partial}{\partial \theta_j} \ln(I + e^{-y_m H(\theta)/T}) \right) \rho_m \right] \end{aligned} \quad (\text{C29})$$

$$= T \text{Tr} \left[\left(\frac{1}{2} \mathbb{E}_{s \sim v, t \sim \gamma} \left[s \Re \left[\frac{y_m H(\theta)}{T} e^{-iy_m H(\theta)st/T} \left(\frac{\partial}{\partial \theta_j} \frac{y_m H(\theta)}{T} \right) e^{-iy_m H(\theta)(1-s)t/T} \right] \right) \right) \rho_m \right] \quad (\text{C30})$$

$$= \text{Tr} \left[\left(-\frac{y_m}{2} H_j + \frac{1}{2} \mathbb{E}_{s \sim v, t \sim \gamma} \left[s \Re \left[\frac{H(\theta)}{T} e^{-iy_m H(\theta)st/T} H_j e^{-iy_m H(\theta)(1-s)t/T} \right] \right] \right) \rho_m \right] \quad (\text{C31})$$

$$\begin{aligned} &= -\frac{y_m}{2} \text{Tr} [H_j \rho_m] \\ &\quad + \frac{1}{2T} \mathbb{E}_{s \sim v, t \sim \gamma} [s \text{Tr} [\Re [H(\theta) e^{-iy_m H(\theta)st/T} H_j e^{-iy_m H(\theta)(1-s)t/T}]] \rho_m]. \end{aligned} \quad (\text{C32})$$

Now consider that

$$\begin{aligned} &\mathbb{E}_{s \sim v, t \sim \gamma} [s \text{Tr} [\Re [H(\theta) e^{-iy_m H(\theta)st/T} H_j e^{-iy_m H(\theta)(1-s)t/T}]] \rho_m] \\ &= \mathbb{E}_{s \sim v, t \sim \gamma} [s \Re [\text{Tr} [H(\theta) e^{-iy_m H(\theta)st/T} H_j e^{-iy_m H(\theta)(1-s)t/T} \rho_m]]] \end{aligned} \quad (\text{C33})$$

$$= \mathbb{E}_{s \sim v, t \sim \gamma} [s \Re [\text{Tr} [H(\theta) H_j e^{-iy_m H(\theta)(1-s)t/T} \rho_m e^{-iy_m H(\theta)st/T}]]] \quad (\text{C34})$$

$$= \mathbb{E}_{s \sim v, t \sim \gamma} [s \Re [\text{Tr} [H(\theta) H_j e^{iy_m H(\theta)(1-s)t/T} \rho_m e^{iy_m H(\theta)st/T}]]] \quad (\text{C35})$$

$$= \mathbb{E}_{s \sim v, t \sim \gamma} [s \Re [\text{Tr} [H(\theta) H_j e^{iy_m H(\theta)t/T} e^{-iy_m H(\theta)st/T} \rho_m e^{iy_m H(\theta)st/T}]]] \quad (\text{C36})$$

$$= \mathbb{E}_{s \sim v, t \sim \gamma} [s \Re [\text{Tr} [H(\theta) H_j e^{iy_m H(\theta)t/T} \mathcal{U}_{st/T}^{y_m H(\theta)}(\rho_m)]]] \quad (\text{C37})$$

$$= \mathbb{E}_{s \sim v, t \sim \gamma} \left[s \Re \left[\text{Tr} \left[\sum_{k \in [J]} \theta_k H_k H_j e^{iy_m H(\theta)t/T} \mathcal{U}_{st/T}^{y_m H(\theta)}(\rho_m) \right] \right] \right] \quad (\text{C38})$$

$$= \|\theta\|_1 \mathbb{E}_{s \sim v, t \sim \gamma} \left[s \Re \left[\text{Tr} \left[\sum_{k \in [J]} \text{sgn}(\theta_k) \frac{|\theta_k|}{\|\theta\|_1} H_k H_j e^{iy_m H(\theta) t/T} \mathcal{U}_{st/T}^{y_m H(\theta)}(\rho_m) \right] \right] \right] \quad (\text{C39})$$

$$= \|\theta\|_1 \mathbb{E}_{s \sim v, t \sim \gamma, k \sim q} \left[s \Re \left[\text{Tr} \left[\text{sgn}(\theta_k) H_k H_j e^{iy_m H(\theta) t/T} \mathcal{U}_{st/T}^{y_m H(\theta)}(\rho_m) \right] \right] \right], \quad (\text{C40})$$

thus concluding the proof. \square

2. Hybrid quantum–classical algorithm for estimating derivative of matrix logistic-loss function

The first term of (63) can be easily estimated by preparing the state ρ and measuring H_j . Under the assumption that each H_j in $H(\theta)$ is both Hermitian and unitary (as in the common case when each H_j is a Pauli string), Algorithm 9 below provides a method for estimating the second term of (63), which we abbreviate as follows:

$$\zeta_j \equiv \frac{1}{2T} \|\theta\|_1 \mathbb{E}_{s \sim v, k \sim q, t \sim \gamma} \left[s \Re \left[\text{Tr} \left[\text{sgn}(\theta_k) H_k H_j e^{iy_m H(\theta) t/T} \mathcal{U}_{st/T}^{y_m H(\theta)}(\rho_m) \right] \right] \right]. \quad (\text{C41})$$

Algorithm 9. A hybrid quantum–classical algorithm for estimating ζ_j in (C41) consists of the following steps:

1. Set $m \leftarrow 1$, and set

$$M \leftarrow O \left(\left(\frac{\|\theta\|_1 \max_{j \in [J]} \|H_j\|}{T \varepsilon} \right)^2 \ln \left(\frac{1}{\delta} \right) \right), \quad (\text{C42})$$

where $\varepsilon > 0$ is the desired accuracy and $\delta \in (0, 1)$ is the desired failure probability.

2. Sample $s \sim v$, $k \sim q$, and $t \sim \gamma$.

3. Prepare the state $\mathcal{U}_{st/T}^{y_m H(\theta)}(\rho_m)$ using one sample of ρ_m and Hamiltonian simulation to realize the unitary channel $\mathcal{U}_{st/T}^{y_m H(\theta)}$.

4. Perform the quantum circuit depicted in Figure 11, with measurement outcomes $Z_m \in \{-1, 1\}$ for the σ_Z measurement and $X_m \in \text{spec}(H_k)$ for the H_k measurement. Set $W_m \leftarrow \frac{\|\theta\|_1}{2T} s \cdot \text{sgn}(\theta_k) Z_m \cdot X_m$. Set $m \leftarrow m + 1$.

5. Repeat Steps 2-4 $M - 1$ more times. Compute the average $\overline{W}_M := \frac{1}{M} \sum_{m=1}^M W_m$ and output this value as an estimate of ζ_j .

By the Hoeffding inequality, we are guaranteed that

$$\Pr \left[\left| \overline{W}_M - \zeta_j \right| \leq \varepsilon \right] \geq 1 - \delta. \quad (\text{C43})$$

3. Alternative formula for logistic-loss function

Similar to the idea behind Theorem 2, we can use Theorem 5 and the fundamental theorem of calculus to derive an expression for the logistic-loss function that can be evaluated by a hybrid quantum–classical algorithm.

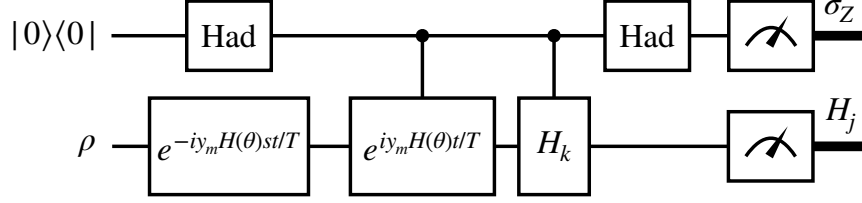


FIG. 11: Quantum circuit used in Algorithm 9 for estimating the second term of (63), denoted by ζ_j in (C41).

Theorem 13. *The following equality holds:*

$$T \operatorname{Tr}[\ln(I + e^{-y_m H(\theta)/T}) \rho_m] = -\frac{y_m}{2} \operatorname{Tr}[H(\theta) \rho_m] + \frac{J}{2T} \mathbb{E}_{\substack{j \sim [J], \\ \lambda, s \sim v, \\ t \sim \gamma}} \left[\|\theta^{(j)}(\lambda)\|_1 \mathbb{E}_{k \sim q_{j,\lambda}} \left[s \Re \left[\operatorname{Tr} \left[\operatorname{sgn}(\theta_k) H_k H_j e^{iy_m H(\theta^{(j)}(\lambda))t/T} \mathcal{U}_{st/T}^{y_m H(\theta^{(j)}(\lambda))}(\rho_m) \right] \right] \right] \right], \quad (\text{C44})$$

where j is selected uniformly at random from $[J]$, λ and s are selected uniformly at random from the unit interval $[0, 1]$, t is selected according to $\gamma(t)$ in (C2),

$$\theta^{(j)}(\lambda) := (0, \dots, 0, \lambda \theta_j, \theta_{j+1}, \dots, \theta_J), \quad (\text{C45})$$

$$\|\theta^{(j)}(\lambda)\|_1 := \lambda |\theta_j| + \sum_{k=j+1}^J |\theta_k|, \quad (\text{C46})$$

$$H(\theta_1, \dots, \theta_J) \equiv H(\theta) = \sum_{j=1}^J \theta_j H_j, \quad (\text{C47})$$

and k is selected according to the conditional probability distribution $q_{j,\lambda}$, defined as

$$q_{j,\lambda}(k) := \begin{cases} \frac{\lambda |\theta_j|}{\|\theta^{(j)}(\lambda)\|_1} & : k = j \\ \frac{|\theta_k|}{\|\theta^{(j)}(\lambda)\|_1} & : k > j \end{cases}. \quad (\text{C48})$$

Proof. Define

$$\mathcal{L}_T(y_m H(\theta)) := T \ln(I + e^{-y_m H(\theta)/T}). \quad (\text{C49})$$

Consider that

$$\begin{aligned} & \operatorname{Tr}[\mathcal{L}_T(y_m H(\theta)) \rho_m] - \operatorname{Tr}[\mathcal{L}_T(y_m H(0, \theta_2, \dots, \theta_J)) \rho_m] \\ &= \operatorname{Tr}[\mathcal{L}_T(y_m H(\theta_1, \theta_2, \dots, \theta_J)) \rho_m] - \operatorname{Tr}[\mathcal{L}_T(y_m H(0, \theta_2, \dots, \theta_J)) \rho_m] \end{aligned} \quad (\text{C50})$$

$$= \operatorname{Tr}[\mathcal{L}_T(y_m H(\theta^{(1)}(1))) \rho_m] - \operatorname{Tr}[\mathcal{L}_T(y_m H(\theta^{(1)}(0))) \rho_m] \quad (\text{C51})$$

$$= \int_0^1 d\lambda_1 \frac{\partial}{\partial \lambda_1} \operatorname{Tr}[\mathcal{L}_T(y_m H(\theta^{(1)}(\lambda_1))) \rho_m] \quad (\text{C52})$$

$$= \int_0^1 d\lambda_1 \left(\begin{aligned} & -\frac{y_m \theta_1}{2} \operatorname{Tr}[H_1 \rho_m] \\ & + \mathbb{E}_{s \sim v, t \sim \gamma} \left[s \Re \left[\operatorname{Tr} \left[H(\theta^{(1)}(\lambda_1)) H_1 e^{iy_m H(\theta^{(1)}(\lambda_1))t/T} \mathcal{U}_{st/T}^{y_m H(\theta^{(1)}(\lambda_1))}(\rho_m) \right] \right] \right] \end{aligned} \right) \quad (\text{C53})$$

$$= -\frac{y_m \theta_1}{2} \operatorname{Tr}[H_1 \rho]$$

$$\begin{aligned}
& + \frac{1}{2T} \mathbb{E}_{\lambda_1, s \sim v, t \sim \gamma} \left[s\Re \left[\text{Tr} \left[H(\theta^{(1)}(\lambda_1)) H_1 e^{iy_m H(\theta^{(1)}(\lambda_1))t/T} \mathcal{U}_{st/T}^{y_m H(\theta^{(1)}(\lambda_1))}(\rho_m) \right] \right] \right] \\
& = -\frac{y_m \theta_1}{2} \text{Tr}[H_1 \rho] \\
& + \frac{1}{2T} \mathbb{E}_{\lambda, s \sim v, t \sim \gamma} \left[s\Re \left[\text{Tr} \left[H(\theta^{(1)}(\lambda)) H_1 e^{iy_m H(\theta^{(1)}(\lambda))t/T} \mathcal{U}_{st/T}^{y_m H(\theta^{(1)}(\lambda))}(\rho_m) \right] \right] \right].
\end{aligned} \tag{C54}$$

$$\begin{aligned}
& + \frac{1}{2T} \mathbb{E}_{\lambda, s \sim v, t \sim \gamma} \left[s\Re \left[\text{Tr} \left[H(\theta^{(1)}(\lambda)) H_1 e^{iy_m H(\theta^{(1)}(\lambda))t/T} \mathcal{U}_{st/T}^{y_m H(\theta^{(1)}(\lambda))}(\rho_m) \right] \right] \right].
\end{aligned} \tag{C55}$$

Additionally,

$$\begin{aligned}
& \text{Tr}[\mathcal{L}_T(y_m H(0, \theta_2, \dots, \theta_J))\rho_m] - \text{Tr}[\mathcal{L}_T(y_m H(0, 0, \theta_3, \dots, \theta_J))\rho_m] \\
& = \text{Tr}[\mathcal{L}_T(y_m H(\theta^{(2)}(1)))\rho_m] - \text{Tr}[\mathcal{L}_T(y_m H(\theta^{(2)}(0)))\rho_m]
\end{aligned} \tag{C56}$$

$$= \int_0^1 d\lambda_2 \frac{\partial}{\partial \lambda_2} \text{Tr}[\mathcal{L}_T(y_m H(\theta^{(2)}(\lambda_2)))\rho_m] \tag{C57}$$

$$= \int_0^1 d\lambda_1 \left(\begin{aligned} & -\frac{y_m \theta_2}{2} \text{Tr}[H_2 \rho_m] \\ & + \mathbb{E}_{s \sim v, t \sim \gamma} \left[s\Re \left[\text{Tr} \left[H(\theta^{(2)}(\lambda_2)) H_2 e^{iy_m H(\theta^{(2)}(\lambda_2))t/T} \mathcal{U}_{st/T}^{y_m H(\theta^{(2)}(\lambda_2))}(\rho_m) \right] \right] \right] \end{aligned} \right) \tag{C58}$$

$$\begin{aligned}
& = -\frac{y_m \theta_2}{2} \text{Tr}[H_2 \rho_m] \\
& + \frac{1}{2T} \mathbb{E}_{\lambda_2, s \sim v, t \sim \gamma} \left[s\Re \left[\text{Tr} \left[H(\theta^{(2)}(\lambda_2)) H_2 e^{iy_m H(\theta^{(2)}(\lambda_2))t/T} \mathcal{U}_{st/T}^{y_m H(\theta^{(2)}(\lambda_2))}(\rho_m) \right] \right] \right]
\end{aligned} \tag{C59}$$

$$\begin{aligned}
& = -\frac{y_m \theta_2}{2} \text{Tr}[H_2 \rho_m] \\
& + \frac{1}{2T} \mathbb{E}_{\lambda, s \sim v, t \sim \gamma} \left[s\Re \left[\text{Tr} \left[H(\theta^{(2)}(\lambda)) H_2 e^{iy_m H(\theta^{(2)}(\lambda))t/T} \mathcal{U}_{st/T}^{y_m H(\theta^{(2)}(\lambda))}(\rho_m) \right] \right] \right].
\end{aligned} \tag{C60}$$

We continue iteratively along these lines and find that the last term is given by

$$\begin{aligned}
& \text{Tr}[\mathcal{L}_T(y_m H(0, \dots, 0, \theta_J))\rho_m] \\
& = \text{Tr}[\mathcal{L}_T(y_m H(0, \dots, 0, \theta_J))\rho_m] - \text{Tr}[\mathcal{L}_T(y_m H(0, \dots, 0, 0))\rho_m]
\end{aligned} \tag{C61}$$

$$= \text{Tr}[\mathcal{L}_T(y_m H(\theta^{(J)}(1)))\rho_m] - \text{Tr}[\mathcal{L}_T(y_m H(\theta^{(J)}(0)))\rho_m] \tag{C62}$$

$$= -\frac{y_m \theta_J}{2} \text{Tr}[H_J \rho] \tag{C63}$$

$$+ \frac{1}{2T} \mathbb{E}_{\lambda, s \sim v, t \sim \gamma} \left[s\Re \left[\text{Tr} \left[H(\theta^{(J)}(\lambda)) H_J e^{iy_m H(\theta^{(J)}(\lambda))t/T} \mathcal{U}_{st/T}^{y_m H(\theta^{(J)}(\lambda))}(\rho_m) \right] \right] \right]. \tag{C64}$$

where we used the fact that

$$\mathcal{L}_T(y_m H(\theta^{(J)}(0))) = \mathcal{L}_T(y_m H(0, \dots, 0)) = \mathcal{L}_T(0) = 0, \tag{C65}$$

given that $T \ln(1 + e^{-x/T})|_{x=0} = 0$. So then we form a telescoping sum and conclude that

$$\begin{aligned}
& \text{Tr}[\mathcal{L}_T(y_m H(\theta))\rho_m] \\
& = \text{Tr}[\mathcal{L}_T(y_m H(\theta))\rho_m] - \text{Tr}[\mathcal{L}_T(y_m H(0, \theta_2, \dots, \theta_J))\rho_m] \\
& \quad + \text{Tr}[\mathcal{L}_T(y_m H(0, \theta_2, \dots, \theta_J))\rho_m] - \text{Tr}[\mathcal{L}_T(y_m H(0, 0, \theta_3, \dots, \theta_J))\rho_m] \\
& \quad + \dots + \text{Tr}[\mathcal{L}_T(y_m H(0, \dots, 0, \theta_J))\rho_m] - \text{Tr}[\mathcal{L}_T(y_m H(0, \dots, 0, 0))\rho_m] \\
& = -\frac{y_m \theta_1}{2} \text{Tr}[H_1 \rho_m] - \frac{y_m \theta_2}{2} \text{Tr}[H_2 \rho_m] - \dots - \frac{y_m \theta_J}{2} \text{Tr}[H_J \rho_m] \\
& \quad + \frac{1}{2T} \mathbb{E}_{\lambda, s \sim v, t \sim \gamma} \left[s\Re \left[\text{Tr} \left[H(\theta^{(1)}(\lambda)) H_1 e^{iy_m H(\theta^{(1)}(\lambda))t/T} \mathcal{U}_{st/T}^{y_m H(\theta^{(1)}(\lambda))}(\rho_m) \right] \right] \right]
\end{aligned} \tag{C66}$$

$$\begin{aligned}
& + \frac{1}{2T} \mathbb{E}_{\lambda, s \sim v, t \sim \gamma} \left[s\Re \left[\text{Tr} \left[H(\theta^{(2)}(\lambda)) H_2 e^{iy_m H(\theta^{(2)}(\lambda)) t/T} \mathcal{U}_{st/T}^{y_m H(\theta^{(2)}(\lambda))}(\rho_m) \right] \right] \right] \\
& + \cdots + \frac{1}{2T} \mathbb{E}_{\lambda, s \sim v, t \sim \gamma} \left[s\Re \left[\text{Tr} \left[H(\theta^{(J)}(\lambda)) H_J e^{iy_m H(\theta^{(J)}(\lambda)) t/T} \mathcal{U}_{st/T}^{y_m H(\theta^{(J)}(\lambda))}(\rho_m) \right] \right] \right] \quad (\text{C67})
\end{aligned}$$

$$= -\frac{y_m}{2} \text{Tr}[H(\theta)\rho_m] + \frac{1}{2T} \sum_{j=1}^J \mathbb{E}_{\lambda, s \sim v, t \sim \gamma} \left[s\Re \left[\text{Tr} \left[H(\theta^{(j)}(\lambda)) H_j e^{iy_m H(\theta^{(j)}(\lambda)) t/T} \mathcal{U}_{st/T}^{y_m H(\theta^{(j)}(\lambda))}(\rho_m) \right] \right] \right]. \quad (\text{C68})$$

Now observe that

$$H(\theta^{(j)}(\lambda)) = \lambda \theta_j H_j + \sum_{k=j+1}^J \theta_k H_k \quad (\text{C69})$$

$$= \|\theta^{(j)}(\lambda)\|_1 \mathbb{E}_{k \sim q_{j,\lambda}} [\text{sgn}(\theta_k) H_k], \quad (\text{C70})$$

where

$$\|\theta^{(j)}(\lambda)\|_1 := \lambda |\theta_j| + \sum_{k=j+1}^J |\theta_k| \quad (\text{C71})$$

$$q_{j,\lambda}(k) := \begin{cases} \frac{\lambda |\theta_j|}{\|\theta^{(j)}(\lambda)\|_1} & : k = j \\ \frac{|\theta_k|}{\|\theta^{(j)}(\lambda)\|_1} & : k > j \end{cases}. \quad (\text{C72})$$

Then

$$\begin{aligned}
& \frac{1}{2T} \sum_{j=1}^J \mathbb{E}_{\lambda, s \sim v, t \sim \gamma} \left[s\Re \left[\text{Tr} \left[H(\theta^{(j)}(\lambda)) H_j e^{iy_m H(\theta^{(j)}(\lambda)) t/T} \mathcal{U}_{st/T}^{y_m H(\theta^{(j)}(\lambda))}(\rho_m) \right] \right] \right] \\
& = \frac{1}{2T} \sum_{j=1}^J \mathbb{E}_{\lambda, s \sim v, t \sim \gamma} \left[\|\theta^{(j)}(\lambda)\|_1 \mathbb{E}_{k \sim q_{j,\lambda}} \left[s\Re \left[\text{Tr} \left[\text{sgn}(\theta_k) H_k H_j e^{iy_m H(\theta^{(j)}(\lambda)) t/T} \mathcal{U}_{st/T}^{y_m H(\theta^{(j)}(\lambda))}(\rho_m) \right] \right] \right] \right] \quad (\text{C73})
\end{aligned}$$

$$= \frac{J}{2T} \mathbb{E}_{\substack{j \sim [J], \\ \lambda, s \sim v, \\ t \sim \gamma}} \left[\|\theta^{(j)}(\lambda)\|_1 \mathbb{E}_{k \sim q_{j,\lambda}} \left[s\Re \left[\text{Tr} \left[\text{sgn}(\theta_k) H_k H_j e^{iy_m H(\theta^{(j)}(\lambda)) t/T} \mathcal{U}_{st/T}^{y_m H(\theta^{(j)}(\lambda))}(\rho_m) \right] \right] \right] \right], \quad (\text{C74})$$

thus completing the proof. \square

4. Hybrid quantum–classical algorithm for estimating logistic-loss function

The expression in (C44) then leads to a hybrid quantum–classical algorithm for estimating the logistic-loss objective function. The first term $-\frac{y_m}{2} \text{Tr}[H(\theta)\rho_m]$ in (C44) can be easily estimated by writing

$$-\frac{y_m}{2} \text{Tr}[H(\theta)\rho_m] = -\frac{y_m}{2} \text{Tr} \left[\sum_{j=1}^J \theta_j H_j \rho_m \right] \quad (\text{C75})$$

$$= -\frac{y_m}{2} \sum_{j=1}^J \theta_j \text{Tr}[H_j \rho_m] \quad (\text{C76})$$

$$= -\frac{\|\theta\|_1 y_m}{2} \sum_{j=1}^J \frac{|\theta_j|}{\|\theta\|_1} \operatorname{sgn}(\theta_j) \operatorname{Tr}[H_j \rho_m]. \quad (\text{C77})$$

Thus, in each iteration of an estimation algorithm, we can pick j at random according to the probability distribution $\frac{|\theta_j|}{\|\theta\|_1}$, prepare the state ρ_m , measure the observable H_j on this state (obtaining an outcome in $\{-1, +1\}$), and multiply the outcome by $-\frac{\|\theta\|_1 y_m}{2} \operatorname{sgn}(\theta_j)$. One then repeats this procedure a number of times and computes the sample mean. The Hoeffding inequality guarantees that a desired accuracy of $\varepsilon > 0$ and a desired failure probability of $\delta \in (0, 1)$ can be achieved using the following number of trials:

$$O\left(\left(\frac{\|\theta\|_1 \max_{j \in [J]} \|H_j\|}{\varepsilon}\right)^2 \ln\left(\frac{1}{\delta}\right)\right). \quad (\text{C78})$$

The second term in (C44), which we abbreviate as

$$\zeta \equiv \frac{J}{2T} \mathbb{E}_{\substack{j \sim [J], \\ \lambda, s \sim v, \\ t \sim \gamma}} \left[\|\theta^{(j)}(\lambda)\|_1 \mathbb{E}_{k \sim q_{j,\lambda}} \left[s \Re \left[\operatorname{Tr} \left[\operatorname{sgn}(\theta_k) H_k H_j e^{iy_m H(\theta^{(j)}(\lambda)) t/T} \mathcal{U}_{st/T}^{y_m H(\theta^{(j)}(\lambda))}(\rho_m) \right] \right] \right] \right], \quad (\text{C79})$$

can be estimated by the following algorithm:

Algorithm 10. A hybrid quantum–classical algorithm for estimating ζ in (C79) consists of the following steps:

1. Set $m \leftarrow 1$, and set

$$M \leftarrow O\left(\left(\frac{J\theta^* h^*}{T\varepsilon}\right)^2 \ln\left(\frac{1}{\delta}\right)\right), \quad (\text{C80})$$

$$\theta^* := \max_{\lambda \in [0,1], j \in [J]} \|\theta^{(j)}(\lambda)\|_1, \quad (\text{C81})$$

$$h^* := \max_{j \in [J]} \|H_j\|, \quad (\text{C82})$$

where $\varepsilon > 0$ is the desired accuracy and $\delta \in (0, 1)$ is the desired failure probability.

2. Sample j according to the uniform distribution on $[J]$, $s \sim v$, $\lambda \sim v$, $t \sim \gamma$, and $k \sim q_{j,\lambda}$.
3. Prepare the state $\mathcal{U}_{st/T}^{y_m H(\theta^{(j)}(\lambda))}(\rho_m)$ using one sample of ρ_m and Hamiltonian simulation to realize the unitary channel $\mathcal{U}_{st/T}^{y_m H(\theta^{(j)}(\lambda))}$.
4. Perform the quantum circuit depicted in Figure 11, with measurement outcomes $Z_m \in \{-1, 1\}$ for the σ_Z measurement and $X_m \in \operatorname{spec}(H_k)$ for the H_k measurement. Set

$$W_m \leftarrow \frac{J \|\theta^{(j)}(\lambda)\|_1}{2T} s \cdot \operatorname{sgn}(\theta_k) Z_m \cdot X_m. \quad (\text{C83})$$

Set $m \leftarrow m + 1$.

5. Repeat Steps 2–4 $M - 1$ more times. Compute the average $\overline{W_M} := \frac{1}{M} \sum_{m=1}^M W_m$ and output this value as an estimate of ζ .

By the Hoeffding inequality, we are guaranteed that

$$\Pr\left[|\overline{W_M} - \zeta| \leq \varepsilon\right] \geq 1 - \delta. \quad (\text{C84})$$

Appendix D: Derivations for smooth rectified linear unit (ReLU)

1. Proof of Theorem 6 (derivative of smooth ReLU function)

Recall from Theorem 5 that

$$\begin{aligned} \frac{\partial}{\partial \theta_j} T \operatorname{Tr} [\ln(I + e^{-y_m H(\theta)/T}) \rho_m] &= -\frac{y_m}{2} \operatorname{Tr}[H_j \rho_m] + \\ &\quad \frac{\|\theta\|_1}{2T} \mathbb{E}_{\substack{s \sim v, \\ k \sim q, \\ t \sim \gamma}} \left[s \Re \left[\operatorname{Tr} \left[\operatorname{sgn}(\theta_k) H_k H_j e^{iy_m H(\theta)t/T} \mathcal{U}_{st/T}^{y_m H(\theta)}(\rho_m) \right] \right] \right]. \end{aligned} \quad (\text{D1})$$

Now set $y_m = 1$ and $\rho_m = \rho$ to get

$$\frac{\partial}{\partial \theta_j} T \operatorname{Tr} [\ln(I + e^{-H(\theta)/T}) \rho] = -\frac{1}{2} \operatorname{Tr}[H_j \rho] + \frac{\|\theta\|_1}{2T} \mathbb{E}_{\substack{s \sim v, \\ k \sim q, \\ t \sim \gamma}} \left[s \Re \left[\operatorname{Tr} \left[\operatorname{sgn}(\theta_k) H_k H_j e^{iH(\theta)t/T} \mathcal{U}_{st/T}^{H(\theta)}(\rho) \right] \right] \right]. \quad (\text{D2})$$

Under the substitution $T \rightarrow -T$, this becomes

$$\begin{aligned} &\frac{\partial}{\partial \theta_j} (-T \operatorname{Tr} [\ln(I + e^{-H(\theta)/-T}) \rho]) \\ &= \frac{\partial}{\partial \theta_j} (-T \operatorname{Tr} [\ln(I + e^{H(\theta)/T}) \rho]) \end{aligned} \quad (\text{D3})$$

$$= -\frac{1}{2} \operatorname{Tr}[H_j \rho] - \frac{\|\theta\|_1}{2T} \mathbb{E}_{\substack{s \sim v, \\ k \sim q, \\ t \sim \gamma}} \left[s \Re \left[\operatorname{Tr} \left[\operatorname{sgn}(\theta_k) H_k H_j e^{-iH(\theta)t/T} \mathcal{U}_{-st/T}^{H(\theta)}(\rho) \right] \right] \right] \quad (\text{D4})$$

$$= -\frac{1}{2} \operatorname{Tr}[H_j \rho] - \frac{\|\theta\|_1}{2T} \mathbb{E}_{\substack{s \sim v, \\ k \sim q, \\ t \sim \gamma}} \left[s \Re \left[\operatorname{Tr} \left[\operatorname{sgn}(\theta_k) H_k H_j e^{iH(\theta)t/T} \mathcal{U}_{st/T}^{H(\theta)}(\rho) \right] \right] \right], \quad (\text{D5})$$

where the last equality follows because γ is an even function. Finally, we conclude that

$$\begin{aligned} &\frac{\partial}{\partial \theta_j} (T \operatorname{Tr} [\ln(I + e^{H(\theta)/T}) \rho]) \\ &= -\frac{\partial}{\partial \theta_j} (-T \operatorname{Tr} [\ln(I + e^{H(\theta)/T}) \rho]) \end{aligned} \quad (\text{D6})$$

$$= \frac{1}{2} \operatorname{Tr}[H_j \rho] + \frac{\|\theta\|_1}{2T} \mathbb{E}_{\substack{s \sim v, \\ k \sim q, \\ t \sim \gamma}} \left[s \Re \left[\operatorname{Tr} \left[\operatorname{sgn}(\theta_k) H_k H_j e^{iH(\theta)t/T} \mathcal{U}_{st/T}^{H(\theta)}(\rho) \right] \right] \right]. \quad (\text{D7})$$

2. Hybrid quantum–classical algorithms for smooth ReLU

a. Hybrid quantum–classical algorithm for estimating gradient of smooth ReLU

In this appendix, we briefly summarize a hybrid quantum–classical algorithm for estimating the formula in (71), i.e., the j th partial derivative of $\operatorname{Tr}[r_T(H(\theta))\rho]$, on a quantum computer.

The first term of (71) can be easily estimated by preparing the state ρ and measuring H_j .

For the second term of (71), let us make the assumption that each H_j in $H(\theta)$ is both Hermitian and unitary (as in the common case when each H_j is a Pauli string). Then Algorithm 9 can be repurposed for estimating the second term of (71), simply by setting $y_m = 1$ and $\rho_m = \rho$ therein. This is due to the expression for the second term of (71) being the same as the second term of (63)

under these substitutions. For completeness, we list the algorithm below. Let us abbreviate the second term of (71) as follows:

$$\zeta_j \equiv \frac{1}{2T} \|\theta\|_1 \mathbb{E}_{s \sim v, k \sim q, t \sim \gamma} \left[s \Re \left[\text{Tr} \left[\text{sgn}(\theta_k) H_k H_j e^{iH(\theta)t/T} \mathcal{U}_{st/T}^{H(\theta)}(\rho) \right] \right] \right]. \quad (\text{D8})$$

Algorithm 11. A hybrid quantum–classical algorithm for estimating ζ_j in (D8) consists of the following steps:

1. Set $m \leftarrow 1$, and set

$$M \leftarrow O \left(\left(\frac{\|\theta\|_1 \max_{j \in [J]} \|H_j\|}{T\varepsilon} \right)^2 \ln \left(\frac{1}{\delta} \right) \right), \quad (\text{D9})$$

where $\varepsilon > 0$ is the desired accuracy and $\delta \in (0, 1)$ is the desired failure probability.

2. Sample $s \sim v$, $k \sim q$, and $t \sim \gamma$.

3. Prepare the state $\mathcal{U}_{st/T}^{H(\theta)}(\rho_m)$ using one sample of ρ and Hamiltonian simulation to realize the unitary channel $\mathcal{U}_{st/T}^{H(\theta)}$.

4. Perform the quantum circuit depicted in Figure 11, with measurement outcomes $Z_m \in \{-1, 1\}$ for the σ_Z measurement and $X_m \in \text{spec}(H_k)$ for the H_k measurement. Set $W_m \leftarrow \frac{\|\theta\|_1}{2T} s \cdot \text{sgn}(\theta_k) Z_m \cdot X_m$. Set $m \leftarrow m + 1$.

5. Repeat Steps 2–4 $M - 1$ more times. Compute the average $\overline{W}_M := \frac{1}{M} \sum_{m=1}^M W_m$ and output this value as an estimate of ζ_j .

By the Hoeffding inequality, we are guaranteed that

$$\Pr \left[\left| \overline{W}_M - \zeta_j \right| \leq \varepsilon \right] \geq 1 - \delta. \quad (\text{D10})$$

b. Hybrid quantum–classical algorithm for estimating smooth ReLU

In this appendix, we detail an alternative formula for the objective function $\text{Tr}[r_T(H(\theta))\rho]$, which is amenable to estimation by means of a hybrid quantum–classical algorithm. The idea behind it is similar to that used for Theorem 13, which in turn is the same idea used in Theorem 2. That is, we can use Theorem 6 and the fundamental theorem of calculus to derive an expression for the smooth ReLU function that can be estimated by a hybrid quantum–classical algorithm.

Theorem 14. The following equality holds:

$$\begin{aligned} \text{Tr}[r_T(H(\theta))\rho] &= \frac{1}{2} \text{Tr}[H(\theta)\rho] + \\ &\frac{J}{2T} \mathbb{E}_{\substack{j \sim [J], \\ \lambda, s \sim v, \\ t \sim \gamma}} \left[\left[\|\theta^{(j)}(\lambda)\|_1 \mathbb{E}_{k \sim q_{j,\lambda}} \left[s \Re \left[\text{Tr} \left[\text{sgn}(\theta_k) H_k H_j e^{iH(\theta^{(j)}(\lambda))t/T} \mathcal{U}_{st/T}^{H(\theta^{(j)}(\lambda))}(\rho) \right] \right] \right] \right] \right], \quad (\text{D11}) \end{aligned}$$

where $r_T(H(\theta))$ is defined from (68), j is selected uniformly at random from $[J]$, λ and s are selected uniformly at random from the unit interval $[0, 1]$, t is selected according to $\gamma(t)$ in (C2),

$$\theta^{(j)}(\lambda) := (0, \dots, 0, \lambda\theta_j, \theta_{j+1}, \dots, \theta_J), \quad (\text{D12})$$

$$\|\theta^{(j)}(\lambda)\|_1 := \lambda |\theta_j| + \sum_{k=j+1}^J |\theta_k|, \quad (\text{D13})$$

$$H(\theta_1, \dots, \theta_J) \equiv H(\theta) = \sum_{j=1}^J \theta_j H_j, \quad (\text{D14})$$

and k is selected according to the conditional probability distribution $q_{j,\lambda}$, defined as

$$q_{j,\lambda}(k) := \begin{cases} \frac{\lambda |\theta_j|}{\|\theta^{(j)}(\lambda)\|_1} & : k = j \\ \frac{|\theta_k|}{\|\theta^{(j)}(\lambda)\|_1} & : k > j \end{cases}. \quad (\text{D15})$$

Proof. This is a direct consequence of the formula in 6 and the same reasoning in the proof of Theorem 13 (note that we set $y_m = 1$ and $\rho_m = \rho$ and the different sign comes about from the same reasoning given in Appendix D 1). \square

Given the similarity of the expressions in (D11) and (C44), it follows that the two terms in (D11) can be estimated by similar algorithms. Indeed, set $y_m = 1$ and $\rho_m = \rho$. Then the algorithm outlined in (C75)–(C77) can be used to estimate the first term in (D11), with the only change being the absence of the minus sign for the first term in (D11). The second term in (D11) can be estimated by Algorithm 10, under the same substitutions $y_m = 1$ and $\rho_m = \rho$. For completeness, we list the algorithm below.

The first term $\frac{1}{2} \text{Tr}[H(\theta)\rho]$ in (D11) can be easily estimated by writing

$$\frac{1}{2} \text{Tr}[H(\theta)\rho] = \frac{1}{2} \text{Tr} \left[\sum_{j=1}^J \theta_j H_j \rho \right] \quad (\text{D16})$$

$$= \frac{1}{2} \sum_{j=1}^J \theta_j \text{Tr}[H_j \rho] \quad (\text{D17})$$

$$= \frac{\|\theta\|_1}{2} \sum_{j=1}^J \frac{|\theta_j|}{\|\theta\|_1} \text{sgn}(\theta_j) \text{Tr}[H_j \rho]. \quad (\text{D18})$$

Thus, in each iteration of an estimation algorithm, we can pick j at random according to the probability distribution $\frac{|\theta_j|}{\|\theta\|_1}$, prepare the state ρ , measure the observable H_j on this state (obtaining an outcome in $\{-1, +1\}$), and multiply the outcome by $\frac{\|\theta\|_1}{2} \text{sgn}(\theta_j)$. One then repeats this procedure a number of times and computes the sample mean. The Hoeffding inequality guarantees that a desired accuracy of $\varepsilon > 0$ and a desired failure probability of $\delta \in (0, 1)$ can be achieved using the following number of trials:

$$O \left(\left(\frac{\|\theta\|_1 \max_{j \in [J]} \|H_j\|}{\varepsilon} \right)^2 \ln \left(\frac{1}{\delta} \right) \right). \quad (\text{D19})$$

The second term in (D11), which we abbreviate as which we abbreviate as

$$\zeta \equiv \frac{J}{2T} \mathbb{E}_{\substack{j \sim [J], \\ \lambda, s \sim v, \\ t \sim \gamma}} \left[\left\| \|\theta^{(j)}(\lambda)\|_1 \mathbb{E}_{k \sim q_{j,\lambda}} \left[s \Re \left[\text{Tr} \left[\text{sgn}(\theta_k) H_k H_j e^{iH(\theta^{(j)}(\lambda))t/T} \mathcal{U}_{st/T}^{H(\theta^{(j)}(\lambda))}(\rho) \right] \right] \right] \right\| \right], \quad (\text{D20})$$

can be estimated by the following algorithm:

Algorithm 12. A hybrid quantum–classical algorithm for estimating ζ in (D20) consists of the following steps:

1. Set $m \leftarrow 1$, and set

$$M \leftarrow O\left(\left(\frac{J\theta^*h^*}{T\varepsilon}\right)^2 \ln\left(\frac{1}{\delta}\right)\right), \quad (\text{D21})$$

$$\theta^* := \max_{\lambda \in [0,1], j \in [J]} \|\theta^{(j)}(\lambda)\|_1, \quad (\text{D22})$$

$$h^* := \max_{j \in [J]} \|H_j\|, \quad (\text{D23})$$

where $\varepsilon > 0$ is the desired accuracy and $\delta \in (0, 1)$ is the desired failure probability.

2. Sample j according to the uniform distribution on $[J]$, $s \sim \nu$, $\lambda \sim \nu$, $t \sim \gamma$, and $k \sim q_{j,\lambda}$.

3. Prepare the state $\mathcal{U}_{st/T}^{H(\theta^{(j)}(\lambda))}(\rho_m)$ using one sample of ρ_m and Hamiltonian simulation to realize the unitary channel $\mathcal{U}_{st/T}^{H(\theta^{(j)}(\lambda))}$.

4. Perform the quantum circuit depicted in Figure 11 (with y_m set to 1), with measurement outcomes $Z_m \in \{-1, 1\}$ for the σ_Z measurement and $X_m \in \text{spec}(H_k)$ for the H_k measurement. Set

$$W_m \leftarrow \frac{J \|\theta^{(j)}(\lambda)\|_1}{2T} s \cdot \text{sgn}(\theta_k) Z_m \cdot X_m. \quad (\text{D24})$$

Set $m \leftarrow m + 1$.

5. Repeat Steps 2–4 $M - 1$ more times. Compute the average $\overline{W}_M := \frac{1}{M} \sum_{m=1}^M W_m$ and output this value as an estimate of ζ .

By the Hoeffding inequality, we are guaranteed that

$$\Pr[|\overline{W}_M - \zeta| \leq \varepsilon] \geq 1 - \delta. \quad (\text{D25})$$

3. Proof of Theorem 7 (correctness of Algorithm 5 for smooth ReLU)

Here we prove that

$$r_T(p) = T_2(\text{ReLU} * \ell_{T_1})\left(\frac{p}{T_2}\right), \quad (\text{D26})$$

for all $p \in \mathbb{R}$, where r_T is defined in (68), ReLU is defined in (67), and ℓ_{T_1} is defined in (38).

Consider that, for all $a \in \mathbb{R}$ and $T > 0$,

$$(\text{ReLU} * \ell_T)(a) = \int_{-\infty}^{\infty} dp \text{ReLU}(p) \ell_T(a - p) \quad (\text{D27})$$

$$= \int_{-\infty}^{\infty} dp \text{ReLU}(p) \ell_T(p - a) \quad (\text{D28})$$

$$= \int_{-\infty}^{\infty} dp \text{ReLU}(p) \frac{e^{(p-a)/T}}{T(e^{(p-a)/T} + 1)^2} \quad (\text{D29})$$

$$= \lim_{R \rightarrow +\infty} \int_{-R}^R dp \operatorname{ReLU}(p) \frac{e^{(p-a)/T}}{T (e^{(p-a)/T} + 1)^2} \quad (\text{D30})$$

$$= \lim_{R \rightarrow +\infty} \int_{-R}^R dp \operatorname{ReLU}(p) \frac{d}{dp} \left(\frac{1}{1 + e^{-(p-a)/T}} \right) \quad (\text{D31})$$

$$= \lim_{R \rightarrow +\infty} \int_0^R dp p \frac{d}{dp} \left(\frac{1}{1 + e^{-(p-a)/T}} \right) \quad (\text{D32})$$

$$\stackrel{(a)}{=} \lim_{R \rightarrow +\infty} \left[\frac{p}{1 + e^{-(p-a)/T}} \Big|_0^R - \int_0^R dp \frac{1}{1 + e^{-(p-a)/T}} \right] \quad (\text{D33})$$

$$= \lim_{R \rightarrow +\infty} \left[\frac{R}{1 + e^{-(R-a)/T}} - \int_0^R dp \frac{1}{1 + e^{-(p-a)/T}} \right] \quad (\text{D34})$$

$$\stackrel{(b)}{=} \lim_{R \rightarrow +\infty} \left[\frac{R}{1 + e^{-(R-a)/T}} - [T \ln(1 + e^{(R-a)/T}) - T \ln(1 + e^{-a/T})] \right] \quad (\text{D35})$$

$$= T \ln(1 + e^{a/T}) + \lim_{R \rightarrow \infty} \left[\frac{R}{1 + e^{-(R-a)/T}} - T \ln(1 + e^{(R-a)/T}) \right] \quad (\text{D36})$$

$$\stackrel{(c)}{=} T \ln(1 + e^{-a/T}) + a \quad (\text{D37})$$

$$= T \ln(1 + e^{-a/T}) + T \ln(e^{a/T}) \quad (\text{D38})$$

$$= T \ln(1 + e^{a/T}). \quad (\text{D39})$$

Now setting $T = T_1 T_2$, for $T_1, T_2 > 0$, this implies that

$$T_2 (\operatorname{ReLU} * \ell_{T_1}) \left(\frac{a}{T_2} \right) = T_1 T_2 \ln(1 + e^{a/(T_1 T_2)}) \quad (\text{D40})$$

$$= T \ln(1 + e^{a/T}) \quad (\text{D41})$$

$$= r_T(a), \quad (\text{D42})$$

thus establishing (D26). The equality (a) follows from integration by parts. The equality (b) follows because, by the substitution $u = \frac{p-a}{T}$,

$$\int_0^R dp \frac{1}{1 + e^{-(p-a)/T}} = T \int_{-a/T}^{(R-a)/T} du \frac{1}{1 + e^{-u}} \quad (\text{D43})$$

$$= T \ln(1 + e^u) \Big|_{-a/T}^{(R-a)/T} \quad (\text{D44})$$

$$= T \ln(1 + e^{(R-a)/T}) - T \ln(1 + e^{-a/T}). \quad (\text{D45})$$

The equality (c) follows because, by setting $S = (R - a) / T$,

$$\begin{aligned} & \lim_{R \rightarrow +\infty} \left[\frac{R}{1 + e^{-(R-a)/T}} - T \ln(1 + e^{(R-a)/T}) \right] \\ &= \lim_{S \rightarrow +\infty} \left[\frac{TS + a}{1 + e^{-S}} - T \ln(1 + e^S) \right] \end{aligned} \quad (\text{D46})$$

$$= \lim_{S \rightarrow +\infty} \left[TS \left(\frac{1}{1 + e^{-S}} \right) + a \left(\frac{1}{1 + e^{-S}} \right) - T \ln(e^S (1 + e^{-S})) \right] \quad (\text{D47})$$

$$= \lim_{S \rightarrow +\infty} \left[TS \left(\frac{1}{1 + e^{-S}} \right) + a \left(\frac{1}{1 + e^{-S}} \right) - TS - T \ln(1 + e^{-S}) \right] \quad (\text{D48})$$

$$= \lim_{s \rightarrow +\infty} \left[TS \left(\frac{1}{1+e^{-s}} - 1 \right) + a \left(\frac{1}{1+e^{-s}} \right) - T \ln(1+e^{-s}) \right] \quad (\text{D49})$$

$$= \lim_{s \rightarrow +\infty} \left[TS \left(\frac{e^{-s}}{1+e^{-s}} \right) + a \left(\frac{1}{1+e^{-s}} \right) - T \ln(1+e^{-s}) \right] \quad (\text{D50})$$

$$= a. \quad (\text{D51})$$

Appendix E: Derivations for sigmoid linear unit (SiLU)

1. Proof of Theorem 8 (derivative of sigmoid linear unit function)

Consider that

$$\text{SiLU}_T(x) := \frac{x}{1+e^{-x/T}}. \quad (\text{E1})$$

The derivative of this function is given by

$$k_T(x) := \frac{\partial}{\partial x} \left(\frac{x}{1+e^{-x/T}} \right) \quad (\text{E2})$$

$$= \frac{1}{1+e^{-x/T}} + \frac{x e^{-x/T}}{T(1+e^{-x/T})^2} \quad (\text{E3})$$

$$= f_T(x) + x \ell_T(-x) \quad (\text{E4})$$

$$= f_T(x) + x \ell_T(x). \quad (\text{E5})$$

Observe also that

$$k_T(x) = \frac{1}{2} \left(1 + g_T \left(\frac{x}{2} \right) \right) + x \ell_T(x) \quad (\text{E6})$$

$$= \frac{1}{2} + \frac{x}{4T} \frac{\tanh\left(\frac{x}{2T}\right)}{\frac{x}{2T}} + x \ell_T(x) \quad (\text{E7})$$

$$= \frac{1}{2} + x \left(\frac{1}{4T} \frac{\tanh\left(\frac{x}{2T}\right)}{\frac{x}{2T}} + \frac{1}{4T} \text{sech}^2\left(\frac{x}{2T}\right) \right) \quad (\text{E8})$$

$$= \frac{1}{2} + \frac{x}{4T} \left(\frac{\tanh\left(\frac{x}{2T}\right)}{\frac{x}{2T}} + \text{sech}^2\left(\frac{x}{2T}\right) \right). \quad (\text{E9})$$

where we used that

$$\ell_T(x) = \frac{e^{x/T}}{T(e^{x/T} + 1)^2} \quad (\text{E10})$$

$$= \frac{1}{4T} \text{sech}^2\left(\frac{x}{2T}\right). \quad (\text{E11})$$

Lemma 3. *Let $x \in \mathbb{R}$, let $x \mapsto A(x)$ be a Hermitian-valued function, and let $T > 0$. Then the following equality holds:*

$$\begin{aligned} \frac{\partial}{\partial x} \text{SiLU}_T(A(x)) &= \frac{1}{2} \frac{\partial}{\partial x} A(x) \\ &+ \frac{1}{2T} \int_{-\infty}^{\infty} dt \left(\frac{\gamma(t) + \mu(t)}{2} \right) \int_0^1 ds s \Re \left[A(x) e^{-isA(x)t/(2T)} \left(\frac{\partial}{\partial x} A(x) \right) e^{-i(1-s)A(x)t/(2T)} \right]. \end{aligned} \quad (\text{E12})$$

Proof. To begin with, let

$$A(x) = \sum_k \lambda_k \Pi_k \quad (\text{E13})$$

be a spectral decomposition of $A(x)$, where we have omitted the dependence on x in the eigenvalues and eigenprojections. Consider that the derivative of the SiLU $_T$ function is given by

$$\frac{\partial}{\partial x} \text{SiLU}_T(A(x)) = \sum_{k,\ell} f_{\text{SiLU}_T}^{[1]}(\lambda_k, \lambda_\ell) \Pi_k \left(\frac{\partial}{\partial x} A(x) \right) \Pi_\ell. \quad (\text{E14})$$

An expression for $f_{\text{SiLU}_T}^{[1]}$ is as follows:

$$f_{\text{SiLU}_T}^{[1]}(y_1, y_2) = \int_0^1 ds k_T(sy_1 + (1-s)y_2). \quad (\text{E15})$$

Defining $\lambda_{s,k,\ell} \equiv s\lambda_k + (1-s)\lambda_\ell$, then we find that

$$\begin{aligned} & \frac{\partial}{\partial x} \text{SiLU}_T(A(x)) \\ &= \sum_{k,\ell} \left(\int_0^1 ds k_T(s\lambda_k + (1-s)\lambda_\ell) \right) \Pi_k \left(\frac{\partial}{\partial x} A(x) \right) \Pi_\ell \end{aligned} \quad (\text{E16})$$

$$= \sum_{k,\ell} \left(\int_0^1 ds \left(\frac{1}{2} + \left(\frac{s\lambda_k + (1-s)\lambda_\ell}{4T} \right) \left(\frac{\tanh\left(\frac{\lambda_{s,k,\ell}}{2T}\right)}{\frac{\lambda_{s,k,\ell}}{2T}} + \text{sech}^2\left(\frac{\lambda_{s,k,\ell}}{2T}\right) \right) \right) \right) \Pi_k \left(\frac{\partial}{\partial x} A(x) \right) \Pi_\ell \quad (\text{E17})$$

$$= \sum_{k,\ell} \left(\frac{1}{2} + \int_0^1 ds \left(\frac{s\lambda_k + (1-s)\lambda_\ell}{4T} \right) \left(\frac{\tanh\left(\frac{\lambda_{s,k,\ell}}{2T}\right)}{\frac{\lambda_{s,k,\ell}}{2T}} + \text{sech}^2\left(\frac{\lambda_{s,k,\ell}}{2T}\right) \right) \right) \Pi_k \left(\frac{\partial}{\partial x} A(x) \right) \Pi_\ell \quad (\text{E18})$$

$$\begin{aligned} &= \frac{1}{2} \sum_{k,\ell} \Pi_k \left(\frac{\partial}{\partial x} A(x) \right) \Pi_\ell \\ &+ \frac{1}{4T} \sum_{k,\ell} \left(\int_0^1 ds (s\lambda_k + (1-s)\lambda_\ell) \left(\frac{\tanh\left(\frac{\lambda_{s,k,\ell}}{2T}\right)}{\frac{\lambda_{s,k,\ell}}{2T}} + \text{sech}^2\left(\frac{\lambda_{s,k,\ell}}{2T}\right) \right) \right) \Pi_k \left(\frac{\partial}{\partial x} A(x) \right) \Pi_\ell \end{aligned} \quad (\text{E19})$$

$$\begin{aligned} &= \frac{1}{2} \frac{\partial}{\partial x} A(x) \\ &+ \frac{1}{4T} \int_0^1 ds \sum_{k,\ell} (s\lambda_k + (1-s)\lambda_\ell) \left(\int_{-\infty}^{\infty} dt (\gamma(t) + \mu(t)) e^{-\frac{i(s\lambda_k + (1-s)\lambda_\ell)t}{2T}} \right) \Pi_k \left(\frac{\partial}{\partial x} A(x) \right) \Pi_\ell. \end{aligned} \quad (\text{E20})$$

We used that

$$\int_{-\infty}^{\infty} dt \gamma(t) e^{-i\omega t} = \frac{\tanh(\omega/2)}{\omega/2}, \quad (\text{E21})$$

$$\int_{-\infty}^{\infty} dt \mu(t) e^{-i\omega t} = \operatorname{sech}^2(\omega). \quad (\text{E22})$$

Now consider that

$$\begin{aligned} & \frac{1}{4T} \int_0^1 ds \sum_{k,\ell} (s\lambda_k + (1-s)\lambda_\ell) \left(\int_{-\infty}^{\infty} dt (\gamma(t) + \mu(t)) e^{-\frac{i(s\lambda_k + (1-s)\lambda_\ell)t}{2T}} \right) \Pi_k \left(\frac{\partial}{\partial x} A(x) \right) \Pi_\ell \\ &= \frac{1}{4T} \int_{-\infty}^{\infty} dt (\gamma(t) + \mu(t)) \int_0^1 ds \sum_{k,\ell} (s\lambda_k + (1-s)\lambda_\ell) \left(e^{-\frac{i(s\lambda_k + (1-s)\lambda_\ell)t}{2T}} \right) \Pi_k \left(\frac{\partial}{\partial x} A(x) \right) \Pi_\ell \quad (\text{E23}) \end{aligned}$$

$$= \frac{1}{4T} \int_{-\infty}^{\infty} dt (\gamma(t) + \mu(t)) \int_0^1 ds \sum_{k,\ell} (s\lambda_k + (1-s)\lambda_\ell) e^{-\frac{is\lambda_k t}{2T}} \Pi_k \left(\frac{\partial}{\partial x} A(x) \right) e^{-\frac{i(1-s)\lambda_\ell t}{2T}} \Pi_\ell \quad (\text{E24})$$

$$\begin{aligned} &= \frac{1}{4T} \int_{-\infty}^{\infty} dt (\gamma(t) + \mu(t)) \int_0^1 ds s \sum_{k,\ell} \lambda_k e^{-\frac{is\lambda_k t}{2T}} \Pi_k \left(\frac{\partial}{\partial x} A(x) \right) e^{-\frac{i(1-s)\lambda_\ell t}{2T}} \Pi_\ell \\ &\quad + \frac{1}{4T} \int_{-\infty}^{\infty} dt (\gamma(t) + \mu(t)) \int_0^1 ds (1-s) \sum_{k,\ell} e^{-\frac{is\lambda_k t}{2T}} \Pi_k \left(\frac{\partial}{\partial x} A(x) \right) \lambda_\ell e^{-\frac{i(1-s)\lambda_\ell t}{2T}} \Pi_\ell \quad (\text{E25}) \end{aligned}$$

$$\begin{aligned} &= \frac{1}{4T} \int_{-\infty}^{\infty} dt (\gamma(t) + \mu(t)) \int_0^1 ds s \left(\sum_k \lambda_k e^{-\frac{is\lambda_k t}{2T}} \Pi_k \right) \left(\frac{\partial}{\partial x} A(x) \right) \left(\sum_\ell e^{-\frac{i(1-s)\lambda_\ell t}{2T}} \Pi_\ell \right) \\ &\quad + \frac{1}{4T} \int_{-\infty}^{\infty} dt (\gamma(t) + \mu(t)) \int_0^1 ds (1-s) \left(\sum_k e^{-\frac{is\lambda_k t}{2T}} \Pi_k \right) \left(\frac{\partial}{\partial x} A(x) \right) \left(\sum_\ell \lambda_\ell e^{-\frac{i(1-s)\lambda_\ell t}{2T}} \Pi_\ell \right) \quad (\text{E26}) \end{aligned}$$

$$\begin{aligned} &= \frac{1}{4T} \int_{-\infty}^{\infty} dt (\gamma(t) + \mu(t)) \int_0^1 ds s A(x) e^{-isA(x)t/(2T)} \left(\frac{\partial}{\partial x} A(x) \right) e^{-i(1-s)A(x)t/(2T)} \\ &\quad + \frac{1}{4T} \int_{-\infty}^{\infty} dt (\gamma(t) + \mu(t)) \int_0^1 ds (1-s) e^{-isA(x)t/(2T)} \left(\frac{\partial}{\partial x} A(x) \right) e^{-i(1-s)A(x)t/(2T)} A(x) \quad (\text{E27}) \end{aligned}$$

$$\begin{aligned} &= \frac{1}{4T} \int_{-\infty}^{\infty} dt (\gamma(t) + \mu(t)) \int_0^1 ds s A(x) e^{-isA(x)t/(2T)} \left(\frac{\partial}{\partial x} A(x) \right) e^{-i(1-s)A(x)t/(2T)} \\ &\quad + \frac{1}{4T} \int_{-\infty}^{\infty} dt (\gamma(t) + \mu(t)) \int_0^1 ds s e^{-i(1-s)A(x)t/(2T)} \left(\frac{\partial}{\partial x} A(x) \right) e^{-isA(x)t/(2T)} A(x) \quad (\text{E28}) \end{aligned}$$

$$\begin{aligned} &= \frac{1}{4T} \int_{-\infty}^{\infty} dt (\gamma(t) + \mu(t)) \int_0^1 ds s A(x) e^{-isA(x)t/(2T)} \left(\frac{\partial}{\partial x} A(x) \right) e^{-i(1-s)A(x)t/(2T)} \\ &\quad + \frac{1}{4T} \int_{-\infty}^{\infty} dt (\gamma(t) + \mu(t)) \int_0^1 ds s e^{i(1-s)A(x)t/(2T)} \left(\frac{\partial}{\partial x} A(x) \right) e^{isA(x)t/(2T)} A(x) \quad (\text{E29}) \end{aligned}$$

$$= \frac{1}{2T} \int_{-\infty}^{\infty} dt \left(\frac{\gamma(t) + \mu(t)}{2} \right) \int_0^1 ds s \Re \left[A(x) e^{-isA(x)t/(2T)} \left(\frac{\partial}{\partial x} A(x) \right) e^{-i(1-s)A(x)t/(2T)} \right], \quad (\text{E30})$$

thus concluding the proof. \square

Theorem (Restatement of Theorem 8). *The following equality holds:*

$$\frac{\partial}{\partial \theta_j} \operatorname{Tr}[\operatorname{SiLU}_T(H(\theta))\rho] = \frac{1}{2} \operatorname{Tr}[H_j \rho] + \frac{\|\theta\|_1}{2T} \mathbb{E}_{\substack{t \sim \xi, \\ s \sim v, \\ k \sim q}} \left[s \Re \left[\operatorname{Tr} \left[\operatorname{sgn}(\theta_k) H_k H_j e^{iH(\theta)t/(2T)} \mathcal{U}_{st/(2T)}^{H(\theta)}(\rho) \right] \right] \right], \quad (\text{E31})$$

where the objective function $\text{Tr}[\text{SiLU}_T(H(\theta))\rho]$ is defined from (74), $\xi(t)$ is the following probability density function

$$\xi(t) := \frac{\gamma(t) + \mu(t)}{2} \quad (\text{E32})$$

v is a uniform random variable on the unit interval $[0, 1]$, q is the following probability distribution:

$$q(k) := \frac{|\theta_k|}{\|\theta\|_1}, \quad (\text{E33})$$

and $\mathcal{U}_t^{H(\theta)}$ is the following unitary quantum channel:

$$\mathcal{U}_t^{H(\theta)}(\cdot) := e^{-iH(\theta)t}(\cdot)e^{iH(\theta)t}. \quad (\text{E34})$$

Proof of Theorem 8. Applying Lemma 3, consider that

$$\begin{aligned} & \frac{\partial}{\partial \theta_j} \text{Tr}[\text{SiLU}_T(H(\theta))\rho] \\ &= \text{Tr} \left[\left(\frac{\partial}{\partial \theta_j} \text{SiLU}_T(H(\theta)) \right) \rho \right] \end{aligned} \quad (\text{E35})$$

$$= \frac{1}{2} \text{Tr}[H_j \rho] + \frac{1}{2T} \int_{-\infty}^{\infty} dt \xi(t) \int_0^1 ds \text{Tr} \left[s \Re \left[H(\theta) e^{-isH(\theta)t/(2T)} \left(\frac{\partial}{\partial \theta_j} H(\theta) \right) e^{-i(1-s)H(\theta)t/(2T)} \right] \rho \right] \quad (\text{E36})$$

$$= \frac{1}{2} \text{Tr}[H_j \rho] + \frac{1}{2T} \mathbb{E}_{\substack{t \sim \xi, \\ s \sim v}} \left[s \text{Tr} \left[\Re \left[H(\theta) e^{-isH(\theta)t/(2T)} \left(\frac{\partial}{\partial \theta_j} H(\theta) \right) e^{-i(1-s)H(\theta)t/(2T)} \right] \rho \right] \right] \quad (\text{E37})$$

$$= \frac{1}{2} \text{Tr}[H_j \rho] + \frac{1}{2T} \mathbb{E}_{\substack{t \sim \xi, \\ s \sim v}} \left[s \Re \left[\text{Tr} \left[e^{-isH(\theta)t/(2T)} H(\theta) H_j e^{-i(1-s)H(\theta)t/(2T)} \rho \right] \right] \right] \quad (\text{E38})$$

$$= \frac{1}{2} \text{Tr}[H_j \rho] + \frac{1}{2T} \mathbb{E}_{\substack{t \sim \xi, \\ s \sim v}} \left[s \Re \left[\text{Tr} \left[H(\theta) H_j e^{-iH(\theta)t/(2T)} e^{isH(\theta)t/(2T)} \rho e^{-istH(\theta)/(2T)} \right] \right] \right] \quad (\text{E39})$$

$$= \frac{1}{2} \text{Tr}[H_j \rho] + \frac{1}{2T} \mathbb{E}_{\substack{t \sim \xi, \\ s \sim v}} \left[s \Re \left[\text{Tr} \left[H(\theta) H_j e^{iH(\theta)t/(2T)} e^{-isH(\theta)t/(2T)} \rho e^{istH(\theta)/(2T)} \right] \right] \right] \quad (\text{E40})$$

$$= \frac{1}{2} \text{Tr}[H_j \rho] + \frac{1}{2T} \mathbb{E}_{\substack{t \sim \xi, \\ s \sim v}} \left[s \Re \left[\text{Tr} \left[H(\theta) H_j e^{iH(\theta)t/(2T)} \mathcal{U}_{st/(2T)}^{H(\theta)}(\rho) \right] \right] \right] \quad (\text{E41})$$

$$= \frac{1}{2} \text{Tr}[H_j \rho] + \frac{\|\theta\|_1}{2T} \mathbb{E}_{\substack{t \sim \xi, \\ s \sim v, \\ k \sim q}} \left[s \Re \left[\text{Tr} \left[\text{sgn}(\theta_k) H_k H_j e^{iH(\theta)t/(2T)} \mathcal{U}_{st/(2T)}^{H(\theta)}(\rho) \right] \right] \right], \quad (\text{E42})$$

thus concluding the proof. \square

2. Hybrid quantum–classical algorithms for SiLU

a. Hybrid quantum–classical algorithm for estimating gradient of SiLU

In this appendix, we briefly summarize a hybrid quantum–classical algorithm for estimating the formula in (76), i.e., the j th partial derivative of $\text{Tr}[\text{SiLU}_T(H(\theta))\rho]$, on a quantum computer.

The first term of (76) can be easily estimated by preparing the state ρ and measuring H_j .

For the second term of (76), let us make the assumption that each H_j in $H(\theta)$ is both Hermitian and unitary (as in the common case when each H_j is a Pauli string). Then an approach similar to Algorithm 9 can be used. We list it below for completeness. Define

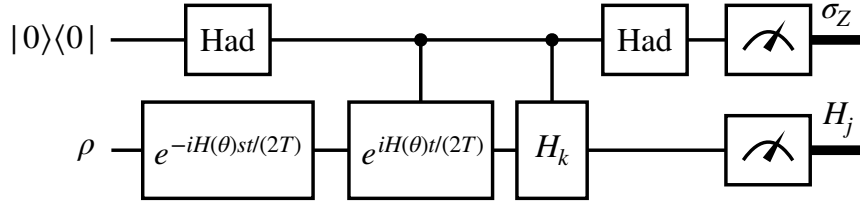


FIG. 12: Quantum circuit used in Algorithm 13 for estimating the second term of (76), denoted by ζ_j in (E43).

$$\zeta_j \equiv \frac{\|\theta\|_1}{2T} \mathbb{E}_{\substack{t \sim \xi, \\ s \sim v, \\ k \sim q}} \left[s \Re \left[\text{Tr} \left[\text{sgn}(\theta_k) H_k H_j e^{iH(\theta)t/(2T)} \mathcal{U}_{st/(2T)}^{H(\theta)}(\rho) \right] \right] \right]. \quad (\text{E43})$$

Algorithm 13. A hybrid quantum–classical algorithm for estimating ζ_j in (E43) consists of the following steps:

1. Set $m \leftarrow 1$, and set

$$M \leftarrow O \left(\left(\frac{\|\theta\|_1 \max_{j \in [J]} \|H_j\|}{T\varepsilon} \right)^2 \ln \left(\frac{1}{\delta} \right) \right), \quad (\text{E44})$$

where $\varepsilon > 0$ is the desired accuracy and $\delta \in (0, 1)$ is the desired failure probability.

2. Sample $s \sim v$, $k \sim q$, and $t \sim \xi$.
3. Prepare the state $\mathcal{U}_{st/(2T)}^{H(\theta)}(\rho)$ using one sample of ρ and Hamiltonian simulation to realize the unitary channel $\mathcal{U}_{st/(2T)}^{H(\theta)}$.
4. Perform the quantum circuit depicted in Figure 12, with measurement outcomes $Z_m \in \{-1, 1\}$ for the σ_Z measurement and $X_m \in \text{spec}(H_k)$ for the H_k measurement. Set $W_m \leftarrow \frac{\|\theta\|_1}{2T} s \cdot \text{sgn}(\theta_k) Z_m \cdot X_m$. Set $m \leftarrow m + 1$.
5. Repeat Steps 2–4 $M - 1$ more times. Compute the average $\overline{W}_M := \frac{1}{M} \sum_{m=1}^M W_m$ and output this value as an estimate of ζ_j .

By the Hoeffding inequality, we are guaranteed that

$$\Pr \left[\left| \overline{W}_M - \zeta_j \right| \leq \varepsilon \right] \geq 1 - \delta. \quad (\text{E45})$$

b. Hybrid quantum–classical algorithm for estimating SiLU

In this appendix, we detail an alternative formula for the objective function $\text{Tr}[\text{SiLU}_T(H(\theta))\rho]$, which is amenable to estimation by means of a hybrid quantum–classical algorithm. The idea behind it is similar to that used for Theorem 13, which in turn is the same idea used in Theorem 2. That is, we can use Theorem 8 and the fundamental theorem of calculus to derive an expression for SiLU that can be estimated by a hybrid quantum–classical algorithm.

Theorem 15. The following equality holds:

$$\begin{aligned} \text{Tr}[\text{SiLU}_T(H(\theta))\rho] &= \frac{1}{2} \text{Tr}[H(\theta)\rho] + \\ &\frac{J}{2T} \mathbb{E}_{\substack{j \sim [J], \\ \lambda, s \sim \mathcal{U}, \\ t \sim \xi}} \left[\|\theta^{(j)}(\lambda)\|_1 \mathbb{E}_{k \sim q_{j,\lambda}} \left[s \Re \left[\text{Tr} \left[\text{sgn}(\theta_k) H_k H_j e^{iH(\theta^{(j)}(\lambda))t/(2T)} \mathcal{U}_{st/(2T)}^{H(\theta^{(j)}(\lambda))}(\rho) \right] \right] \right] \right], \end{aligned} \quad (\text{E46})$$

where $\text{SiLU}_T(H(\theta))$ is defined from (74), j is selected uniformly at random from $[J]$, λ and s are selected uniformly at random from the unit interval $[0, 1]$, t is selected according to $\xi(t)$ in (E32),

$$\theta^{(j)}(\lambda) := (0, \dots, 0, \lambda\theta_j, \theta_{j+1}, \dots, \theta_J), \quad (\text{E47})$$

$$\|\theta^{(j)}(\lambda)\|_1 := \lambda|\theta_j| + \sum_{k=j+1}^J |\theta_k|, \quad (\text{E48})$$

$$H(\theta_1, \dots, \theta_J) \equiv H(\theta) = \sum_{j=1}^J \theta_j H_j, \quad (\text{E49})$$

and k is selected according to the conditional probability distribution $q_{j,\lambda}$, defined as

$$q_{j,\lambda}(k) := \begin{cases} \frac{\lambda|\theta_j|}{\|\theta^{(j)}(\lambda)\|_1} & : k = j \\ \frac{|\theta_k|}{\|\theta^{(j)}(\lambda)\|_1} & : k > j \end{cases}. \quad (\text{E50})$$

Proof. The proof goes along the same lines as in the proof of Theorem 13 (see also Theorem 14), but using the expression in (76) instead of that in (71). \square

For completeness, we delineate the hybrid quantum–classical algorithm that estimates $\text{Tr}[\text{SiLU}_T(H(\theta))\rho]$, using the expression in (E46). The first term $\frac{1}{2} \text{Tr}[H(\theta)\rho]$ in (E46) can be easily estimated by writing

$$\frac{1}{2} \text{Tr}[H(\theta)\rho] = \frac{1}{2} \text{Tr} \left[\sum_{j=1}^J \theta_j H_j \rho \right] \quad (\text{E51})$$

$$= \frac{1}{2} \sum_{j=1}^J \theta_j \text{Tr}[H_j \rho] \quad (\text{E52})$$

$$= \frac{\|\theta\|_1}{2} \sum_{j=1}^J \frac{|\theta_j|}{\|\theta\|_1} \text{sgn}(\theta_j) \text{Tr}[H_j \rho]. \quad (\text{E53})$$

Thus, in each iteration of an estimation algorithm, we can pick j at random according to the probability distribution $\frac{|\theta_j|}{\|\theta\|_1}$, prepare the state ρ , measure the observable H_j on this state (obtaining an outcome in $\{-1, +1\}$), and multiply the outcome by $\frac{\|\theta\|_1}{2} \text{sgn}(\theta_j)$. One then repeats this procedure a number of times and computes the sample mean. The Hoeffding inequality guarantees that a desired accuracy of $\varepsilon > 0$ and a desired failure probability of $\delta \in (0, 1)$ can be achieved using the following number of trials:

$$O \left(\left(\frac{\|\theta\|_1 \max_{j \in [J]} \|H_j\|}{\varepsilon} \right)^2 \ln \left(\frac{1}{\delta} \right) \right). \quad (\text{E54})$$

The second term in (E46), which we abbreviate as

$$\zeta \equiv \frac{J}{2T} \mathbb{E}_{\substack{j \sim [J], \\ \lambda, s \sim v, \\ t \sim \xi}} \left[\left\| \theta^{(j)}(\lambda) \right\|_1 \mathbb{E}_{k \sim q_{j,\lambda}} \left[s \Re \left[\text{Tr} \left[\text{sgn}(\theta_k) H_k H_j e^{iH(\theta^{(j)}(\lambda))t/(2T)} \mathcal{U}_{st/(2T)}^{H(\theta^{(j)}(\lambda))}(\rho_m) \right] \right] \right] \right], \quad (\text{E55})$$

can be estimated by the following algorithm:

Algorithm 14. *A hybrid quantum–classical algorithm for estimating ζ in (E55) consists of the following steps:*

1. Set $m \leftarrow 1$, and set

$$M \leftarrow O \left(\left(\frac{J\theta^* h^*}{T\varepsilon} \right)^2 \ln \left(\frac{1}{\delta} \right) \right), \quad (\text{E56})$$

$$\theta^* := \max_{\lambda \in [0,1], j \in [J]} \left\| \theta^{(j)}(\lambda) \right\|_1, \quad (\text{E57})$$

$$h^* := \max_{j \in [J]} \|H_j\|, \quad (\text{E58})$$

where $\varepsilon > 0$ is the desired accuracy and $\delta \in (0, 1)$ is the desired failure probability.

2. Sample j according to the uniform distribution on $[J]$, $s \sim v$, $\lambda \sim v$, $t \sim \xi$, and $k \sim q_{j,\lambda}$.
3. Prepare the state $\mathcal{U}_{st/(2T)}^{H(\theta^{(j)}(\lambda))}(\rho)$ using one sample of ρ and Hamiltonian simulation to realize the unitary channel $\mathcal{U}_{st/(2T)}^{H(\theta^{(j)}(\lambda))}$.
4. Perform the quantum circuit depicted in Figure 12, with measurement outcomes $Z_m \in \{-1, 1\}$ for the σ_Z measurement and $X_m \in \text{spec}(H_k)$ for the H_k measurement. Set

$$W_m \leftarrow \frac{J \left\| \theta^{(j)}(\lambda) \right\|_1}{2T} s \cdot \text{sgn}(\theta_k) Z_m \cdot X_m. \quad (\text{E59})$$

Set $m \leftarrow m + 1$.

5. Repeat Steps 2–4 $M - 1$ more times. Compute the average $\overline{W}_M := \frac{1}{M} \sum_{m=1}^M W_m$ and output this value as an estimate of ζ .

By the Hoeffding inequality, we are guaranteed that

$$\Pr \left[\left| \overline{W}_M - \zeta \right| \leq \varepsilon \right] \geq 1 - \delta. \quad (\text{E60})$$

3. Proof of Theorem 9 (expected value of quantum convolution and multiplication algorithm)

Following the same reasoning as in (A49)–(A53), we conclude that, for $i \in \{1, 2\}$, $|q_i\rangle$ is a state vector if q_i is a probability density. As in Appendix A3, let us first suppose that the state of the data register is pure and given by $|\varphi\rangle\langle\varphi|$, where $|\varphi\rangle$ is a state vector. Suppose that a spectral decomposition of A is given by

$$A = \sum_i a_i |i\rangle\langle i|. \quad (\text{E61})$$

This implies that

$$e^{i\hat{x}\otimes A} = \sum_i \int_{-\infty}^{\infty} dx e^{ix a_i} |x\rangle\langle x| \otimes |i\rangle\langle i|. \quad (\text{E62})$$

We begin under the assumption that $t_1 = t_2 = 1$. The probability density that Step 3 of Algorithm 6 outputs $p_1, p_2 \in \mathbb{R}$ is equal to

$$\|(\langle p_1| \otimes \langle p_2| \otimes I) e^{i\hat{x}_2 \otimes A_3} e^{i\hat{x}_1 \otimes A_3} (|q_1\rangle \otimes |q_2\rangle \otimes |\varphi\rangle)\|^2. \quad (\text{E63})$$

Thus, the expected value of the output of Algorithm 6 is

$$\int_{-\infty}^{\infty} dp_1 \int_{-\infty}^{\infty} dp_2 r_1(p_1) r_2(p_2) \|(\langle p_1| \otimes \langle p_2| \otimes I) e^{i\hat{x}_2 \otimes A_3} e^{i\hat{x}_1 \otimes A_3} (|q_1\rangle \otimes |q_2\rangle \otimes |\varphi\rangle)\|^2. \quad (\text{E64})$$

Consider that

$$\begin{aligned} & (\langle p_1| \otimes \langle p_2| \otimes I) e^{i\hat{x}_2 \otimes A_3} e^{i\hat{x}_1 \otimes A_3} (|q_1\rangle \otimes |q_2\rangle \otimes |\varphi\rangle) \\ &= (\langle p_1| \otimes \langle p_2| \otimes I) \left(I \otimes \sum_j \int_{-\infty}^{\infty} dx_2 e^{ix_2 a_j} |x_2\rangle\langle x_2| \otimes |j\rangle\langle j| \right) \times \\ & \quad \left(\sum_i \int_{-\infty}^{\infty} dx_1 e^{ix_1 a_i} |x_1\rangle\langle x_1| \otimes I \otimes |i\rangle\langle i| \right) \times \\ & \quad \left(\int_{-\infty}^{\infty} dp'_1 \sqrt{q_1(p'_1)} |p'_1\rangle \otimes \int_{-\infty}^{\infty} dp'_2 \sqrt{q_2(p'_2)} |p'_2\rangle \otimes |\varphi\rangle \right) \end{aligned} \quad (\text{E65})$$

$$\begin{aligned} &= \sum_{i,j} \int_{-\infty}^{\infty} dx_2 \int_{-\infty}^{\infty} dx_1 \int_{-\infty}^{\infty} dp'_1 \int_{-\infty}^{\infty} dp'_2 e^{ix_2 a_j} e^{ix_1 a_i} \sqrt{q_1(p'_1) q_2(p'_2)} \times \\ & \quad \langle p_1|x_1\rangle \langle x_1|p'_1\rangle \langle p_2|x_2\rangle \langle x_2|p'_2\rangle |j\rangle\langle j| |i\rangle\langle i| \langle i|\varphi\rangle \end{aligned} \quad (\text{E66})$$

$$\begin{aligned} &= \sum_i \int_{-\infty}^{\infty} dp'_1 \int_{-\infty}^{\infty} dp'_2 \left(\int_{-\infty}^{\infty} dx_1 e^{ix_1 a_i} \langle p_1|x_1\rangle \langle x_1|p'_1\rangle \right) \times \\ & \quad \left(\int_{-\infty}^{\infty} dx_2 e^{ix_2 a_i} \langle p_2|x_2\rangle \langle x_2|p'_2\rangle \right) \sqrt{q_1(p'_1) q_2(p'_2)} |i\rangle\langle i|\varphi \end{aligned} \quad (\text{E67})$$

$$= \sum_i \int_{-\infty}^{\infty} dp'_1 \int_{-\infty}^{\infty} dp'_2 \delta(p'_1 - p_1 + a_i) \delta(p'_2 - p_2 + a_i) \sqrt{q_1(p'_1) q_2(p'_2)} |i\rangle\langle i|\varphi \quad (\text{E68})$$

$$= \sum_i \sqrt{q_1(p_1 - a_i) q_2(p_2 - a_i)} |i\rangle\langle i|\varphi \quad (\text{E69})$$

$$= \sum_i \sqrt{q_1(a_i - p_1) q_2(a_i - p_2)} |i\rangle\langle i|\varphi. \quad (\text{E70})$$

The fourth equality follows from reasoning similar to that given in (A63)–(A65). The last equality follows from the assumption that q_1 and q_2 are even functions. So then

$$\begin{aligned} & \|(\langle p_1| \otimes \langle p_2| \otimes I) e^{i\hat{x}_2 \otimes A_3} e^{i\hat{x}_1 \otimes A_3} (|q_1\rangle \otimes |q_2\rangle \otimes |\varphi\rangle)\|^2 \\ &= \left\| \sum_i \sqrt{q_1(a_i - p_1) q_2(a_i - p_2)} |i\rangle\langle i|\varphi \right\|^2 \end{aligned} \quad (\text{E71})$$

$$= \langle \varphi | \left(\sum_i q_1(a_i - p_1) q_2(a_i - p_2) |i\rangle\langle i| \right) | \varphi \rangle. \quad (\text{E72})$$

Then we conclude that the expected value is given by

$$\begin{aligned} & \int_{-\infty}^{\infty} dp_1 \int_{-\infty}^{\infty} dp_2 r_1(p_1) r_2(p_2) \left\| \left(\langle p_1 | \otimes \langle p_2 | \otimes I \right) e^{i\hat{x}_2 \otimes A_3} e^{i\hat{x}_1 \otimes A_3} (|q_1\rangle \otimes |q_2\rangle \otimes |\varphi\rangle) \right\|^2 \\ &= \int_{-\infty}^{\infty} dp_1 \int_{-\infty}^{\infty} dp_2 r_1(p_1) r_2(p_2) \langle \varphi | \left(\sum_i q_1(a_i - p_1) q_2(a_i - p_2) |i\rangle\langle i| \right) | \varphi \rangle \end{aligned} \quad (\text{E73})$$

$$= \langle \varphi | \left(\sum_i \left(\int_{-\infty}^{\infty} dp_1 r_1(p_1) q_1(a_i - p_1) \right) \left(\int_{-\infty}^{\infty} dp_2 r_2(p_2) q_2(a_i - p_2) \right) |i\rangle\langle i| \right) | \varphi \rangle \quad (\text{E74})$$

$$= \langle \varphi | \left(\sum_i s_1(a_i) s_2(a_i) |i\rangle\langle i| \right) | \varphi \rangle \quad (\text{E75})$$

$$= \langle \varphi | s_1(A) s_2(A) | \varphi \rangle. \quad (\text{E76})$$

The result generalizes to an arbitrary state ρ because every such state can be written as a convex combination of pure states as

$$\rho = \sum_z t(z) |\varphi_z\rangle\langle \varphi_z|, \quad (\text{E77})$$

so that

$$\begin{aligned} & \int_{-\infty}^{\infty} dp_1 \int_{-\infty}^{\infty} dp_2 r_1(p_1) r_2(p_2) \text{Tr} \left[\begin{array}{l} (|p_1\rangle\langle p_1| \otimes |p_2\rangle\langle p_2| \otimes I) e^{i\hat{x}_2 \otimes A_3} e^{i\hat{x}_1 \otimes A_3} \times \\ (|q_1\rangle\langle q_1| \otimes |q_2\rangle\langle q_2| \otimes \rho) e^{-i\hat{x}_1 \otimes A_3} e^{-i\hat{x}_2 \otimes A_3} \end{array} \right] \\ &= \sum_z t(z) \int_{-\infty}^{\infty} dp_1 \int_{-\infty}^{\infty} dp_2 r_1(p_1) r_2(p_2) \text{Tr} \left[\begin{array}{l} (|p_1\rangle\langle p_1| \otimes |p_2\rangle\langle p_2| \otimes I) e^{i\hat{x}_2 \otimes A_3} e^{i\hat{x}_1 \otimes A_3} \times \\ (|q_1\rangle\langle q_1| \otimes |q_2\rangle\langle q_2| \otimes |\varphi_z\rangle\langle \varphi_z|) e^{-i\hat{x}_1 \otimes A_3} e^{-i\hat{x}_2 \otimes A_3} \end{array} \right] \end{aligned} \quad (\text{E78})$$

$$= \sum_z t(z) \int_{-\infty}^{\infty} dp_1 \int_{-\infty}^{\infty} dp_2 r_1(p_1) r_2(p_2) \left\| \left(\langle p_1 | \otimes \langle p_2 | \otimes I \right) e^{i\hat{x}_2 \otimes A_3} e^{i\hat{x}_1 \otimes A_3} (|q_1\rangle \otimes |q_2\rangle \otimes |\varphi_z\rangle) \right\|^2 \quad (\text{E79})$$

$$= \sum_z t(z) \text{Tr}[s_1(A) s_2(A) |\varphi_z\rangle\langle \varphi_z|] \quad (\text{E80})$$

$$= \text{Tr}[s_1(A) s_2(A) \rho], \quad (\text{E81})$$

where the penultimate equality follows from (E76).

Finally, the claim for different times t_1 and t_2 follows because

$$\begin{aligned} & \int_{-\infty}^{\infty} dp_1 \int_{-\infty}^{\infty} dp_2 r_1(p_1) r_2(p_2) \text{Tr} \left[\begin{array}{l} (|p_1\rangle\langle p_1| \otimes |p_2\rangle\langle p_2| \otimes I) e^{i\hat{x}_2 \otimes A_3 t_2} e^{i\hat{x}_1 \otimes A_3 t_1} \times \\ (|q_1\rangle\langle q_1| \otimes |q_2\rangle\langle q_2| \otimes \rho) e^{-i\hat{x}_1 \otimes A_3 t_1} e^{-i\hat{x}_2 \otimes A_3 t_2} \end{array} \right] \\ &= \text{Tr}[s_1(At_1) s_2(At_2) \rho]. \end{aligned} \quad (\text{E82})$$

4. Proof of Theorem 10 (correctness of Algorithm 7 for SiLU)

This is an application of Theorem 9. Given that the first control qumode is prepared in the vacuum state, its representation in the momentum eigenbasis is

$$|0\rangle = \int dp \sqrt{\phi(p)} |p\rangle, \quad (\text{E83})$$

$$\phi(p) := \frac{e^{-p^2}}{\sqrt{\pi}}. \quad (\text{E84})$$

This means that $q_1 = \phi$. Additionally, $q_2 = \ell_{T_1}$. Since the output of Algorithm 7 is $p_1 \mathbf{1}_{p_2 \geq 0}$, we can take

$$r_1(p_1) = p_1, \quad (\text{E85})$$

$$r_2(p_2) = \mathbf{1}_{p_2 \geq 0}. \quad (\text{E86})$$

By Theorem 9, the expected value equals

$$\text{Tr}[(q_1 * r_1)(H(\theta))(q_2 * r_2)(H(\theta)/T_2)\rho], \quad (\text{E87})$$

because the second controlled evolution uses $H(\theta)/T_2$. Thus, to conclude the proof, we need to show that

$$(q_1 * r_1)(p)(q_2 * r_2)(p/T_2) = \text{SiLU}_T(p). \quad (\text{E88})$$

To this end, consider that

$$(q_1 * r_1)(p) = \int_{-\infty}^{\infty} dp' q_1(p') r_1(p - p') \quad (\text{E89})$$

$$= \int_{-\infty}^{\infty} dp' \phi(p')(p - p') \quad (\text{E90})$$

$$= \int_{-\infty}^{\infty} dp' \phi(p') p - \int_{-\infty}^{\infty} dp' \phi(p') p' \quad (\text{E91})$$

$$= p \int_{-\infty}^{\infty} dp' \phi(p') \quad (\text{E92})$$

$$= p. \quad (\text{E93})$$

The penultimate equality follows because ϕ is a probability density function and because it has zero mean. Now consider that

$$(q_2 * r_2)(p/T_2) = (\ell_{T_1} * \mathbf{1}_{p \geq 0})(p/T_2) \quad (\text{E94})$$

$$= \int_{-\infty}^{\infty} dp' \mathbf{1}_{p' \geq 0} \ell_{T_1}(p/T_2 - p') \quad (\text{E95})$$

$$= \int_0^{\infty} dp' \ell_{T_1}(p/T_2 - p') \quad (\text{E96})$$

$$= \int_0^{\infty} dp' \ell_{T_1}(p' - p/T_2) \quad (\text{E97})$$

$$= \int_{-p/T_2}^{\infty} dp' \ell_{T_1}(p') \quad (\text{E98})$$

$$= \int_{-p/T_2}^{\infty} dp' \frac{d}{dp'} f_{T_1}(p') \quad (\text{E99})$$

$$= f_{T_1}(\infty) - f_{T_1}(-p/T_2) \quad (\text{E100})$$

$$= 1 - f_{T_1 T_2}(-p) \quad (\text{E101})$$

$$= 1 - f_T(-p) \quad (\text{E102})$$

$$= f_T(p), \quad (\text{E103})$$

thus concluding the proof.

Appendix F: Derivations for quantizing Gaussian activation functions

Let us denote the cumulative Gaussian distribution function as

$$\Phi(x) := \frac{1}{\sqrt{2\pi}} \int_{-\infty}^x dy e^{-\frac{1}{2}y^2} \quad (\text{F1})$$

and let us denote the standard Gaussian probability density function as

$$\phi(x) := \frac{1}{\sqrt{2\pi}} e^{-\frac{1}{2}x^2}. \quad (\text{F2})$$

1. Proof of Equation (90)

Our goal is to prove (90), which we recall here:

$$(\phi_{T_1} * r)(p/T_2) = 2\Phi\left(\frac{2p}{T}\right) - 1 =: \operatorname{erf}\left(\frac{\sqrt{2}p}{T}\right), \quad (\text{F3})$$

for all $p \in \mathbb{R}$, with r set as in (39) and $T/2 = T_1 T_2$.

Following the same approach as in (A80)–(A90) and noting that

$$\Phi\left(\frac{p}{T_1}\right) = \int_{-\infty}^p dp' \phi_{T_1}(p'), \quad (\text{F4})$$

consider that

$$(\phi_{T_1} * r)(p/T_2) = (\phi_{T_1} * \mathbf{1}_{p \geq 0})(p/T_2) - (\phi_{T_1} * \mathbf{1}_{p < 0})(p/T_2) \quad (\text{F5})$$

$$= \int_{-\infty}^{\infty} dp' \mathbf{1}_{p' \geq 0} \phi_{T_1}(p/T_2 - p') - \int_{-\infty}^{\infty} dp' \mathbf{1}_{p' < 0} \phi_{T_1}(p/T_2 - p') \quad (\text{F6})$$

$$= \int_0^{\infty} dp' \phi_{T_1}(p/T_2 - p') - \int_{-\infty}^0 dp' \phi_{T_1}(p/T_2 - p') \quad (\text{F7})$$

$$= \int_0^{\infty} dp' \phi_{T_1}(p' - p/T_2) - \int_{-\infty}^0 dp' \phi_{T_1}(p' - p/T_2) \quad (\text{F8})$$

$$= \int_{-p/T_2}^{\infty} dp' \phi_{T_1}(p') - \int_{-\infty}^{-p/T_2} dp' \phi_{T_1}(p') \quad (\text{F9})$$

$$= \int_{-p/T_2}^{\infty} dp' \frac{d}{dp'} \Phi\left(\frac{p'}{T_1}\right) - \int_{-\infty}^{-p/T_2} dp' \frac{d}{dp'} \Phi\left(\frac{p'}{T_1}\right) \quad (\text{F10})$$

$$= \Phi(\infty) - \Phi\left(-\frac{p}{T_1 T_2}\right) - \Phi\left(-\frac{p}{T_1 T_2}\right) + \Phi(-\infty) \quad (\text{F11})$$

$$= 1 - 2\Phi\left(-\frac{2p}{T}\right) \quad (\text{F12})$$

$$= 2\Phi\left(\frac{2p}{T}\right) - 1 \quad (\text{F13})$$

$$= \operatorname{erf}\left(\frac{\sqrt{2}p}{T}\right), \quad (\text{F14})$$

where the fourth equality follows because ϕ_{T_1} is an even function and the penultimate equality follows because $\Phi(-x) = 1 - \Phi(x)$.

2. Gradient of expectation of Gaussian error function activation observable

In this appendix, we derive a formula for the gradient of $\frac{\partial}{\partial \theta_j} \text{Tr} \left[\text{erf} \left(\frac{\sqrt{2}H(\theta)}{T} \right) \rho \right]$ that is useful for estimation on quantum computers. The development here mirrors that in Appendix A 1.

We begin by deriving a formula for the derivative of the matrix Gaussian error function. Recall that

$$\text{erf}(x) = 2\Phi(\sqrt{2}x) - 1, \quad (\text{F15})$$

which implies that

$$\frac{\partial}{\partial x} \text{erf}(x) = 2\sqrt{2}\phi(\sqrt{2}x). \quad (\text{F16})$$

Lemma 4. *Let $x \in \mathbb{R}$, and let $x \mapsto A(x)$ be a Hermitian-valued function. Then the following equality holds:*

$$\frac{\partial}{\partial x} \text{erf}(A(x)) = \frac{2}{\sqrt{\pi}} \int_{-\infty}^{\infty} dt \phi(t) \int_0^1 ds e^{i\sqrt{2}tsA(x)} \left(\frac{\partial}{\partial x} A(x) \right) e^{i\sqrt{2}t(1-s)A(x)}, \quad (\text{F17})$$

where $\phi(t)$ is the standard Gaussian probability density function in (F2).

Proof. To begin with, let

$$A(x) = \sum_k \lambda_k \Pi_k \quad (\text{F18})$$

be a spectral decomposition of $A(x)$, where we have omitted the dependence on x in the eigenvalues and eigenprojections. Consider that the derivative of the matrix Gaussian error function is given by

$$\frac{\partial}{\partial x} \text{erf}(A(x)) = \sum_{k,\ell} f_{\text{erf}}^{[1]}(\lambda_k, \lambda_\ell) \Pi_k \left(\frac{\partial}{\partial x} A(x) \right) \Pi_\ell, \quad (\text{F19})$$

where $f_{\text{erf}}^{[1]}$ is the first divided difference of the Gaussian error function, which is given by

$$f_{\text{erf}}^{[1]}(y_1, y_2) = 2\sqrt{2} \int_0^1 ds \phi\left(\sqrt{2}(sy_1 + (1-s)y_2)\right), \quad (\text{F20})$$

as a consequence of the fundamental theorem of calculus and that

$$\frac{d}{ds} \text{erf}(sy_1 + (1-s)y_2) = 2\sqrt{2}\phi\left(\sqrt{2}(sy_1 + (1-s)y_2)\right) (y_1 - y_2). \quad (\text{F21})$$

Then it follows that

$$\frac{\partial}{\partial x} \text{erf}(A(x)) = 2\sqrt{2} \sum_{k,\ell} \int_0^1 ds \phi\left(\sqrt{2}(s\lambda_k + (1-s)\lambda_\ell)\right) \Pi_k \left(\frac{\partial}{\partial x} A(x) \right) \Pi_\ell. \quad (\text{F22})$$

Now consider that the Fourier transform of $\phi(x)$ is as follows:

$$\phi(x) = \frac{1}{\sqrt{2\pi}} \int_{-\infty}^{\infty} dt \phi(t) e^{itx}, \quad (\text{F23})$$

where $\phi(t)$ is the standard Gaussian probability density function. Then it follows that

$$\frac{\partial}{\partial x} \operatorname{erf}(A(x)) = 2\sqrt{2} \left(\frac{1}{\sqrt{2\pi}} \right) \sum_{k,\ell} \int_0^1 ds \int_{-\infty}^{\infty} dt \phi(t) e^{it\sqrt{2}(s\lambda_k+(1-s)\lambda_\ell)} \Pi_k \left(\frac{\partial}{\partial x} A(x) \right) \Pi_\ell \quad (\text{F24})$$

$$= \frac{2}{\sqrt{\pi}} \int_{-\infty}^{\infty} dt \phi(t) \int_0^1 ds \sum_{k,\ell} e^{it\sqrt{2}(s\lambda_k+(1-s)\lambda_\ell)} \Pi_k \left(\frac{\partial}{\partial x} A(x) \right) \Pi_\ell \quad (\text{F25})$$

$$= \frac{2}{\sqrt{\pi}} \int_{-\infty}^{\infty} dt \phi(t) \int_0^1 ds \left(\sum_k e^{i\sqrt{2}ts\lambda_k} \Pi_k \right) \left(\frac{\partial}{\partial x} A(x) \right) \sum_\ell e^{i\sqrt{2}t(1-s)\lambda_\ell} \Pi_\ell \quad (\text{F26})$$

$$= \frac{2}{\sqrt{\pi}} \int_{-\infty}^{\infty} dt \phi(t) \int_0^1 ds e^{i\sqrt{2}tsA(x)} \left(\frac{\partial}{\partial x} A(x) \right) e^{i\sqrt{2}t(1-s)A(x)}, \quad (\text{F27})$$

thus concluding the proof. \square

Remark 4. For Hermitian matrices A and H , we can write the Fréchet derivative of $\operatorname{erf}(A)$ at H as follows:

$$D \operatorname{erf}(A)[H] = \frac{2}{\sqrt{\pi}} \int_{-\infty}^{\infty} dt \phi(t) \int_0^1 ds e^{i\sqrt{2}tsA} H e^{i\sqrt{2}t(1-s)A}. \quad (\text{F28})$$

Theorem 16. *The following equality holds:*

$$\frac{\partial}{\partial \theta_j} \operatorname{Tr} \left[\operatorname{erf} \left(\frac{\sqrt{2}H(\theta)}{T} \right) \rho \right] = \frac{2}{T} \sqrt{\frac{2}{\pi}} \mathbb{E}_{t \sim \phi, s \sim v} \left[\Re \left[\operatorname{Tr} \left[H_j e^{iH(\theta)2t/T} \mathcal{U}_{2st/T}^{H(\theta)}(\rho) \right] \right] \right], \quad (\text{F29})$$

where $\phi(t)$ is the standard Gaussian probability density function in (F2), v is a uniform random variable on the unit interval $[0, 1]$, and $\mathcal{U}_t^{H(\theta)}$ is the following unitary quantum channel:

$$\mathcal{U}_t^{H(\theta)}(\cdot) := e^{-iH(\theta)t}(\cdot)e^{iH(\theta)t}, \quad (\text{F30})$$

Proof. Consider that

$$\begin{aligned} & \frac{\partial}{\partial \theta_j} \operatorname{Tr} \left[\operatorname{erf} \left(\frac{\sqrt{2}H(\theta)}{T} \right) \rho \right] \\ &= \operatorname{Tr} \left[\left(\frac{\partial}{\partial \theta_j} \operatorname{erf} \left(\frac{\sqrt{2}H(\theta)}{T} \right) \right) \rho \right] \end{aligned} \quad (\text{F31})$$

$$= \operatorname{Tr} \left[\frac{2}{\sqrt{\pi}} \int_{-\infty}^{\infty} dt \phi(t) \int_0^1 ds e^{i\sqrt{2}ts(\sqrt{2}H(\theta)/T)} \left(\frac{\partial}{\partial \theta_j} \frac{\sqrt{2}H(\theta)}{T} \right) e^{i\sqrt{2}t(1-s)(\sqrt{2}H(\theta)/T)} \rho \right] \quad (\text{F32})$$

$$= \frac{2}{T} \sqrt{\frac{2}{\pi}} \int_{-\infty}^{\infty} dt \phi(t) \int_0^1 ds \operatorname{Tr} \left[e^{i2tsH(\theta)/T} H_j e^{i2t(1-s)H(\theta)/T} \rho \right] \quad (\text{F33})$$

$$= \frac{2}{T} \sqrt{\frac{2}{\pi}} \int_{-\infty}^{\infty} dt \phi(t) \int_0^1 ds \operatorname{Tr} \left[H_j e^{i2t(1-s)H(\theta)/T} \rho e^{i2tsH(\theta)/T} \right]. \quad (\text{F34})$$

Using the conventions in the statement of the lemma, we can rewrite the expression once more as follows:

$$\frac{\partial}{\partial \theta_j} \operatorname{Tr} \left[\operatorname{erf} \left(\frac{\sqrt{2}H(\theta)}{T} \right) \rho \right] = \frac{2}{T} \sqrt{\frac{2}{\pi}} \mathbb{E}_{t \sim \phi, s \sim v} \left[\operatorname{Tr} \left[H_j e^{iH(\theta)2t/T} \mathcal{U}_{2st/T}^{H(\theta)}(\rho) \right] \right]. \quad (\text{F35})$$

We conclude the statement of the theorem by employing the same arguments used at the end of the proof of Theorem 1. \square

3. Proof of Equation (94)

Our goal is to prove (94), which we recall here:

$$\text{GReLU}_T(x) := x\Phi\left(\frac{x}{T}\right) + T\phi\left(\frac{x}{T}\right) \quad (\text{F36})$$

$$= T_2 (\text{ReLU} * \phi_{T_1})\left(\frac{x}{T_2}\right), \quad (\text{F37})$$

where $T = T_1 T_2$.

Consider that, for all $a \in \mathbb{R}$ and $T > 0$,

$$(\text{ReLU} * \phi_T)(a) = \int_{-\infty}^{\infty} dp \text{ReLU}(p) \phi_T(a-p) \quad (\text{F38})$$

$$= \int_{-\infty}^{\infty} dp \text{ReLU}(p) \phi_T(p-a) \quad (\text{F39})$$

$$= \frac{1}{\sqrt{2\pi}T} \int_{-\infty}^{\infty} dp \text{ReLU}(p) \exp\left(-\frac{(p-a)^2}{2T^2}\right) \quad (\text{F40})$$

$$= \frac{1}{\sqrt{2\pi}T} \int_0^{\infty} dp p \exp\left(-\frac{(p-a)^2}{2T^2}\right) \quad (\text{F41})$$

$$= \frac{1}{\sqrt{2\pi}T} \int_{-a}^{\infty} dp' (p' + a) \exp\left(-\frac{(p')^2}{2T^2}\right) \quad (\text{F42})$$

$$= \frac{1}{\sqrt{2\pi}} \int_{-a/T}^{\infty} dz (Tz + a) \exp\left(-\frac{z^2}{2}\right) \quad (\text{F43})$$

$$= T \frac{1}{\sqrt{2\pi}} \int_{-a/T}^{\infty} dz z \exp\left(-\frac{z^2}{2}\right) + a \frac{1}{\sqrt{2\pi}} \int_{-a/T}^{\infty} dz \exp\left(-\frac{z^2}{2}\right) \quad (\text{F44})$$

$$\stackrel{(a)}{=} T \frac{1}{\sqrt{2\pi}} \left[-\exp\left(-\frac{z^2}{2}\right) \Big|_{-a/T}^{\infty} \right] + a\Phi(a/T) \quad (\text{F45})$$

$$= T \frac{1}{\sqrt{2\pi}} \exp\left(-\frac{(a/T)^2}{2}\right) + a\Phi(a/T) \quad (\text{F46})$$

$$= T\phi\left(\frac{a}{T}\right) + a\Phi\left(\frac{a}{T}\right), \quad (\text{F47})$$

where the equality (a) follows because

$$\frac{1}{\sqrt{2\pi}} \int_{-a/T}^{\infty} dz \exp\left(-\frac{z^2}{2}\right) = \frac{1}{\sqrt{2\pi}} \int_{-\infty}^{\infty} dz \exp\left(-\frac{z^2}{2}\right) - \frac{1}{\sqrt{2\pi}} \int_{-\infty}^{-a/T} dz \exp\left(-\frac{z^2}{2}\right) \quad (\text{F48})$$

$$= 1 - \Phi(-a/T) \quad (\text{F49})$$

$$= \Phi(a/T). \quad (\text{F50})$$

Now setting $T = T_1 T_2$, for $T_1, T_2 > 0$, this implies that

$$T_2 (\text{ReLU} * \phi_{T_1}) \left(\frac{x}{T_2} \right) = T_2 \left[T_1 \phi \left(\frac{x}{T_1 T_2} \right) + \frac{x}{T_2} \Phi \left(\frac{x}{T_1 T_2} \right) \right] \quad (\text{F51})$$

$$= T_1 T_2 \phi \left(\frac{x}{T_1 T_2} \right) + x \Phi \left(\frac{x}{T_1 T_2} \right) \quad (\text{F52})$$

$$= T \phi \left(\frac{x}{T} \right) + x \Phi \left(\frac{x}{T} \right). \quad (\text{F53})$$

4. Derivative of Gaussian smoothed rectified linear unit (GReLU)

We begin by proving (96). Consider that

$$\frac{\partial}{\partial x} [\text{GReLU}_T(x)] = \frac{\partial}{\partial x} \left[x \Phi \left(\frac{x}{T} \right) + T \phi \left(\frac{x}{T} \right) \right] \quad (\text{F54})$$

$$= \Phi \left(\frac{x}{T} \right) + x \left[\frac{\partial}{\partial x} \Phi \left(\frac{x}{T} \right) \right] + T \frac{\partial}{\partial x} \phi \left(\frac{x}{T} \right) \quad (\text{F55})$$

$$= \Phi \left(\frac{x}{T} \right) + \frac{x}{T} \phi \left(\frac{x}{T} \right) - T \left(\frac{x}{T} \right) \phi \left(\frac{x}{T} \right) \frac{1}{T} \quad (\text{F56})$$

$$= \Phi \left(\frac{x}{T} \right). \quad (\text{F57})$$

Lemma 5. *The following equality holds:*

$$\frac{\partial}{\partial x} [\text{GReLU}_T(x)] = \frac{1}{2} + \frac{1}{\sqrt{2\pi}} \left(\frac{x}{T} \right) \mathbb{E}_{t \sim \nu_T, v \sim \nu} [e^{-ixvt}], \quad (\text{F58})$$

where $\nu_T(t)$ is the following Gaussian probability density function on $t \in \mathbb{R}$:

$$\nu_T(t) := \frac{T}{\sqrt{2\pi}} e^{-T^2 t^2 / 2}, \quad (\text{F59})$$

and v is a uniform random variable over the unit interval $[0, 1]$.

Proof. Consider that

$$\frac{\partial}{\partial x} [\text{GReLU}_T(x)] = \Phi \left(\frac{x}{T} \right) \quad (\text{F60})$$

$$= \frac{1}{2} + \frac{1}{2} \operatorname{erf} \left(\frac{x}{\sqrt{2}T} \right) \quad (\text{F61})$$

$$= \frac{1}{2} + \frac{x}{\sqrt{2\pi}T} \int_0^1 dv e^{-\frac{x^2 v^2}{2T^2}} \quad (\text{F62})$$

$$= \frac{1}{2} + \frac{x}{T} \int_0^1 dv \left(\frac{T}{\sqrt{2\pi}} \int_{-\infty}^{\infty} dt e^{-T^2 t^2 / 2} \left(\frac{1}{\sqrt{2\pi}} e^{-ixvt} \right) \right) \quad (\text{F63})$$

$$= \frac{1}{2} + \frac{x}{\sqrt{2\pi}T} \mathbb{E}_{t \sim \nu_T, v \sim \nu} [e^{-ixvt}] \quad (\text{F64})$$

$$= \frac{1}{2} + \frac{1}{\sqrt{2\pi}} \left(\frac{x}{T} \right) \mathbb{E}_{t \sim \nu_T, v \sim \nu} [e^{-ixvt}], \quad (\text{F65})$$

thus concluding the proof. \square

Lemma 6. Let $x \in \mathbb{R}$, let $x \mapsto A(x)$ be a Hermitian-valued function, and let $T > 0$. Then the following equality holds:

$$\frac{\partial}{\partial x} \text{GReLU}_T(A(x)) = \frac{1}{2} \frac{\partial}{\partial x} A(x) + \sqrt{\frac{2}{\pi}} \left(\frac{1}{T} \right) \mathbb{E}_{t \sim \nu_T, v \sim \nu} \left[s \Re \left[A(x) e^{-isA(x)vt} \left(\frac{\partial}{\partial x} A(x) \right) e^{-i(1-s)A(x)vt} \right] \right], \quad (\text{F66})$$

where ν_T is the probability measure defined in (F59) and v is a uniform random variable over the unit interval $[0, 1]$.

Proof. To begin with, let

$$A(x) = \sum_k \lambda_k \Pi_k \quad (\text{F67})$$

be a spectral decomposition of $A(x)$, where we have omitted the dependence on x in the eigenvalues and eigenprojections. Consider that the derivative of the GReLU_T function is given by

$$\frac{\partial}{\partial x} \text{GReLU}_T(A(x)) = \sum_{k, \ell} f_{\text{GReLU}_T}^{[1]}(\lambda_k, \lambda_\ell) \Pi_k \left(\frac{\partial}{\partial x} A(x) \right) \Pi_\ell, \quad (\text{F68})$$

where $f_{\text{GReLU}_T}^{[1]}$ denotes the first divided difference of GReLU_T . An expression for $f_{\text{GReLU}_T}^{[1]}$ is as follows:

$$f_{\text{GReLU}_T}^{[1]}(y_1, y_2) = \int_0^1 ds \left(\frac{1}{2} + \frac{(sy_1 + (1-s)y_2)}{\sqrt{2\pi T}} \mathbb{E}_{t \sim \nu_T, v \sim \nu} [e^{-i(sy_1 + (1-s)y_2)vt}] \right), \quad (\text{F69})$$

where we used Lemma 5 and the fact that

$$f^{[1]}(y_1, y_2) = \int_0^1 ds f'(sy_1 + (1-s)y_2). \quad (\text{F70})$$

Defining $\lambda_{s,k,\ell} \equiv s\lambda_k + (1-s)\lambda_\ell$, then we find that

$$\begin{aligned} & \frac{\partial}{\partial x} \text{GReLU}_T(A(x)) \\ &= \sum_{k, \ell} \left(\int_0^1 ds \left(\frac{1}{2} + \frac{\lambda_{s,k,\ell}}{\sqrt{2\pi T}} \mathbb{E}_{t \sim \nu_T, v \sim \nu} [e^{-i\lambda_{s,k,\ell}vt}] \right) \right) \Pi_k \left(\frac{\partial}{\partial x} A(x) \right) \Pi_\ell \end{aligned} \quad (\text{F71})$$

$$= \sum_{k, \ell} \left(\frac{1}{2} + \int_0^1 ds \frac{\lambda_{s,k,\ell}}{\sqrt{2\pi T}} \mathbb{E}_{t \sim \nu_T, v \sim \nu} [e^{-i\lambda_{s,k,\ell}vt}] \right) \Pi_k \left(\frac{\partial}{\partial x} A(x) \right) \Pi_\ell \quad (\text{F72})$$

$$\begin{aligned} &= \frac{1}{2} \sum_{k, \ell} \Pi_k \left(\frac{\partial}{\partial x} A(x) \right) \Pi_\ell \\ &\quad + \frac{1}{\sqrt{2\pi T}} \sum_{k, \ell} \left(\int_0^1 ds \lambda_{s,k,\ell} \mathbb{E}_{t \sim \nu_T, v \sim \nu} [e^{-i\lambda_{s,k,\ell}vt}] \right) \Pi_k \left(\frac{\partial}{\partial x} A(x) \right) \Pi_\ell \end{aligned} \quad (\text{F73})$$

$$\begin{aligned} &= \frac{1}{2} \frac{\partial}{\partial x} A(x) \\ &\quad + \frac{1}{\sqrt{2\pi T}} \int_0^1 ds \sum_{k, \ell} (s\lambda_k + (1-s)\lambda_\ell) \mathbb{E}_{t \sim \nu_T, v \sim \nu} [e^{-i(s\lambda_k + (1-s)\lambda_\ell)vt}] \Pi_k \left(\frac{\partial}{\partial x} A(x) \right) \Pi_\ell. \end{aligned} \quad (\text{F74})$$

Now consider that

$$\begin{aligned} & \int_0^1 ds \sum_{k,\ell} (s\lambda_k + (1-s)\lambda_\ell) \mathbb{E}_{t \sim \nu_T, v \sim \nu} [e^{-i(s\lambda_k + (1-s)\lambda_\ell)vt}] \Pi_k \left(\frac{\partial}{\partial x} A(x) \right) \Pi_\ell \\ &= \mathbb{E}_{t \sim \nu_T, v \sim \nu} \left[\int_0^1 ds \sum_{k,\ell} (s\lambda_k + (1-s)\lambda_\ell) e^{-i(s\lambda_k + (1-s)\lambda_\ell)vt} \Pi_k \left(\frac{\partial}{\partial x} A(x) \right) \Pi_\ell \right] \end{aligned} \quad (\text{F75})$$

$$= \mathbb{E}_{t \sim \nu_T, v \sim \nu} \left[\int_0^1 ds \sum_{k,\ell} (s\lambda_k + (1-s)\lambda_\ell) e^{-is\lambda_k vt} \Pi_k \left(\frac{\partial}{\partial x} A(x) \right) e^{-i(1-s)\lambda_\ell vt} \Pi_\ell \right] \quad (\text{F76})$$

$$\begin{aligned} &= \mathbb{E}_{t \sim \nu_T, v \sim \nu} \left[\int_0^1 ds s \sum_{k,\ell} \lambda_k e^{-is\lambda_k vt} \Pi_k \left(\frac{\partial}{\partial x} A(x) \right) e^{-i(1-s)\lambda_\ell vt} \Pi_\ell \right] \\ &\quad + \mathbb{E}_{t \sim \nu_T, v \sim \nu} \left[\int_0^1 ds (1-s) \sum_{k,\ell} e^{-is\lambda_k vt} \Pi_k \left(\frac{\partial}{\partial x} A(x) \right) \lambda_\ell e^{-i(1-s)\lambda_\ell vt} \Pi_\ell \right] \end{aligned} \quad (\text{F77})$$

$$\begin{aligned} &= \mathbb{E}_{t \sim \nu_T, v \sim \nu} \left[\int_0^1 ds s \left(\sum_k \lambda_k e^{-is\lambda_k vt} \Pi_k \right) \left(\frac{\partial}{\partial x} A(x) \right) \left(\sum_\ell e^{-i(1-s)\lambda_\ell vt} \Pi_\ell \right) \right] \\ &\quad + \mathbb{E}_{t \sim \nu_T, v \sim \nu} \left[\int_0^1 ds (1-s) \left(\sum_k e^{-is\lambda_k vt} \Pi_k \right) \left(\frac{\partial}{\partial x} A(x) \right) \left(\sum_\ell \lambda_\ell e^{-i(1-s)\lambda_\ell vt} \Pi_\ell \right) \right] \end{aligned} \quad (\text{F78})$$

$$\begin{aligned} &= \mathbb{E}_{t \sim \nu_T, v \sim \nu} \left[\int_0^1 ds s A(x) e^{-isA(x)vt} \left(\frac{\partial}{\partial x} A(x) \right) e^{-i(1-s)A(x)vt} \right] \\ &\quad + \mathbb{E}_{t \sim \nu_T, v \sim \nu} \left[\int_0^1 ds (1-s) e^{-isA(x)vt} \left(\frac{\partial}{\partial x} A(x) \right) e^{-i(1-s)A(x)vt} A(x) \right] \end{aligned} \quad (\text{F79})$$

$$\begin{aligned} &= \mathbb{E}_{t \sim \nu_T, v \sim \nu, s \sim \nu} \left[s A(x) e^{-isA(x)vt} \left(\frac{\partial}{\partial x} A(x) \right) e^{-i(1-s)A(x)vt} \right] \\ &\quad + \mathbb{E}_{t \sim \nu_T, v \sim \nu} \left[\int_0^1 ds s e^{-i(1-s)A(x)vt} \left(\frac{\partial}{\partial x} A(x) \right) e^{-isA(x)vt} A(x) \right] \end{aligned} \quad (\text{F80})$$

$$\begin{aligned} &= \mathbb{E}_{t \sim \nu_T, v \sim \nu, s \sim \nu} \left[s A(x) e^{-isA(x)vt} \left(\frac{\partial}{\partial x} A(x) \right) e^{-i(1-s)A(x)vt} \right] \\ &\quad + \mathbb{E}_{t \sim \nu_T, v \sim \nu} \left[\int_0^1 ds s e^{i(1-s)A(x)vt} \left(\frac{\partial}{\partial x} A(x) \right) e^{isA(x)vt} A(x) \right] \end{aligned} \quad (\text{F81})$$

$$\begin{aligned} &= \mathbb{E}_{t \sim \nu_T, v \sim \nu, s \sim \nu} \left[s A(x) e^{-isA(x)vt} \left(\frac{\partial}{\partial x} A(x) \right) e^{-i(1-s)A(x)vt} \right] \\ &\quad + \mathbb{E}_{t \sim \nu_T, v \sim \nu, s \sim \nu} \left[s e^{i(1-s)A(x)vt} \left(\frac{\partial}{\partial x} A(x) \right) e^{isA(x)vt} A(x) \right] \end{aligned} \quad (\text{F82})$$

$$= 2\mathbb{E}_{t \sim \nu_T, v \sim \nu, s \sim \nu} \left[s \Re \left[A(x) e^{-isA(x)vt} \left(\frac{\partial}{\partial x} A(x) \right) e^{-i(1-s)A(x)vt} \right] \right], \quad (\text{F83})$$

thus concluding the proof. \square

Theorem 17. *The following equality holds:*

$$\frac{\partial}{\partial \theta_j} \text{Tr}[\text{GReLU}_T(H(\theta))\rho] = \frac{1}{2} \text{Tr}[H_j \rho]$$

$$+ \sqrt{\frac{2}{\pi}} \left(\frac{1}{T} \right) \|\theta\|_1 \mathbb{E}_{t \sim \nu_T, k \sim q, v, s \sim \nu} \left[s \Re \left[\text{Tr} \left[\text{sgn}(\theta_k) H_k H_j e^{iH(\theta)vt} \mathcal{U}_{svt}^{H(\theta)}(\rho) \right] \right] \right], \quad (\text{F84})$$

where the objective function $\text{Tr}[\text{GReLU}_T(H(\theta))\rho]$ is defined from (92), the probability densities ν_T and ν are defined in Lemma 6, q is the following probability distribution:

$$q(k) := \frac{|\theta_k|}{\|\theta\|_1}, \quad (\text{F85})$$

and $\mathcal{U}_t^{H(\theta)}$ is the following unitary quantum channel:

$$\mathcal{U}_t^{H(\theta)}(\cdot) := e^{-iH(\theta)t}(\cdot)e^{iH(\theta)t}. \quad (\text{F86})$$

Proof. Applying Lemma 6, consider that

$$\begin{aligned} & \frac{\partial}{\partial \theta_j} \text{Tr}[\text{GReLU}_T(H(\theta))\rho] \\ &= \text{Tr} \left[\left(\frac{\partial}{\partial \theta_j} \text{GReLU}_T(H(\theta)) \right) \rho \right] \end{aligned} \quad (\text{F87})$$

$$= \frac{1}{2} \text{Tr}[H_j \rho] + \sqrt{\frac{2}{\pi}} \left(\frac{1}{T} \right) \mathbb{E}_{t \sim \nu_T, v, s \sim \nu} \left[\text{Tr} \left[s \Re \left[H(\theta) e^{-isH(\theta)vt} \left(\frac{\partial}{\partial \theta_j} H(\theta) \right) e^{-i(1-s)H(\theta)vt} \right] \rho \right] \right] \quad (\text{F88})$$

$$= \frac{1}{2} \text{Tr}[H_j \rho] + \sqrt{\frac{2}{\pi}} \left(\frac{1}{T} \right) \mathbb{E}_{t \sim \nu_T, v, s \sim \nu} \left[s \text{Tr} \left[\Re \left[H(\theta) e^{-isH(\theta)vt} H_j e^{-i(1-s)H(\theta)vt} \right] \rho \right] \right] \quad (\text{F89})$$

$$= \frac{1}{2} \text{Tr}[H_j \rho] + \sqrt{\frac{2}{\pi}} \left(\frac{1}{T} \right) \mathbb{E}_{t \sim \nu_T, v, s \sim \nu} \left[s \Re \left[\text{Tr} \left[e^{-isH(\theta)vt} H(\theta) H_j e^{-i(1-s)H(\theta)vt} \rho \right] \right] \right] \quad (\text{F90})$$

$$= \frac{1}{2} \text{Tr}[H_j \rho] + \sqrt{\frac{2}{\pi}} \left(\frac{1}{T} \right) \mathbb{E}_{t \sim \nu_T, v, s \sim \nu} \left[s \Re \left[\text{Tr} \left[H(\theta) H_j e^{-iH(\theta)vt} e^{isH(\theta)vt} \rho e^{-isvtH(\theta)} \right] \right] \right] \quad (\text{F91})$$

$$= \frac{1}{2} \text{Tr}[H_j \rho] + \sqrt{\frac{2}{\pi}} \left(\frac{1}{T} \right) \mathbb{E}_{t \sim \nu_T, v, s \sim \nu} \left[s \Re \left[\text{Tr} \left[H(\theta) H_j e^{iH(\theta)vt} e^{-isH(\theta)vt} \rho e^{isvtH(\theta)} \right] \right] \right] \quad (\text{F92})$$

$$= \frac{1}{2} \text{Tr}[H_j \rho] + \sqrt{\frac{2}{\pi}} \left(\frac{1}{T} \right) \mathbb{E}_{t \sim \nu_T, v, s \sim \nu} \left[s \Re \left[\text{Tr} \left[H(\theta) H_j e^{iH(\theta)vt} \mathcal{U}_{svt}^{H(\theta)}(\rho) \right] \right] \right] \quad (\text{F93})$$

$$= \frac{1}{2} \text{Tr}[H_j \rho] + \sqrt{\frac{2}{\pi}} \left(\frac{1}{T} \right) \|\theta\|_1 \mathbb{E}_{t \sim \nu_T, v, s \sim \nu, k \sim q} \left[s \Re \left[\text{Tr} \left[\text{sgn}(\theta_k) H_k H_j e^{iH(\theta)vt} \mathcal{U}_{svt}^{H(\theta)}(\rho) \right] \right] \right], \quad (\text{F94})$$

thus concluding the proof. \square

5. Derivative of Gaussian error linear unit (GeLU)

Lemma 7. *The following equality holds:*

$$\frac{\partial}{\partial x} \left[x \Phi \left(\frac{x}{T} \right) \right] = \frac{1}{2} + \sqrt{\frac{2}{\pi}} \left(\frac{x}{T} \right) \mathbb{E}_{t \sim \nu_T, v \sim \kappa} \left[e^{-ixvt} \right], \quad (\text{F95})$$

where $\nu_T(t)$ is the following Gaussian probability density function on $t \in \mathbb{R}$:

$$\nu_T(t) := \frac{T}{\sqrt{2\pi}} e^{-T^2 t^2 / 2}, \quad (\text{F96})$$

and κ is the following probability measure:

$$d\kappa(v) := \frac{1}{2}\delta_1(dv) + \frac{1}{2}\mathbf{1}_{[0,1]}(v) dv. \quad (\text{F97})$$

Proof. Consider that

$$\frac{\partial}{\partial x} \left[x\Phi\left(\frac{x}{T}\right) \right] = \Phi\left(\frac{x}{T}\right) + \frac{x}{T}\phi\left(\frac{x}{T}\right) \quad (\text{F98})$$

$$= \frac{1}{2} \left(1 + \operatorname{erf}\left(\frac{x}{\sqrt{2}T}\right) \right) + \frac{x}{T}\phi\left(\frac{x}{T}\right) \quad (\text{F99})$$

$$= \frac{1}{2} + \frac{1}{2} \operatorname{erf}\left(\frac{x}{\sqrt{2}T}\right) + \frac{x}{T}\phi\left(\frac{x}{T}\right). \quad (\text{F100})$$

Furthermore,

$$\frac{x}{T}\phi\left(\frac{x}{T}\right) = \frac{x}{T} \left(\frac{1}{\sqrt{2\pi}} e^{-\frac{x^2}{2T^2}} \right) \quad (\text{F101})$$

$$= \frac{x}{\sqrt{2\pi}T} \left(\frac{T}{\sqrt{2\pi}} \int_{-\infty}^{\infty} dt e^{-T^2 t^2/2} e^{-ixt} \right) \quad (\text{F102})$$

$$= \frac{x}{\sqrt{2\pi}T} \mathbb{E}_{t \sim \nu_T} [e^{-ixt}]. \quad (\text{F103})$$

Also,

$$\Phi\left(\frac{x}{T}\right) = \frac{1}{2} + \frac{1}{2} \operatorname{erf}\left(\frac{x}{\sqrt{2}T}\right) \quad (\text{F104})$$

$$= \frac{1}{2} + \frac{x}{\sqrt{2\pi}T} \int_0^1 dv e^{-\frac{x^2 v^2}{2T^2}} \quad (\text{F105})$$

$$= \frac{1}{2} + \frac{x}{T} \int_0^1 dv \left(\frac{T}{\sqrt{2\pi}} \int_{-\infty}^{\infty} dt e^{-T^2 t^2/2} \left(\frac{1}{\sqrt{2\pi}} e^{-ixvt} \right) \right) \quad (\text{F106})$$

$$= \frac{1}{2} + \frac{x}{\sqrt{2\pi}T} \mathbb{E}_{t \sim \nu_T, v \sim \nu} [e^{-ixvt}]. \quad (\text{F107})$$

So this implies that

$$\frac{\partial}{\partial x} \left[x\Phi\left(\frac{x}{T}\right) \right] = \frac{1}{2} + \frac{x}{\sqrt{2\pi}T} \left(\mathbb{E}_{t \sim \nu_T, v \sim \nu} [e^{-ixvt}] + \mathbb{E}_{t \sim \nu_T} [e^{-ixt}] \right). \quad (\text{F108})$$

Using the probability measure κ , it follows that

$$\mathbb{E}_{v \sim \kappa} [e^{-ixvt}] = \frac{1}{2} e^{-ixt} + \frac{1}{2} \int_0^1 dv e^{-ixvt}, \quad (\text{F109})$$

so that

$$\frac{\partial}{\partial x} \left[x\Phi\left(\frac{x}{T}\right) \right] = \frac{1}{2} + \frac{2x}{\sqrt{2\pi}T} \mathbb{E}_{t \sim \nu_T, v \sim \kappa} [e^{-ixvt}] \quad (\text{F110})$$

$$= \frac{1}{2} + \sqrt{\frac{2}{\pi}} \left(\frac{x}{T} \right) \mathbb{E}_{t \sim \nu_T, v \sim \kappa} [e^{-ixvt}], \quad (\text{F111})$$

thus concluding the proof. \square

Lemma 8. Let $x \in \mathbb{R}$, let $x \mapsto A(x)$ be a Hermitian-valued function, and let $T > 0$. Then the following equality holds:

$$\frac{\partial}{\partial x} \text{GeLU}_T(A(x)) = \frac{1}{2} \frac{\partial}{\partial x} A(x) + \sqrt{\frac{2}{\pi}} \left(\frac{2}{T} \right) \mathbb{E}_{\substack{t \sim \nu_T, \\ v \sim \kappa, \\ s \sim v}} \left[s \Re \left[A(x) e^{-isA(x)vt} \left(\frac{\partial}{\partial x} A(x) \right) e^{-i(1-s)A(x)vt} \right] \right], \quad (\text{F112})$$

where ν_T is the probability measure defined in (F96), κ is the probability measure defined in (F97), and v is a uniform random variable over the unit interval $[0, 1]$.

Proof. To begin with, let

$$A(x) = \sum_k \lambda_k \Pi_k \quad (\text{F113})$$

be a spectral decomposition of $A(x)$, where we have omitted the dependence on x in the eigenvalues and eigenprojections. Consider that the derivative of the GeLU_T function is given by

$$\frac{\partial}{\partial x} \text{GeLU}_T(A(x)) = \sum_{k,\ell} f_{\text{GeLU}_T}^{[1]}(\lambda_k, \lambda_\ell) \Pi_k \left(\frac{\partial}{\partial x} A(x) \right) \Pi_\ell, \quad (\text{F114})$$

where $f_{\text{GeLU}_T}^{[1]}$ denotes the first divided difference of GeLU_T . An expression for $f_{\text{GeLU}_T}^{[1]}$ is as follows:

$$f_{\text{GeLU}_T}^{[1]}(y_1, y_2) = \int_0^1 ds \left(\frac{1}{2} + \frac{2(sy_1 + (1-s)y_2)}{\sqrt{2\pi T}} \mathbb{E}_{t \sim \nu_T, v \sim \kappa} [e^{-i(sy_1 + (1-s)y_2)vt}] \right), \quad (\text{F115})$$

where we used Lemma 7 and the fact that

$$f^{[1]}(y_1, y_2) = \int_0^1 ds f'(sy_1 + (1-s)y_2). \quad (\text{F116})$$

Defining $\lambda_{s,k,\ell} \equiv s\lambda_k + (1-s)\lambda_\ell$, then we find that

$$\begin{aligned} & \frac{\partial}{\partial x} \text{GeLU}_T(A(x)) \\ &= \sum_{k,\ell} \left(\int_0^1 ds \left(\frac{1}{2} + \frac{2\lambda_{s,k,\ell}}{\sqrt{2\pi T}} \mathbb{E}_{t \sim \nu_T, v \sim \kappa} [e^{-i\lambda_{s,k,\ell}vt}] \right) \right) \Pi_k \left(\frac{\partial}{\partial x} A(x) \right) \Pi_\ell \end{aligned} \quad (\text{F117})$$

$$= \sum_{k,\ell} \left(\frac{1}{2} + \int_0^1 ds \frac{2\lambda_{s,k,\ell}}{\sqrt{2\pi T}} \mathbb{E}_{t \sim \nu_T, v \sim \kappa} [e^{-i\lambda_{s,k,\ell}vt}] \right) \Pi_k \left(\frac{\partial}{\partial x} A(x) \right) \Pi_\ell \quad (\text{F118})$$

$$\begin{aligned} &= \frac{1}{2} \sum_{k,\ell} \Pi_k \left(\frac{\partial}{\partial x} A(x) \right) \Pi_\ell \\ &\quad + \sqrt{\frac{2}{\pi}} \left(\frac{1}{T} \right) \sum_{k,\ell} \left(\int_0^1 ds \lambda_{s,k,\ell} \mathbb{E}_{t \sim \nu_T, v \sim \kappa} [e^{-i\lambda_{s,k,\ell}vt}] \right) \Pi_k \left(\frac{\partial}{\partial x} A(x) \right) \Pi_\ell \end{aligned} \quad (\text{F119})$$

$$\begin{aligned} &= \frac{1}{2} \frac{\partial}{\partial x} A(x) \\ &\quad + \sqrt{\frac{2}{\pi}} \left(\frac{1}{T} \right) \int_0^1 ds \sum_{k,\ell} (s\lambda_k + (1-s)\lambda_\ell) \mathbb{E}_{t \sim \nu_T, v \sim \kappa} [e^{-i(s\lambda_k + (1-s)\lambda_\ell)vt}] \Pi_k \left(\frac{\partial}{\partial x} A(x) \right) \Pi_\ell. \end{aligned} \quad (\text{F120})$$

Following the same steps as in (F75)–(F83), but with $v \sim \kappa$ instead of $v \sim v$, we conclude that

$$\begin{aligned} & \int_0^1 ds \sum_{k,\ell} (s\lambda_k + (1-s)\lambda_\ell) \mathbb{E}_{t \sim \nu_T, v \sim \kappa} [e^{-i(s\lambda_k + (1-s)\lambda_\ell)vt}] \Pi_k \left(\frac{\partial}{\partial x} A(x) \right) \Pi_\ell \\ & = 2\mathbb{E}_{\substack{t \sim \nu_T, \\ v \sim \kappa, s \sim v}} \left[s \Re \left[A(x) e^{-isA(x)vt} \left(\frac{\partial}{\partial x} A(x) \right) e^{-i(1-s)A(x)vt} \right] \right], \end{aligned} \quad (\text{F121})$$

thus completing the proof. \square

Theorem 18. *The following equality holds:*

$$\begin{aligned} \frac{\partial}{\partial \theta_j} \text{Tr}[\text{GeLU}_T(H(\theta))\rho] &= \frac{1}{2} \text{Tr}[H_j \rho] \\ &+ \sqrt{\frac{2}{\pi}} \left(\frac{2}{T} \right) \|\theta\|_1 \mathbb{E}_{\substack{t \sim \nu_T, v \sim \kappa, \\ s \sim v, k \sim q}} \left[s \Re \left[\text{Tr} \left[\text{sgn}(\theta_k) H_k H_j e^{iH(\theta)vt} \mathcal{U}_{svt}^{H(\theta)}(\rho) \right] \right] \right], \end{aligned} \quad (\text{F122})$$

where the objective function $\text{Tr}[\text{GeLU}_T(H(\theta))\rho]$ is defined from (97), the probability densities ν_T , κ , and v are defined in Lemma 8, q is the following probability distribution:

$$q(k) := \frac{|\theta_k|}{\|\theta\|_1}, \quad (\text{F123})$$

and $\mathcal{U}_t^{H(\theta)}$ is the following unitary quantum channel:

$$\mathcal{U}_t^{H(\theta)}(\cdot) := e^{-iH(\theta)t}(\cdot)e^{iH(\theta)t}. \quad (\text{F124})$$

Proof. Applying Lemma 8 and following the same steps as in (F88)–(F94), but with $v \sim \kappa$ instead of $v \sim v$, consider that

$$\begin{aligned} & \frac{\partial}{\partial \theta_j} \text{Tr}[\text{GeLU}_T(H(\theta))\rho] \\ &= \text{Tr} \left[\left(\frac{\partial}{\partial \theta_j} \text{GeLU}_T(H(\theta)) \right) \rho \right] \end{aligned} \quad (\text{F125})$$

$$= \frac{1}{2} \text{Tr}[H_j \rho] + \sqrt{\frac{2}{\pi}} \left(\frac{2}{T} \right) \mathbb{E}_{\substack{t \sim \nu_T, \\ v \sim \kappa, \\ s \sim v}} \left[\text{Tr} \left[s \Re \left[H(\theta) e^{-isH(\theta)vt} \left(\frac{\partial}{\partial \theta_j} H(\theta) \right) e^{-i(1-s)H(\theta)vt} \right] \rho \right] \right] \quad (\text{F126})$$

$$= \frac{1}{2} \text{Tr}[H_j \rho] + \sqrt{\frac{2}{\pi}} \left(\frac{2}{T} \right) \|\theta\|_1 \mathbb{E}_{\substack{t \sim \nu_T, \\ v \sim \kappa, \\ s \sim v, k \sim q}} \left[s \Re \left[\text{Tr} \left[\text{sgn}(\theta_k) H_k H_j e^{iH(\theta)vt} \mathcal{U}_{svt}^{H(\theta)}(\rho) \right] \right] \right], \quad (\text{F127})$$

thus concluding the proof. \square

Appendix G: Gradient formulas for quantum observable networks

In this appendix, we derive formulas for the gradient of two-, three-, and L -layer quantum observable networks. In our formulas for general L -layer networks, we show how the gradient formulas can be expressed in terms of a backpropagation rule, generalizing that of [49, 71]. While our derivations focus on hyperbolic tangent activation functions, we note that they can be generalized to an arbitrary activation function.

1. Two-layer gradient formulas

In this appendix, we show how to calculate the gradient for a two-layer quantum observable network of the form in (143)–(146), specializing to the case when φ_1 and φ_2 are both tanh.

Theorem 19. *The following formulas hold for the partial derivatives of a quantum observable network of the form in (143)–(146):*

$$\frac{\partial}{\partial \theta_{kj}^{(2)}} \text{Tr} \left[\varphi_2 \left(\sum_{j'=1}^{J_1} \theta_{kj'}^{(2)} A_{j'}^{(1)} \right) \rho \right] = \text{Tr} \left[\mathcal{D}_{B_k^{(2)}(\theta^{(2)})} \left(A_j^{(1)} \right) \rho \right], \quad (\text{G1})$$

$$\frac{\partial}{\partial \theta_{ji}^{(1)}} \text{Tr} \left[\varphi_2 \left(\sum_{j'=1}^{J_1} \theta_{kj'}^{(2)} \varphi_1 \left(\sum_{i'=1}^{J_0} \theta_{j'i'}^{(1)} H_{i'} \right) \right) \rho \right] = \theta_{kj}^{(2)} \text{Tr} \left[\left(\mathcal{D}_{B_k^{(2)}(\theta^{(2)})} \circ \mathcal{D}_{B_j^{(1)}(\theta^{(1)})} \right) (H_i) \rho \right], \quad (\text{G2})$$

where φ_1 and φ_2 are both tanh, ρ is a quantum state, the superoperator \mathcal{D}_H is defined for a Hamiltonian H as

$$\mathcal{D}_H(X) := \mathbb{E}_{t \sim \mu, s \sim \nu} \left[e^{iHst} X e^{iH(1-s)t} \right], \quad (\text{G3})$$

$\mu(t)$ is the probability density function defined in (A2), ν is a uniform random variable on the unit interval $[0, 1]$,

$$B_k^{(2)}(\theta^{(2)}) := \sum_{j=1}^{J_1} \theta_{kj}^{(2)} A_j^{(1)}, \quad (\text{G4})$$

$$B_j^{(1)}(\theta^{(1)}) := \sum_{i=1}^{J_0} \theta_{ji}^{(1)} A_i^{(0)} = \sum_{i=1}^{J_0} \theta_{ji}^{(1)} H_i. \quad (\text{G5})$$

Proof. Applying Lemma 1, i.e.,

$$\frac{\partial}{\partial x} \tanh(A(x)) = \mathbb{E}_{t \sim \mu, s \sim \nu} \left[e^{itsA(x)} \left(\frac{\partial}{\partial x} A(x) \right) e^{it(1-s)A(x)} \right], \quad (\text{G6})$$

$$= \mathcal{D}_{A(x)} \left(\frac{\partial}{\partial x} A(x) \right) \quad (\text{G7})$$

we find that

$$\frac{\partial}{\partial \theta_{kj}^{(2)}} \text{Tr} \left[\varphi_2 \left(\sum_{j'=1}^{J_1} \theta_{kj'}^{(2)} A_{j'}^{(1)} \right) \rho \right] = \frac{\partial}{\partial \theta_{kj}^{(2)}} \text{Tr} \left[\tanh \left(\sum_{j'=1}^{J_1} \theta_{kj'}^{(2)} A_{j'}^{(1)} \right) \rho \right] \quad (\text{G8})$$

$$= \mathbb{E}_{t \sim \mu, s \sim \nu} \left[\text{Tr} \left[\mathcal{D}_{B_k^{(2)}(\theta^{(2)})} \left(\frac{\partial}{\partial \theta_{kj}^{(2)}} \sum_{j'=1}^{J_1} \theta_{kj'}^{(2)} A_{j'}^{(1)} \right) \rho \right] \right] \quad (\text{G9})$$

$$= \text{Tr} \left[\mathcal{D}_{B_k^{(2)}(\theta^{(2)})} \left(A_j^{(1)} \right) \rho \right]. \quad (\text{G10})$$

Recalling from (143)–(146) that

$$A_k^{(2)}(\theta^{(2)}) = \tanh \left(\sum_{i=1}^{J_1} \theta_{ki}^{(2)} A_i^{(1)}(\theta^{(1)}) \right), \quad (\text{G11})$$

and applying Lemma 1, the other partial derivative to calculate is as follows:

$$\begin{aligned} & \frac{\partial}{\partial \theta_{ji}^{(1)}} \operatorname{Tr} \left[\varphi_2 \left(\sum_{j'=1}^{J_1} \theta_{kj'}^{(2)} \varphi_1 \left(\sum_{i'=1}^{J_0} \theta_{j'i'}^{(1)} H_{i'} \right) \right) \rho \right] \\ &= \frac{\partial}{\partial \theta_{ji}^{(1)}} \operatorname{Tr} \left[\tanh \left(\sum_{j'=1}^{J_1} \theta_{kj'}^{(2)} \tanh \left(B_{j'}^{(1)}(\theta^{(1)}) \right) \right) \rho \right] \end{aligned} \quad (\text{G12})$$

$$= \operatorname{Tr} \left[\frac{\partial}{\partial \theta_{ji}^{(1)}} \tanh \left(B_k^{(2)}(\theta^{(2)}) \right) \rho \right] \quad (\text{G13})$$

$$= \operatorname{Tr} \left[\mathcal{D}_{B_k^{(2)}(\theta^{(2)})} \left(\frac{\partial}{\partial \theta_{ji}^{(1)}} B_k^{(2)}(\theta^{(2)}) \right) \rho \right] \quad (\text{G14})$$

$$= \operatorname{Tr} \left[\mathcal{D}_{B_k^{(2)}(\theta^{(2)})} \left(\frac{\partial}{\partial \theta_{ji}^{(1)}} \sum_{j'=1}^{J_1} \theta_{kj'}^{(2)} A_{j'}^{(1)} \right) \rho \right] \quad (\text{G15})$$

$$= \sum_{j'=1}^{J_1} \theta_{kj'}^{(2)} \operatorname{Tr} \left[\mathcal{D}_{B_k^{(2)}(\theta^{(2)})} \left(\frac{\partial}{\partial \theta_{ji}^{(1)}} A_{j'}^{(1)} \right) \rho \right] \quad (\text{G16})$$

$$= \sum_{j'=1}^{J_1} \theta_{kj'}^{(2)} \operatorname{Tr} \left[\mathcal{D}_{B_k^{(2)}(\theta^{(2)})} \left(\frac{\partial}{\partial \theta_{ji}^{(1)}} \tanh \left(B_{j'}^{(1)}(\theta^{(1)}) \right) \right) \rho \right] \quad (\text{G17})$$

$$= \sum_{j'=1}^{J_1} \theta_{kj'}^{(2)} \operatorname{Tr} \left[\mathcal{D}_{B_k^{(2)}(\theta^{(2)})} \left(\mathcal{D}_{B_{j'}^{(1)}(\theta^{(1)})} \left(\frac{\partial}{\partial \theta_{ji}^{(1)}} B_{j'}^{(1)}(\theta^{(1)}) \right) \right) \rho \right] \quad (\text{G18})$$

$$= \sum_{j'=1}^{J_1} \theta_{kj'}^{(2)} \operatorname{Tr} \left[\left(\mathcal{D}_{B_k^{(2)}(\theta^{(2)})} \circ \mathcal{D}_{B_{j'}^{(1)}(\theta^{(1)})} \right) \left(\frac{\partial}{\partial \theta_{ji}^{(1)}} \sum_{i'=1}^{J_0} \theta_{j'i'}^{(1)} H_{i'} \right) \rho \right] \quad (\text{G19})$$

$$= \theta_{kj}^{(2)} \operatorname{Tr} \left[\left(\mathcal{D}_{B_k^{(2)}(\theta^{(2)})} \circ \mathcal{D}_{B_j^{(1)}(\theta^{(1)})} \right) (H_i) \rho \right]. \quad (\text{G20})$$

The last equality follows because

$$\frac{\partial}{\partial \theta_{ji}^{(1)}} \sum_{i'=1}^{J_0} \theta_{j'i'}^{(1)} H_{i'} = \sum_{i'=1}^{J_0} \left(\frac{\partial}{\partial \theta_{ji}^{(1)}} \theta_{j'i'}^{(1)} \right) H_{i'} \quad (\text{G21})$$

$$= \sum_{i'=1}^{J_0} \delta_{jj'} \delta_{ii'} H_{i'} \quad (\text{G22})$$

$$= \delta_{jj'} H_i, \quad (\text{G23})$$

thus concluding the proof. \square

Remark 5. In order to estimate these partial derivatives, we require the ability to perform Hamiltonian simulation according to the Hamiltonian $B_k^{(2)}(\theta^{(2)})$. Given that $B_k^{(2)}(\theta^{(2)})$ is itself a composition of Hamiltonians, it is not generally a local Hamiltonian, and so standard approaches do not apply. One can potentially make use of the formalism of block encoding and quantum singular value transformation [53] to address this problem, but we leave it as the topic of future research.

2. Three-layer gradient formulas

Now we consider the three-layer case, where the objective function is

$$\mathrm{Tr} \left[\varphi_3 \left(B_k^{(3)}(\theta^{(3)}) \right) \rho \right], \quad (\text{G24})$$

and

$$B_k^{(3)}(\theta^{(3)}) := \sum_{j_2=1}^{J_2} \theta_{kj_2}^{(3)} A_{j_2}^{(2)}(\theta^{(2)}), \quad (\text{G25})$$

$$A_{j_2}^{(2)}(\theta^{(2)}) := \varphi_2 \left(B_{j_2}^{(2)}(\theta^{(2)}) \right), \quad (\text{G26})$$

$$B_{j_2}^{(2)}(\theta^{(2)}) := \sum_{j_1=1}^{J_1} \theta_{j_2 j_1}^{(2)} A_{j_1}^{(1)}(\theta^{(1)}) \quad (\text{G27})$$

$$A_{j_1}^{(1)}(\theta^{(1)}) := \varphi_1 \left(B_{j_1}^{(1)}(\theta^{(1)}) \right), \quad (\text{G28})$$

$$B_{j_1}^{(1)}(\theta^{(1)}) := \sum_{j_0=1}^{J_0} \theta_{j_1 j_0}^{(1)} A_{j_0}^{(0)} = \sum_{j_0=1}^{J_0} \theta_{j_1 j_0}^{(1)} H_{j_0}. \quad (\text{G29})$$

Theorem 20. *The gradient formulas for a three-layer quantum observable network of the form in (139)–(142) are given by*

$$\frac{\partial}{\partial \theta_{kj_2}^{(3)}} \mathrm{Tr} \left[\varphi_3 \left(B_k^{(3)}(\theta^{(3)}) \right) \rho \right] = \mathrm{Tr} \left[\mathcal{D}_{B_k^{(3)}(\theta^{(3)})} \left(A_{j_2}^{(2)}(\theta^{(2)}) \right) \rho \right], \quad (\text{G30})$$

$$\frac{\partial}{\partial \theta_{j_2 j_1}^{(2)}} \mathrm{Tr} \left[\varphi_3 \left(B_k^{(3)}(\theta^{(3)}) \right) \rho \right] = \theta_{kj_2}^{(3)} \mathrm{Tr} \left[\left(\mathcal{D}_{B_k^{(3)}(\theta^{(3)})} \circ \mathcal{D}_{B_{j_2}^{(2)}(\theta^{(2)})} \right) \left(A_{j_1}^{(1)}(\theta^{(1)}) \right) \rho \right], \quad (\text{G31})$$

$$\frac{\partial}{\partial \theta_{j_1 j_0}^{(1)}} \mathrm{Tr} \left[\varphi_3 \left(B_k^{(3)}(\theta^{(3)}) \right) \rho \right] = \sum_{j_2=1}^{J_2} \theta_{kj_2}^{(3)} \theta_{j_2 j_1}^{(2)} \mathrm{Tr} \left[\left(\mathcal{D}_{B_k^{(3)}(\theta^{(3)})} \circ \mathcal{D}_{B_{j_2}^{(2)}(\theta^{(2)})} \circ \mathcal{D}_{B_{j_1}^{(1)}(\theta^{(1)})} \right) (H_{j_0}) \rho \right]. \quad (\text{G32})$$

Proof. Consider that

$$\frac{\partial}{\partial \theta_{kj_2}^{(3)}} \mathrm{Tr} \left[\varphi_3 \left(B_k^{(3)}(\theta^{(3)}) \right) \rho \right] = \mathrm{Tr} \left[\mathcal{D}_{B_k^{(3)}(\theta^{(3)})} \left(\frac{\partial}{\partial \theta_{kj_2}^{(3)}} B_k^{(3)}(\theta^{(3)}) \right) \rho \right] \quad (\text{G33})$$

$$= \mathrm{Tr} \left[\mathcal{D}_{B_k^{(3)}(\theta^{(3)})} \left(\frac{\partial}{\partial \theta_{kj_2}^{(3)}} \sum_{j_2=1}^{J_2} \theta_{kj_2}^{(3)} A_{j_2}^{(2)}(\theta^{(2)}) \right) \rho \right] \quad (\text{G34})$$

$$= \mathrm{Tr} \left[\mathcal{D}_{B_k^{(3)}(\theta^{(3)})} \left(\sum_{j_2=1}^{J_2} \left(\frac{\partial}{\partial \theta_{kj_2}^{(3)}} \theta_{kj_2}^{(3)} \right) A_{j_2}^{(2)}(\theta^{(2)}) \right) \rho \right] \quad (\text{G35})$$

$$= \mathrm{Tr} \left[\mathcal{D}_{B_k^{(3)}(\theta^{(3)})} \left(A_{j_2}^{(2)}(\theta^{(2)}) \right) \rho \right]. \quad (\text{G36})$$

Also,

$$\frac{\partial}{\partial \theta_{j_2 j_1}^{(2)}} \mathrm{Tr} \left[\varphi_3 \left(B_k^{(3)}(\theta^{(3)}) \right) \rho \right]$$

$$= \text{Tr} \left[\mathcal{D}_{B_k^{(3)}(\theta^{(3)})} \left(\frac{\partial}{\partial \theta_{j_2 j_1}^{(2)}} B_k^{(3)}(\theta^{(3)}) \right) \rho \right] \quad (\text{G37})$$

$$= \text{Tr} \left[\mathcal{D}_{B_k^{(3)}(\theta^{(3)})} \left(\frac{\partial}{\partial \theta_{j_2 j_1}^{(2)}} \sum_{j'_2=1}^{J_2} \theta_{k j'_2}^{(3)} A_{j'_2}^{(2)}(\theta^{(2)}) \right) \rho \right] \quad (\text{G38})$$

$$= \sum_{j'_2=1}^{J_2} \theta_{k j'_2}^{(3)} \text{Tr} \left[\mathcal{D}_{B_k^{(3)}(\theta^{(3)})} \left(\frac{\partial}{\partial \theta_{j_2 j_1}^{(2)}} A_{j'_2}^{(2)}(\theta^{(2)}) \right) \rho \right] \quad (\text{G39})$$

$$= \sum_{j'_2=1}^{J_2} \theta_{k j'_2}^{(3)} \text{Tr} \left[\mathcal{D}_{B_k^{(3)}(\theta^{(3)})} \left(\frac{\partial}{\partial \theta_{j_2 j_1}^{(2)}} \varphi_2 \left(B_{j'_2}^{(2)}(\theta^{(2)}) \right) \right) \rho \right] \quad (\text{G40})$$

$$= \sum_{j'_2=1}^{J_2} \theta_{k j'_2}^{(3)} \text{Tr} \left[\mathcal{D}_{B_k^{(3)}(\theta^{(3)})} \left(\mathcal{D}_{B_{j'_2}^{(2)}(\theta^{(2)})} \left(\frac{\partial}{\partial \theta_{j_2 j_1}^{(2)}} B_{j'_2}^{(2)}(\theta^{(2)}) \right) \right) \rho \right] \quad (\text{G41})$$

$$= \sum_{j'_2=1}^{J_2} \theta_{k j'_2}^{(3)} \text{Tr} \left[\mathcal{D}_{B_k^{(3)}(\theta^{(3)})} \left(\mathcal{D}_{B_{j'_2}^{(2)}(\theta^{(2)})} \left(\frac{\partial}{\partial \theta_{j_2 j_1}^{(2)}} \sum_{j'_1=1}^{J_1} \theta_{j'_2 j'_1}^{(2)} A_{j'_1}^{(1)}(\theta^{(1)}) \right) \right) \rho \right] \quad (\text{G42})$$

$$= \sum_{j'_2=1}^{J_2} \theta_{k j'_2}^{(3)} \text{Tr} \left[\mathcal{D}_{B_k^{(3)}(\theta^{(3)})} \left(\mathcal{D}_{B_{j'_2}^{(2)}(\theta^{(2)})} \left(\sum_{j'_1=1}^{J_1} \left(\frac{\partial}{\partial \theta_{j_2 j_1}^{(2)}} \theta_{j'_2 j'_1}^{(2)} \right) A_{j'_1}^{(1)}(\theta^{(1)}) \right) \right) \rho \right] \quad (\text{G43})$$

$$= \theta_{k j_2}^{(3)} \text{Tr} \left[\mathcal{D}_{B_k^{(3)}(\theta^{(3)})} \left(\mathcal{D}_{B_{j_2}^{(2)}(\theta^{(2)})} \left(A_{j_1}^{(1)}(\theta^{(1)}) \right) \right) \rho \right] \quad (\text{G44})$$

$$= \theta_{k j_2}^{(3)} \text{Tr} \left[\left(\mathcal{D}_{B_k^{(3)}(\theta^{(3)})} \circ \mathcal{D}_{B_{j_2}^{(2)}(\theta^{(2)})} \right) \left(A_{j_1}^{(1)}(\theta^{(1)}) \right) \rho \right]. \quad (\text{G45})$$

Finally, consider that

$$\begin{aligned} & \frac{\partial}{\partial \theta_{j_1 j_0}^{(1)}} \text{Tr} \left[\varphi_3 \left(B_k^{(3)}(\theta^{(3)}) \right) \rho \right] \\ &= \text{Tr} \left[\mathcal{D}_{B_k^{(3)}(\theta^{(3)})} \left(\frac{\partial}{\partial \theta_{j_1 j_0}^{(1)}} B_k^{(3)}(\theta^{(3)}) \right) \rho \right] \end{aligned} \quad (\text{G46})$$

$$= \text{Tr} \left[\mathcal{D}_{B_k^{(3)}(\theta^{(3)})} \left(\frac{\partial}{\partial \theta_{j_1 j_0}^{(1)}} \sum_{j'_2=1}^{J_2} \theta_{k j'_2}^{(3)} A_{j'_2}^{(2)}(\theta^{(2)}) \right) \rho \right] \quad (\text{G47})$$

$$= \sum_{j'_2=1}^{J_2} \theta_{k j'_2}^{(3)} \text{Tr} \left[\mathcal{D}_{B_k^{(3)}(\theta^{(3)})} \left(\frac{\partial}{\partial \theta_{j_1 j_0}^{(1)}} \varphi_2 \left(B_{j'_2}^{(2)}(\theta^{(2)}) \right) \right) \rho \right] \quad (\text{G48})$$

$$= \sum_{j'_2=1}^{J_2} \theta_{k j'_2}^{(3)} \text{Tr} \left[\mathcal{D}_{B_k^{(3)}(\theta^{(3)})} \left(\mathcal{D}_{B_{j'_2}^{(2)}(\theta^{(2)})} \left(\frac{\partial}{\partial \theta_{j_1 j_0}^{(1)}} B_{j'_2}^{(2)}(\theta^{(2)}) \right) \right) \rho \right] \quad (\text{G49})$$

$$= \sum_{j'_2=1}^{J_2} \theta_{k j'_2}^{(3)} \text{Tr} \left[\mathcal{D}_{B_k^{(3)}(\theta^{(3)})} \left(\mathcal{D}_{B_{j'_2}^{(2)}(\theta^{(2)})} \left(\frac{\partial}{\partial \theta_{j_1 j_0}^{(1)}} \sum_{j'_1=1}^{J_1} \theta_{j'_2 j'_1}^{(2)} A_{j'_1}^{(1)}(\theta^{(1)}) \right) \right) \rho \right] \quad (\text{G50})$$

$$= \sum_{j'_2=1}^{J_2} \theta_{kj'_2}^{(3)} \sum_{j'_1=1}^{J_1} \theta_{j'_2j'_1}^{(2)} \text{Tr} \left[\mathcal{D}_{B_k^{(3)}(\theta^{(3)})} \left(\mathcal{D}_{B_{j'_2}^{(2)}(\theta^{(2)})} \left(\frac{\partial}{\partial \theta_{j_1j_0}^{(1)}} \varphi_1 \left(B_{j'_1}^{(1)}(\theta^{(1)}) \right) \right) \right) \rho \right] \quad (\text{G51})$$

$$= \sum_{j'_2=1}^{J_2} \theta_{kj'_2}^{(3)} \sum_{j'_1=1}^{J_1} \theta_{j'_2j'_1}^{(2)} \text{Tr} \left[\mathcal{D}_{B_k^{(3)}(\theta^{(3)})} \left(\mathcal{D}_{B_{j'_2}^{(2)}(\theta^{(2)})} \left(\mathcal{D}_{B_{j'_1}^{(1)}(\theta^{(1)})} \frac{\partial}{\partial \theta_{j_1j_0}^{(1)}} B_{j'_1}^{(1)}(\theta^{(1)}) \right) \right) \rho \right] \quad (\text{G52})$$

$$= \sum_{j'_2=1}^{J_2} \theta_{kj'_2}^{(3)} \sum_{j'_1=1}^{J_1} \theta_{j'_2j'_1}^{(2)} \text{Tr} \left[\left(\mathcal{D}_{B_k^{(3)}(\theta^{(3)})} \circ \mathcal{D}_{B_{j'_2}^{(2)}(\theta^{(2)})} \circ \mathcal{D}_{B_{j'_1}^{(1)}(\theta^{(1)})} \right) \left(\frac{\partial}{\partial \theta_{j_1j_0}^{(1)}} B_{j'_1}^{(1)}(\theta^{(1)}) \right) \rho \right] \quad (\text{G53})$$

$$= \sum_{j'_2=1}^{J_2} \theta_{kj'_2}^{(3)} \sum_{j'_1=1}^{J_1} \theta_{j'_2j'_1}^{(2)} \text{Tr} \left[\left(\mathcal{D}_{B_k^{(3)}(\theta^{(3)})} \circ \mathcal{D}_{B_{j'_2}^{(2)}(\theta^{(2)})} \circ \mathcal{D}_{B_{j'_1}^{(1)}(\theta^{(1)})} \right) \left(\frac{\partial}{\partial \theta_{j_1j_0}^{(1)}} \sum_{j'_0=1}^{J_0} \theta_{j'_1j'_0}^{(1)} H_{j'_0} \right) \rho \right] \quad (\text{G54})$$

$$= \sum_{j'_2=1}^{J_2} \theta_{kj'_2}^{(3)} \theta_{j'_2j_1}^{(2)} \text{Tr} \left[\left(\mathcal{D}_{B_k^{(3)}(\theta^{(3)})} \circ \mathcal{D}_{B_{j'_2}^{(2)}(\theta^{(2)})} \circ \mathcal{D}_{B_{j_1}^{(1)}(\theta^{(1)})} \right) (H_{j_0}) \rho \right], \quad (\text{G55})$$

thus concluding the proof. \square

3. L -layer gradient formulas

The gradient formulas for an L -layer quantum observable network of the form in (139)–(142) are then given by

$$\frac{\partial}{\partial \theta_{kj_{L-1}}^{(L)}} \text{Tr} \left[\varphi_L \left(B_k^{(L)}(\theta^{(L)}) \right) \rho \right] = \text{Tr} \left[\mathcal{D}_{B_k^{(L)}(\theta^{(L)})} \left(A_{j_{L-1}}^{(L-1)}(\theta^{(L-1)}) \right) \rho \right]. \quad (\text{G56})$$

For $\ell = L - 1, \dots, 2$, we have that

$$\begin{aligned} \frac{\partial}{\partial \theta_{j_\ell j_{\ell-1}}^{(\ell)}} \text{Tr} \left[\varphi_L \left(B_k^{(L)}(\theta^{(L)}) \right) \rho \right] &= \sum_{j'_{L-1}=1}^{J_{L-1}} \sum_{j'_{L-2}=1}^{J_{L-2}} \dots \sum_{j'_{\ell+1}=1}^{J_{\ell+1}} \theta_{kj'_{L-1}}^{(L)} \theta_{j'_{L-1}j'_{L-2}}^{(L-1)} \dots \theta_{j'_{\ell+1}j_\ell}^{(\ell+1)} \times \\ &\text{Tr} \left[\left(\mathcal{D}_{B_k^{(L)}(\theta^{(L)})} \circ \mathcal{D}_{B_{j'_{L-1}}^{(L-1)}(\theta^{(L-1)})} \circ \dots \circ \mathcal{D}_{B_{j'_\ell}^{(\ell)}(\theta^{(\ell)})} \right) \left(A_{j_{\ell-1}}^{(\ell-1)}(\theta^{(\ell-1)}) \right) \rho \right]. \end{aligned} \quad (\text{G57})$$

Finally, we have that

$$\begin{aligned} \frac{\partial}{\partial \theta_{j_1j_0}^{(1)}} \text{Tr} \left[\varphi_L \left(B_k^{(L)}(\theta^{(L)}) \right) \rho \right] &= \sum_{j'_{L-1}=1}^{J_{L-1}} \sum_{j'_{L-2}=1}^{J_{L-2}} \dots \sum_{j'_2=1}^{J_2} \theta_{kj'_{L-1}}^{(L)} \theta_{j'_{L-1}j'_{L-2}}^{(L-1)} \dots \theta_{j'_2j_1}^{(2)} \times \\ &\text{Tr} \left[\left(\mathcal{D}_{B_k^{(L)}(\theta^{(L)})} \circ \mathcal{D}_{B_{j'_{L-1}}^{(L-1)}(\theta^{(L-1)})} \circ \dots \circ \mathcal{D}_{B_{j_1}^{(1)}(\theta^{(1)})} \right) (H_{j_0}) \rho \right]. \end{aligned} \quad (\text{G58})$$

From these formulas, we can derive a recursive formulation similar to backpropagation [71, 72]. Define

$$\Gamma_{kj_{L-1}}^{(L)} := \theta_{kj_{L-1}}^{(L)} \mathcal{D}_{B_k^{(L)}(\theta^{(L)})}, \quad (\text{G59})$$

$$\Gamma_{kj_{L-2}}^{(L-1)} := \sum_{j_{L-1}=1}^{J_{L-1}} \theta_{j_{L-1}j_{L-2}}^{(L-1)} \left(\Gamma_{kj_{L-1}}^{(L)} \circ \mathcal{D}_{B_{j_{L-1}}^{(L-1)}(\theta^{(L-1)})} \right), \quad (\text{G60})$$

$$\Gamma_{kj_{L-3}}^{(L-2)} := \sum_{j_{L-2}=1}^{J_{L-2}} \theta_{j_{L-2}j_{L-3}}^{(L-2)} \left(\Gamma_{kj_{L-2}}^{(L-1)} \circ \mathcal{D}_{B_{j_{L-2}}^{(L-2)}(\theta^{(L-2)})} \right), \quad (\text{G61})$$

$$\vdots \quad (\text{G62})$$

$$\Gamma_{kj_\ell}^{(\ell+1)} := \sum_{j_{\ell+1}=1}^{J_{\ell+1}} \theta_{j_{\ell+1}j_\ell}^{(\ell+1)} \left(\Gamma_{kj_{\ell+1}}^{(\ell+2)} \circ \mathcal{D}_{B_{j_{\ell+1}}^{(\ell+1)}(\theta^{(\ell+1)})} \right). \quad (\text{G63})$$

So then, for $\ell = L - 1, \dots, 2, 1$, we have that

$$\frac{\partial}{\partial \theta_{j_\ell j_{\ell-1}}^{(\ell)}} \text{Tr} \left[\varphi_L \left(B_k^{(L)}(\theta^{(L)}) \right) \rho \right] = \text{Tr} \left[\left(\Gamma_{kj_\ell}^{(\ell+1)} \circ \mathcal{D}_{B_{j_\ell}^{(\ell)}(\theta^{(\ell)})} \right) \left(A_{j_{\ell-1}}^{(\ell-1)}(\theta^{(\ell-1)}) \right) \rho \right]. \quad (\text{G64})$$

Remark 6. If one is performing a classical simulation of quantum observable networks, then the recursive relations in (G59)–(G63) can be used to evaluate gradients efficiently through a reverse-mode propagation procedure analogous to the classical backpropagation algorithm [49, 71]. In particular, the superoperators $\Gamma_{kj_\ell}^{(\ell+1)}$ play the role of recursively propagated error maps, with the Fréchet derivative superoperators $\mathcal{D}_{B_{j_\ell}^{(\ell)}(\theta^{(\ell)})}$ replacing the scalar derivatives that appear in classical neural networks.

However, it is less clear how to exploit this recursive structure in order to obtain an efficient quantum implementation of backpropagation. Unlike the classical setting, the quantities propagated backward through the network are superoperators acting on observables, rather than classical vectors or tensors. Furthermore, implementing compositions of Fréchet derivative superoperators coherently on a quantum computer appears to require nontrivial higher-order transformations of quantum states and observables. Determining whether there exists an efficient quantum algorithm for reverse-mode differentiation in quantum observable networks therefore remains an open problem.

Appendix H: Proof of Theorem 11 (complexity theoretic-evidence against classical simulation)

Containment in BQP follows from Algorithm 2.

To see that Problem 1 is BQP-hard for $k \geq 5$, we can use the Feynman–Kitaev circuit-to-Hamiltonian construction [76, 77] (see also [78, 79]). Let $A \equiv (A_{\text{yes}}, A_{\text{no}})$ be a promise problem in BQP, and let $x \in \{0, 1\}^n$ be an input. Let $U_x := U_M U_{M-1} \cdots U_2 U_1$ be a sequence of $M = \text{poly}(n)$ 2-local unitary gates, acting on $|0\rangle^{\otimes p(n)}$, where $p(n) = \text{poly}(n)$, such that the acceptance probability

$$p_{\text{acc}} \equiv \left\| \left(\langle 1 | \otimes I^{\otimes p(n)-1} \right) U_x |0\rangle^{\otimes p(n)} \right\|^2 \quad (\text{H1})$$

satisfies $p_{\text{acc}} \geq 1 - \varepsilon$ in the case of a YES instance and $p_{\text{acc}} \leq \varepsilon$ in the case of a NO instance, where $\varepsilon \in [0, 1/2)$. By the standard error reduction for BQP (i.e., repeating the circuit polynomially many times and taking a majority vote), we can take $\varepsilon = 2^{-q(n)}$ for some $q(n) = \text{poly}(n)$. Without loss of generality, we then suppose that U_x achieves the error probability $\varepsilon = 2^{-q(n)}$.

We now pre-idle the verifier, by performing $L = \text{poly}(n)$ identity gates before applying U_x , and define $W_x := W_{M+L} W_{M+L-1} \cdots W_2 W_1$, where

$$W_k := \begin{cases} I & : k \in \{1, \dots, L\} \\ U_{k-L} & : k \in \{L+1, \dots, M+L\} \end{cases}. \quad (\text{H2})$$

Following [76] and setting $K \equiv M + L$, we define the Hamiltonian H as follows:

$$H := \Delta (H_{\text{in}} + H_{\text{prop}} + H_{\text{stab}}) + H_{\text{out}}, \quad (\text{H3})$$

where Δ ,

$$H_{\text{in}} := \sum_{i=1}^{p(n)} |1\rangle\langle 1|_i \otimes |0\rangle\langle 0|_C, \quad (\text{H4})$$

$$H_{\text{prop}} := \frac{1}{2} \sum_{k=1}^K \left(I \otimes (|k\rangle\langle k|_C + |k-1\rangle\langle k-1|_C) - W_k \otimes |k\rangle\langle k-1|_C - W_k^\dagger \otimes |k-1\rangle\langle k|_C \right), \quad (\text{H5})$$

$$H_{\text{stab}} := I \otimes \sum_{j=1}^{K-1} |0\rangle\langle 0|_{C_j} \otimes |1\rangle\langle 1|_{C_{j+1}}, \quad (\text{H6})$$

$$H_{\text{out}} := |0\rangle\langle 0| \otimes I^{\otimes p(n)-1} \otimes |K\rangle\langle K|_C, \quad (\text{H7})$$

where the clock states are encoded in unary, as done in the standard construction [76]. Here we use the shorthand $|k\rangle_C$ for the unary clock state corresponding to time step k . Each term in the construction acts nontrivially on at most five qubits, so the Hamiltonian is 5-local. Each local term appearing in the construction has operator norm at most $O(\Delta)$, and we return to this issue at the end of the proof.

The history state corresponding to the computation W_x is as follows:

$$|\eta\rangle := \frac{1}{\sqrt{K+1}} \sum_{k=0}^K W_k \cdots W_1 |0\rangle |k\rangle_C, \quad (\text{H8})$$

satisfying

$$\langle \eta | (H_{\text{in}} + H_{\text{prop}} + H_{\text{stab}}) | \eta \rangle = 0, \quad (\text{H9})$$

$$\langle \eta | H_{\text{out}} | \eta \rangle \leq \frac{\varepsilon}{K+1} = \frac{2^{-q(n)}}{K+1}, \quad (\text{H10})$$

in the case of a YES instance. Also, in the case of a NO instance, we have that

$$\langle \eta | H_{\text{out}} | \eta \rangle \geq \frac{1-\varepsilon}{K+1} = \frac{1-2^{-q(n)}}{K+1}. \quad (\text{H11})$$

While the history state depends on the computation, the following state, featuring a uniform superposition over the clock register, does not:

$$|v\rangle := |0\rangle^{\otimes p(n)} \otimes \left(\frac{1}{\sqrt{L+1}} \sum_{k=0}^L |k\rangle_C \right). \quad (\text{H12})$$

Observe that

$$|\langle v | \eta \rangle|^2 = \left| \left(\langle 0 |^{\otimes p(n)} \otimes \left(\frac{1}{\sqrt{L+1}} \sum_{k'=0}^L \langle k' |_C \right) \right) \left(\frac{1}{\sqrt{K+1}} \sum_{k=0}^K W_k \cdots W_1 |0\rangle^{\otimes p(n)} |k\rangle_C \right) \right|^2 \quad (\text{H13})$$

$$= \frac{1}{(L+1)(K+1)} \left| \sum_{k'=0}^L \sum_{k=0}^K \langle 0 |^{\otimes p(n)} W_k \cdots W_1 |0\rangle^{\otimes p(n)} \langle k' |_C |k\rangle_C \right|^2 \quad (\text{H14})$$

$$= \frac{1}{(L+1)(K+1)} \left| \sum_{k'=0}^L \langle 0|0 \rangle^{\otimes p(n)} \right|^2 \quad (\text{H15})$$

$$= \frac{L+1}{K+1} \quad (\text{H16})$$

$$= \frac{L+1}{L+M+1}. \quad (\text{H17})$$

We can then take $L = \text{poly}(n)$ such that $|\langle v|\eta \rangle|^2 \geq 1 - \frac{1}{r(n)}$, where $r(n) = \text{poly}(n)$.

Eq. (12) of [47] guarantees that

$$\| |g\rangle - |\eta\rangle \| = O\left(\left(\frac{\Delta}{K^2}\right)^{-1}\right), \quad (\text{H18})$$

where $|g\rangle$ is the ground state of H , and we can choose Δ such that

$$O\left(\left(\frac{\Delta}{K^2}\right)^{-1}\right) = O\left(\frac{1}{\text{poly}(n)}\right). \quad (\text{H19})$$

The first-order effective Hamiltonian is then given by

$$H_{\text{eff}} \equiv |\eta\rangle\langle\eta| H_{\text{out}} |\eta\rangle\langle\eta|. \quad (\text{H20})$$

Combining (H10), (H11), (H18), and (H19), we conclude that the ground-state energy of H differs from $\langle\eta|H_{\text{out}}|\eta\rangle$ by at most $O(1/\text{poly}(n))$. Appealing now to (H10) and (H11), the ground-state energy of H lies in the range $\pm O\left(\frac{1}{\text{poly}(n)}\right)$ if $x \in A_{\text{yes}}$ and in the range of $\frac{1}{K+1} \pm O\left(\frac{1}{\text{poly}(n)}\right)$ if $x \in A_{\text{no}}$.

We then shift the spectrum of the Hamiltonian by taking $H' := H - \delta I$, where $\delta := \frac{1}{2(K+1)}$, while noting that this modification does not change the locality of the Hamiltonian. Thus, the ground-state energy E_0 of H' lies in the range $-\frac{1}{2(K+1)} \pm O\left(\frac{1}{\text{poly}(n)}\right)$ if $x \in A_{\text{yes}}$ and in the range of $\frac{1}{2(K+1)} \pm O\left(\frac{1}{\text{poly}(n)}\right)$ if $x \in A_{\text{no}}$. In fact, we have that

$$E_0 \leq -\frac{1}{3(K+1)} \quad \text{if } x \in A_{\text{yes}}, \quad (\text{H21})$$

$$E_0 \geq \frac{1}{3(K+1)} \quad \text{if } x \in A_{\text{no}}. \quad (\text{H22})$$

Now consider the following. The Hamiltonian H' has spectral decomposition

$$H' = E_0 |g\rangle\langle g| + \sum_{j \geq 1} E_j |E_j\rangle\langle E_j| \quad (\text{H23})$$

where, for all $j \geq 1$, $E_j \geq \frac{1}{\text{poly}(n)}$. This follows from the spectral gap of the Feynman–Kitaev Hamiltonian together with the choice of spectral shift δ . Recall that $|\langle v|g \rangle|^2 \geq 1 - \varepsilon_v$, where $\varepsilon_v = \frac{1}{\text{poly}(n)}$. Writing

$$|v\rangle = \alpha_0 |g\rangle + \sum_{j \geq 1} \alpha_j |E_j\rangle, \quad (\text{H24})$$

we know that

$$|\alpha_0|^2 \geq 1 - \varepsilon_v, \quad \sum_{j \geq 1} |\alpha_j|^2 \leq \varepsilon_v. \quad (\text{H25})$$

Recall that $g_T(x) := \tanh(x/T)$. Then

$$\langle v | g_T(H') | v \rangle = |\alpha_0|^2 g_T(E_0) + \sum_{j \geq 1} |\alpha_j|^2 g_T(E_j), \quad (\text{H26})$$

which implies that

$$|\langle v | g_T(H') | v \rangle - g_T(E_0)| \leq 2\varepsilon_v, \quad (\text{H27})$$

given that

$$\sum_{j \geq 1} |\alpha_j|^2 g_T(E_j) \leq \sum_{j \geq 1} |\alpha_j|^2 |g_T(E_j)| \leq \sum_{j \geq 1} |\alpha_j|^2 \leq \varepsilon_v, \quad (\text{H28})$$

where we used that $|g_T(y)| \leq 1$ for all $y \in \mathbb{R}$.

Now choose the temperature

$$T = \frac{1}{10(K+1)}. \quad (\text{H29})$$

For $x \in A_{\text{yes}}$, (H21) and (H29) imply that $\frac{E_0}{T} \leq -\frac{10}{3}$. Then

$$g_T(E_0) = \tanh(E_0/T) \leq \tanh(-10/3) \leq -0.99. \quad (\text{H30})$$

Combined with (H27) and choosing parameters such that $2\varepsilon_v \leq 0.01$, we conclude that

$$\langle v | g_T(H') | v \rangle \leq -0.98. \quad (\text{H31})$$

Similarly, for $x \in A_{\text{no}}$, (H22) and (H29) imply that $\frac{E_0}{T} \geq \frac{10}{3}$. Then

$$g_T(E_0) = \tanh(E_0/T) \geq \tanh(10/3) \geq 0.99. \quad (\text{H32})$$

Combined with (H27) and the same choice of parameters such that $2\varepsilon_v \leq 0.01$, we conclude that

$$\langle v | g_T(H') | v \rangle \geq 0.98. \quad (\text{H33})$$

Finally, note that the local terms appearing in the construction in (H3) have operator norm at most $O(\Delta)$, where $\Delta = \text{poly}(n)$. To normalize the terms, define the rescaled Hamiltonian $\tilde{H} := H/\Delta$ and the rescaled temperature $\tilde{T} := T/\Delta$. Then $\tanh(H/T) = \tanh(\tilde{H}/\tilde{T})$, and therefore $\text{Tr}[\tanh(H/T)\rho] = \text{Tr}[\tanh(\tilde{H}/\tilde{T})\rho]$. Since $\Delta = \text{poly}(n)$, the temperature \tilde{T} remains inverse-polynomially bounded, while every local term of \tilde{H} has norm $O(1)$. After rescaling by an additional constant factor if necessary, we may therefore assume that $\|H_j\| \leq 1$ for all local terms.

Appendix I: Derivations for cross entropy and log partition function estimation

1. Proof of Theorem 12 (derivation of formula for cross entropy)

Using the notation in Theorem 12, consider that

$$\Xi(\eta \| \rho(\theta)) - \Xi(\eta \| \rho(0, \theta_2, \dots, \theta_J)) = \Xi(\eta \| \rho(\theta_1, \theta_2, \dots, \theta_J)) - \Xi(\eta \| \rho(0, \theta_2, \dots, \theta_J)) \quad (\text{I1})$$

$$= \Xi(\eta\|\rho(\theta^{(1)}(1))) - \Xi(\eta\|\rho(\theta^{(1)}(0))) \quad (\text{I2})$$

$$= \int_0^1 d\lambda_1 \frac{\partial}{\partial \lambda_1} \Xi(\eta\|\rho(\theta^{(1)}(\lambda_1))) \quad (\text{I3})$$

$$= \int_0^1 d\lambda_1 \theta_1 \left(\langle H_1 \rangle_\eta - \langle H_1 \rangle_{\rho(\theta^{(1)}(\lambda_1))} \right) \quad (\text{I4})$$

$$= \theta_1 \left(\langle H_1 \rangle_\eta - \int_0^1 d\lambda \langle H_1 \rangle_{\rho(\theta^{(1)}(\lambda))} \right) \quad (\text{I5})$$

$$= \theta_1 \left(\langle H_1 \rangle_\eta - \mathbb{E}_{\lambda \sim v} \left[\langle H_1 \rangle_{\rho(\theta^{(1)}(\lambda))} \right] \right). \quad (\text{I6})$$

The fourth equality follows from (161), while accounting for the fact that

$$\frac{\partial}{\partial \lambda_1} H(\theta^{(1)}(\lambda_1)) = \theta_1 H_1. \quad (\text{I7})$$

Additionally,

$$\Xi(\eta\|\rho(0, \theta_2, \dots, \theta_J)) - \Xi(\eta\|\rho(0, 0, \theta_3, \dots, \theta_J)) = \Xi(\eta\|\rho(\theta^{(2)}(1))) - \Xi(\eta\|\rho(\theta^{(2)}(0))) \quad (\text{I8})$$

$$= \int_0^1 d\lambda_2 \frac{\partial}{\partial \lambda_2} \Xi(\eta\|\rho(\theta^{(2)}(\lambda_2))) \quad (\text{I9})$$

$$= \int_0^1 d\lambda_2 \theta_2 \left(\langle H_2 \rangle_\eta - \langle H_2 \rangle_{\rho(\theta^{(2)}(\lambda_2))} \right) \quad (\text{I10})$$

$$= \theta_2 \left(\langle H_2 \rangle_\eta - \mathbb{E}_{\lambda \sim v} \left[\langle H_2 \rangle_{\rho(\theta^{(2)}(\lambda))} \right] \right). \quad (\text{I11})$$

We continue iteratively along these lines and find that the last term is given by

$$\Xi(\eta\|\rho(0, \dots, 0, \theta_J)) - \ln d = \Xi(\eta\|\rho(0, \dots, 0, \theta_J)) - \Xi(\eta\|\rho(0, \dots, 0, 0)) \quad (\text{I12})$$

$$= \Xi(\eta\|\rho(\theta^{(J)}(1))) - \Xi(\eta\|\rho(\theta^{(J)}(0))) \quad (\text{I13})$$

$$= \theta_J \left(\langle H_J \rangle_\eta - \mathbb{E}_{\lambda \sim v} \left[\langle H_J \rangle_{\rho(\theta^{(J)}(\lambda))} \right] \right), \quad (\text{I14})$$

where we used the fact that

$$\rho(0, \dots, 0) = \frac{I}{d}, \quad (\text{I15})$$

which implies that

$$\Xi(\eta\|\rho(0, \dots, 0)) = -\text{Tr}[\eta \ln(\rho(0, \dots, 0))] = -\text{Tr} \left[\eta \ln \left(\frac{I}{d} \right) \right] = \ln d. \quad (\text{I16})$$

So then we form a telescoping sum and conclude that

$$\begin{aligned} \Xi(\eta\|\rho(\theta)) - \ln d &= \Xi(\eta\|\rho(\theta)) - \Xi(\eta\|\rho(0, \theta_2, \dots, \theta_J)) \\ &\quad + \Xi(\eta\|\rho(0, \theta_2, \dots, \theta_J)) - \Xi(\eta\|\rho(0, 0, \theta_3, \dots, \theta_J)) \\ &\quad + \dots + \Xi(\eta\|\rho(0, \dots, 0, \theta_J)) - \Xi(\eta\|\rho(0, \dots, 0, 0)) \\ &= \theta_1 \left(\langle H_1 \rangle_\eta - \mathbb{E}_{\lambda \sim v} \left[\langle H_1 \rangle_{\rho(\theta^{(1)}(\lambda))} \right] \right) \\ &\quad + \theta_2 \left(\langle H_2 \rangle_\eta - \mathbb{E}_{\lambda \sim v} \left[\langle H_2 \rangle_{\rho(\theta^{(2)}(\lambda))} \right] \right) \end{aligned} \quad (\text{I17})$$

$$+ \cdots + \theta_J \left(\langle H_J \rangle_\eta - \mathbb{E}_{\lambda \sim v} \left[\langle H_J \rangle_{\rho(\theta^{(J)}(\lambda))} \right] \right) \quad (\text{I18})$$

$$= \sum_{j=1}^J \theta_j \left(\langle H_j \rangle_\eta - \mathbb{E}_{\lambda \sim v} \left[\langle H_j \rangle_{\rho(\theta^{(j)}(\lambda))} \right] \right) \quad (\text{I19})$$

$$= \langle H(\theta) \rangle_\eta - \sum_{j=1}^J \theta_j \mathbb{E}_{\lambda \sim v} \left[\langle H_j \rangle_{\rho(\theta^{(j)}(\lambda))} \right] \quad (\text{I20})$$

$$= \langle H(\theta) \rangle_\eta - \|\theta\|_1 \sum_{j=1}^J \frac{|\theta_j|}{\|\theta\|_1} \mathbb{E}_{\lambda \sim v} \left[\text{sgn}(\theta_j) \langle H_j \rangle_{\rho(\theta^{(j)}(\lambda))} \right] \quad (\text{I21})$$

$$= \langle H(\theta) \rangle_\eta - \|\theta\|_1 \mathbb{E}_{j \sim q, \lambda \sim v} \left[\text{sgn}(\theta_j) \langle H_j \rangle_{\rho(\theta^{(j)}(\lambda))} \right]. \quad (\text{I22})$$

Note that we can also write

$$\begin{aligned} & \langle H(\theta) \rangle_\eta - \|\theta\|_1 \mathbb{E}_{j \sim q, \lambda \sim v} \left[\text{sgn}(\theta_j) \langle H_j \rangle_{\rho(\theta^{(j)}(\lambda))} \right] \\ &= \|\theta\|_1 \mathbb{E}_{j \sim q} \left[\text{sgn}(\theta_j) \langle H_j \rangle_\eta \right] - \|\theta\|_1 \mathbb{E}_{j \sim q, \lambda \sim v} \left[\text{sgn}(\theta_j) \langle H_j \rangle_{\rho(\theta^{(j)}(\lambda))} \right] \end{aligned} \quad (\text{I23})$$

$$= \|\theta\|_1 \mathbb{E}_{j \sim q, \lambda \sim v} \left[\text{sgn}(\theta_j) \left(\langle H_j \rangle_\eta - \langle H_j \rangle_{\rho(\theta^{(j)}(\lambda))} \right) \right]. \quad (\text{I24})$$

2. Hybrid quantum–classical algorithm for cross entropy and log partition function estimation

This leads to the following hybrid quantum–classical algorithm for estimating the cross entropy:

Algorithm 15. *A hybrid quantum–classical algorithm for estimating the cross entropy $\Xi(\eta \parallel \rho(\theta))$ consists of the following steps:*

1. Set $k \leftarrow 1$, and set

$$K \leftarrow O \left(\left(\frac{\|\theta\|_1 \max_{j \in [J]} \|H_j\|}{\varepsilon} \right)^2 \ln \left(\frac{1}{\delta} \right) \right), \quad (\text{I25})$$

where $\varepsilon > 0$ is the desired accuracy and $\delta \in (0, 1)$ is the desired failure probability.

2. Sample $j \sim q$ and $\lambda \sim v$.

3. Prepare the state η and the thermal state $\rho(\theta^{(j)}(\lambda))$.

4. Measure the observable H_j on each state, with measurement outcomes $X_k^\eta, X_k^\rho \in \text{spec}(H_j)$. Set $W_k \leftarrow \|\theta\|_1 \cdot \text{sgn}(\theta_j) (X_k^\eta - X_k^\rho)$. Set $k \leftarrow k + 1$.

5. Repeat Steps 2–4 $K - 1$ more times. Compute the average $\overline{W}_K := \frac{1}{K} \sum_{k=1}^K W_k$ and output $\ln d + \overline{W}_K$ as an estimate of $\Xi(\eta \parallel \rho(\theta))$.

By the Hoeffding inequality, we are guaranteed that

$$\Pr \left[\left| \ln d + \overline{W}_K - \Xi(\eta \parallel \rho(\theta)) \right| \leq \varepsilon \right] \geq 1 - \delta. \quad (\text{I26})$$

Let us finally note that one can estimate the log-partition function $\ln Z(\theta)$ by means of the same algorithm, but with steps 3 and 4 replaced by the following:

1. Prepare the thermal state $\rho(\theta^{(j)}(\lambda))$.
2. Measure the observable H_j on this state, with measurement outcome $X_k^\rho \in \text{spec}(H_j)$. Set $W_k \leftarrow -\|\theta\|_1 \cdot \text{sgn}(\theta_j) X_k^\rho$. Set $k \leftarrow k + 1$.